Applied Catalysis B: Environment and Energy 352 (2024) 124043

Contents lists available at ScienceDirect

Applied Catalysis B: Environment and Energy

journal homepage: www.elsevier.com/locate/apcatb

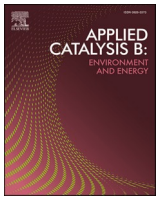

Molecular modification: A promising strategy for the design of donor-acceptor-type organic polymers photocatalyst

Yaocheng Deng [a,*], Yu Shi [a], Ling Li [a,b], Rongdi Tang [a,c], Zhanpeng Zhou [a,b], Sheng Xiong [a], Wenbo Li [a,b], Jiawei Liu [a], Ying Huang [b,*]

[a] College of Environment & Ecology, Hunan Agricultural University, Changsha 410128, China
[b] College of Resources, Hunan Agricultural University, Changsha 410128, China
[c] College of Environmental Science and Engineering, Hunan University and Key Laboratory of Environmental Biology and Pollution Control (Hunan University), Ministry of Education, Changsha 410082, China

ARTICLE INFO

Keywords:
Organic polymers
Donor-acceptor structure
Molecular modification
Charge transfer dynamics
Pollutant degradation

ABSTRACT

Organic polymers (OPs), including conjugated polymers, conjugated microporous polymers, and conjugated organic frameworks, have garnered increasing attention in recent years due to their exceptional photocatalytic performance and recombinable molecular building blocks. The intramolecular charge transfer (ICT) within OPs is instrumental in achieving efficient photocatalysis. Moreover, the intermolecular electron donor-acceptor (D-A) structure is aimed at optimizing ICT, which could be accomplished by molecular modification. In this paper, we outline the comprehensive approaches for constructing D-A structure through molecular modification, and discuss the fundamental principles of enhancing the photocatalytic activity of D-A OPs in detail. Furthermore, we summarize the application of modified D-A OPs in resolving prevalent environmental and energy problems. This method is widely recognized as a promising solution to address the current bottleneck in photocatalysis. Thus, this review aims to enhance the fundamental comprehension of D-A OPs created through molecular modification and explore innovative strategies for addressing existing environmental challenges.

1. Introduction

Global environmental pollution and energy shortages are escalating in severity today. Researchers are making great efforts to realize a greener and more efficient production capacity system. Therefore, in view of its advantages of being more low-energy, high-efficiency, green and non-polluting compared to other methods of degrading pollutants, the development of photocatalytic technology has received widespread attention since 1967 [1]. With the development of artificial photocatalysis systems, researchers are trying to explore the photocatalyst with strong photocatalysis capability [2–6]. The general photocatalysts in recent years are categorized into organic photocatalysts and inorganic photocatalysts. Among them, inorganic photocatalysts, such as TiO_2, SnO_2, MnO_2, sulfides, and their composite products, have been respected by many researchers in the development of photocatalytic technology due to their low price and better redox ability [7–9]. However, its fatal drawbacks are revealed in the process. For example, sulfides and their complex products will inevitably produce toxic by-products during the reaction, and the abuse of metal oxides in photocatalysis, resulting in the leakage of metal ions thereby polluting the water. Moreover, the durability and photostability of inorganic photocatalysts, particularly those incorporating metallic elements, present inherent limitations that compromise their practicality. Therefore, researchers have investigated the organic photocatalysts with identical semiconductor properties due to its environmentally friendly nature and favorable photostability. On the one hand, most organic photocatalysts are structurally stable polymers that rarely produce reaction by-products and change their inherent structure in the reaction. On the other hand, its extreme plasticity provides more possibilities to further improve the photocatalytic efficiency and create different application. However, with the deeper research, many problems are discovered. The pure organic photocatalysts, such as g-C_3N_4 [10–12], carbazole [13] and pyrene [14] also have inevitable drawbacks when used as the single photocatalyst in the photocatalysis. They may perform low internal charge transfer rate, narrow optical response range, fast electron-hole recombination, or low environmental durability. Fortunately, to solve above problems as far as possible, researchers have found that the composite photocatalysts prepared by metal doping [15–18], synthetic heterojunction [19–21] or

* Corresponding authors.
E-mail addresses: dengyaocheng@hunau.edu.cn (Y. Deng), huangying@hunau.edu.cn (Y. Huang).

https://doi.org/10.1016/j.apcatb.2024.124043
Received 15 November 2023; Received in revised form 27 March 2024; Accepted 4 April 2024
Available online 5 April 2024

homojunction [22–24], molecular modification [25–27], and other methods which could well optimize the deficiencies of single photocatalysts in the photocatalytic reaction process for the promoted photocatalytic efficiency and excellent durability [28–30]. Among the above methods, molecular modification could be considered as one of the most suitable approaches for modifying organic polymers (OPs) photocatalysts, owing to the inherent characteristic of modular molecular structure in OPs. The single-type organic photocatalysts have been subjected to molecular modification by incorporating diverse micromolecule units, leading to the synthesis of a novel composite organic photocatalyst [31]. In this process, the incorporation of molecular building blocks exhibiting excellent durability to construct the composite organic photocatalyst could successfully enhanced its overall durability. For instance, the environmental durability of OPs systems containing thiazolo[5,4-*d*]thiazole has been demonstrated owing to their stable polymeric structure and extended conjugated framework [32,33]. Moreover, the incorporation of molecular units featuring robust linkages, such as amide bonds, into OPs could confer remarkable durability upon them [34]. In the composite OPs systems, due to the different electronegativity or the bonding mode between the molecular building blocks of OPs, resulting in the emergence of electron D-A structure within it [35,36]. According to the function of the molecular building blocks in the D-A molecular unit, its role is also different. When the molecular building block provides electrons or oxidation sites during electron transfer, it could be defined as D unit. Similarly, when the other molecular building block accepts electrons or provides reduction sites during electron transfer, it could be defined as A unit [37–39]. If π-π bonds are existed in the D-A structure, it could be called donor-π-acceptor (D-π-A) structure [40–42].

Besides, it has been demonstrated that the presence of pronounced charge separation and migration within the molecular structure is pivotal for photocatalysts to exhibit efficient light responsivity [43–45]. Recent studies have demonstrated that the formation of robust covalent bonds between molecular units in the OPs represents an effective strategy for achieving large dipole moment [46]. When the catalyst is in the photoexcited state, the large dipole moment of the molecule could form a stronger build-in electric field [47]. It is widely considered that building the build-in electric field is a feasible strategy for inducing effective intramolecular charge transfer (ICT) [48,49]. This process induces the transfer of electrons from the highest occupied molecular orbitals (HOMO) of the donor unit to the lower unoccupied molecular orbitals (LUMO) of the acceptor unit, resulting in electron accumulation in the acceptor units and hole formation in the donor units, thereby maximizing light-induced carrier separation [50,51]. Thus, the photocatalytic performance is effectively promoted and the original photocatalyst is more efficient in the process of photocatalytic oxidation. For example, Zhang *et al.* [52] have prepared TBPA-COF, a conjugated organic polymer (COP) with D-A structure. It utilizes 2,4,6-trimethyl-1, 3,5-triazine as the electron-donor unit and bis(4-formylphenyl) acetylene as the electron-acceptor unit through organic acid-induced solve molecular condensation reaction. The D-A structure enhances the intramolecular carrier separation and migration capabilities, thereby improving overall performance. Similarly, Che *et al.* [53] have also employed thermal copolymerization reaction to synthesize the 4-methoxyphenyl-grafted polymeric carbon nitride (PCN) framework, aiming to enhance the photocatalytic degradation of nitenpyram (NTP).

Among the various methods employed for the synthesis of D-A OPs, molecular modification has gained significant attention from researchers due to its evident impact on modifying properties and straightforward operational procedure [42]. Since the inception of molecular modification [54], there has been an exponential increase in related studies (Fig. 1). Particularly after 2020, this growth has been remarkable, highlighting the immense potential of molecular modification in enhancing photocatalytic performance. This could be attributed to the fact that the properties of D-A OPs, following molecular modification, exhibit a closer resemblance to those of the ideal

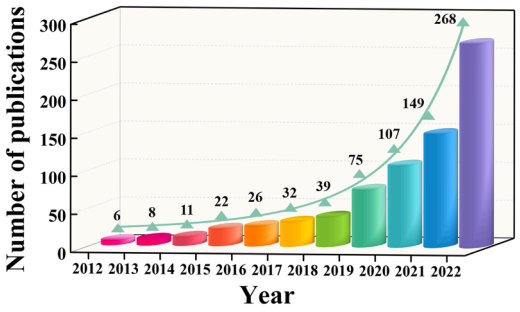

Fig. 1. Number of publications on molecular modification builds D-A structure in the last decade.

photocatalyst compared to D-A OPs modified through alternative methods [55,56]. And the ideal photocatalyst should fulfill several criteria as broad visible light absorption range, appropriate bandgap structure, and efficient charge transfer ability [57,58]. Consequently, the modified OPs could overcome existing limitations and achieve higher conversion efficiencies. Moreover, OPs play a crucial role as substrate materials for constructing D-A structure within traditional organic photocatalysts [59–62]. The flexible and versatile modular units present in OPs are more conducive to facilitating the formation of D-A structure through molecular modification, while ensuring their stability through polymerization state control. It also provides the potential for subsequent investigations into the functional customization of photocatalysts based on OPs [63–65]. The D-A OPs exhibit unique photoelectric semiconductor properties: (a) Organic molecules possessing electron D-A structure demonstrate characteristics akin to rectification effects observed in inorganic semiconductor p-n junctions [66]; (b) electron donor and electron acceptor moieties effectively regulate energy levels within the molecule [67,68]; (c) light-induced energy transfer and electron transfer occur between donor and acceptor within the molecule itself [69,70]. The application of photocatalysis technology in environmental renewable restoration has gained widespread recognition in recent years, particularly in the fields of photocatalytic overall water splitting [71] (hydrogen evolution reaction (HER), oxygen evolution reaction (OER)); CO_2 reduction [72]; photocatalytic degradation of water pollutants (nitenpyram [53], rhodamine B [73], methyl orange [74], atrazine [75], etc.); photocatalytic promoting other redox reactions [76]; pH visualization [73]; etc. Changing the type of molecular building blocks by molecular modification offers to tailor photocatalyst performance [77], such as altering energy levels, expanding light absorption range, and facilitating efficient separation of electron-hole pairs. As molecular modification enables the conferment of fascinating properties on OPs, the concept of designing molecular building blocks has revolutionized the study of it since 1998 [54]. Before 2011, early research reports mainly focused on how different construction types affected optical properties [68,69,78]. Over a decade's worth of development in designing molecular blocks has laid a strong theoretical foundation for subsequent rapid advancements in molecular modification research. Since 2011 [44], there has been a shift towards investigating charge transfer dynamics between different molecular building blocks, recognizing that it could facilitate the formation of electron D-A structure thereby promoting complete charge transfer [79]. A significant milestone has been reached in 2015 [80], the breakthrough occurred with the introduction of ICT as an explanation for the photocatalytic behavior of g-C_3N_4 when exposed to long-wave light irradiation. The concept introduced in 2016, which bridges combinations among different molecular units, offers new perspectives for future diversification in molecular modifications [81,82]. Building upon two decades' worth of prior research, recent years have witnessed an explosive increase in related research reports, particularly focusing on practical applications such as environmentally sustainable remediation within the field of constructing electronic D-A OPs through molecular modification

[83,84]. This developmental process (Fig. 2) underscores both solid research foundations and broad prospects for further exploration on molecular modification. In comparison to other reviews of similar nature, this work has delved deeper into the representative papers from different developmental periods of molecular modification D-A OPs, providing a more comprehensive and visually illustrative depiction of the evolutionary trajectory in molecular modification for D-A OPs [85, 86].

In this review, we present a thorough overview of the latest developments in techniques for molecular modification to improve the performance of unaltered photocatalysts. We elucidate the underlying principles governing the formation of D-A structure and its role in promoting photocatalytic processes. Based on it, we critically revisit and reevaluate the concept of molecular modification. Additionally, this paper primarily focuses on elucidating the alterations in energy band structure and charge characteristics observed in composite photocatalysts with D-A structure because of molecular modification. And, these modifications hold significant potential for enhancing the photocatalytic properties of corresponding OPs and expanding their application scope. The D-A OPs constructed through molecular modification precisely fulfills a range of prerequisites for ideal photocatalysts, thus rendering the strategy of molecular modification highly captivating in recent. Regrettably, no comprehensive and meticulous synthesis has been conducted on this topic thus far. Therefore, to enhance the advancement of research in the field of molecular modification and achieve groundbreaking accomplishments, we conducted this study. Furthermore, considering the current developmental status and existing challenges associated with molecular modify OPs, several future-oriented aspects that require attention are proposed. This endeavor holds immense significance in surmounting forthcoming hurdles faced by OPs photocatalysts.

2. Types of molecular modifications

The molecular building blocks could be customized thereby highly selectively influencing the shape and physicochemical properties of OPs. Until now, most of the molecular modification known to us have been used to establish the electronic push-pull model in OPs [87–89]. As crucial components of the inherent electronic push-pull model, the electron donor and acceptor play a significant role in enhancing the efficiency of electron transmission during photocatalysis. And the generation of a built-in electric field stands out as a pivotal element in augmenting the effectiveness of electron transfer within the photocatalysis process. Based on it, D-A OPs with great potential in catalysis, semiconductor, antibacterial and drug delivery have been designed. Based on the distinct electronic functionalities of the molecular building blocks upon integration with the main molecular unit, the newly incorporated molecular building blocks and main molecular units can be categorized as electronic D unit and electronic A unit, collectively constituting an electronic D-A architecture. When a single type of molecular building block is introduced to the main molecular unit with a quantity of one, this process could be defined as the monomolecular modification (Fig. 3a). The introduction of multiple types or quantities of building blocks to modify the subject molecule, this process could be defined as the multimolecular modification (Fig. 3b-g). Among them, the types of multimolecular modification could be roughly divided into two categories: a) when two or more types of molecular building blocks modify the same main molecular unit simultaneously, they play different roles due to their varying mutual electronegativity (Fig. 3b-e); b) by increasing the amount of D or A units in the original D-A molecular model, the OPs with the combination of D-A_1-A_1 or A-D_1-D_1 molecular units are obtained (Fig. 3f-g). Furthermore, when the molecular building block replaces the original molecular position in a manner that entails substitution rather than addition to the main unit, this process could be defined as molecular substitution (Fig. 3h). Currently, the existing strategies for implementing molecular modification processes are generally categorized into thermal copolymerization reaction, Tautomerism strategy, Knoevenagel condensation reaction, Suzuki condensation reaction, Povarov reaction, and Suzuki-Miyaura coupling reaction. Among them, the thermal copolymerization reaction and Suzuki condensation reaction are normally used in molecular modification.

Compared to the other two methods, monomolecular modification has been favored by more researchers for the customization of individual OPs photocatalysts due to its simplified material synthesis process and the more straightforward approach towards analyzing photoreaction mechanisms. Specifically, a type of small molecular units is selectively grafted into the periphery of the major OPs or form periodic links with other organic molecular units, which could be directly achieved through one-step thermal polycondensation and alternative methods [90]. In contrast, commonly employed preparation methods for multimolecular modification include Suzuki condensation reaction, statistical copolymerization, and trimerization reaction [91,92]. The above methods, in comparison, exhibit drawbacks such as complex process, and lengthy preparation cycle [26,87]. Consequently, their application in the preparation of electronic D-A OPs is limited. On the other hand, the successful establishment of intermolecular electron D-A structures in the OPs through monomolecular modification, particularly in determining the respective roles as electron donor or acceptor, could be effectively validated through straightforward density functional theory calculations [45,84]. However, the OPs modified by the other two methods exhibit some issues such as complex types of molecular

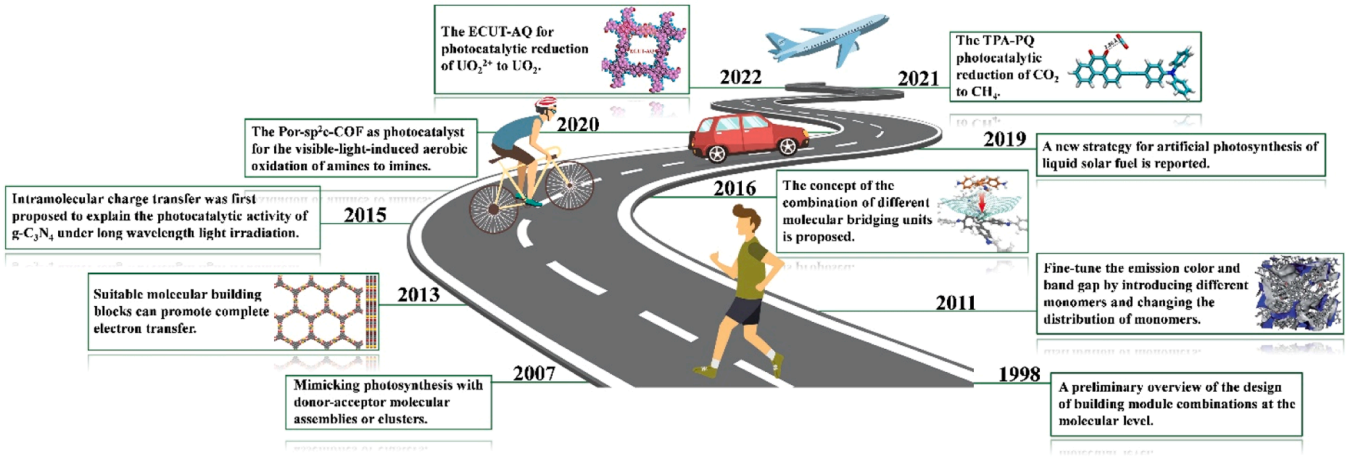

Fig. 2. Development of D-A OPs modified by molecular modification.

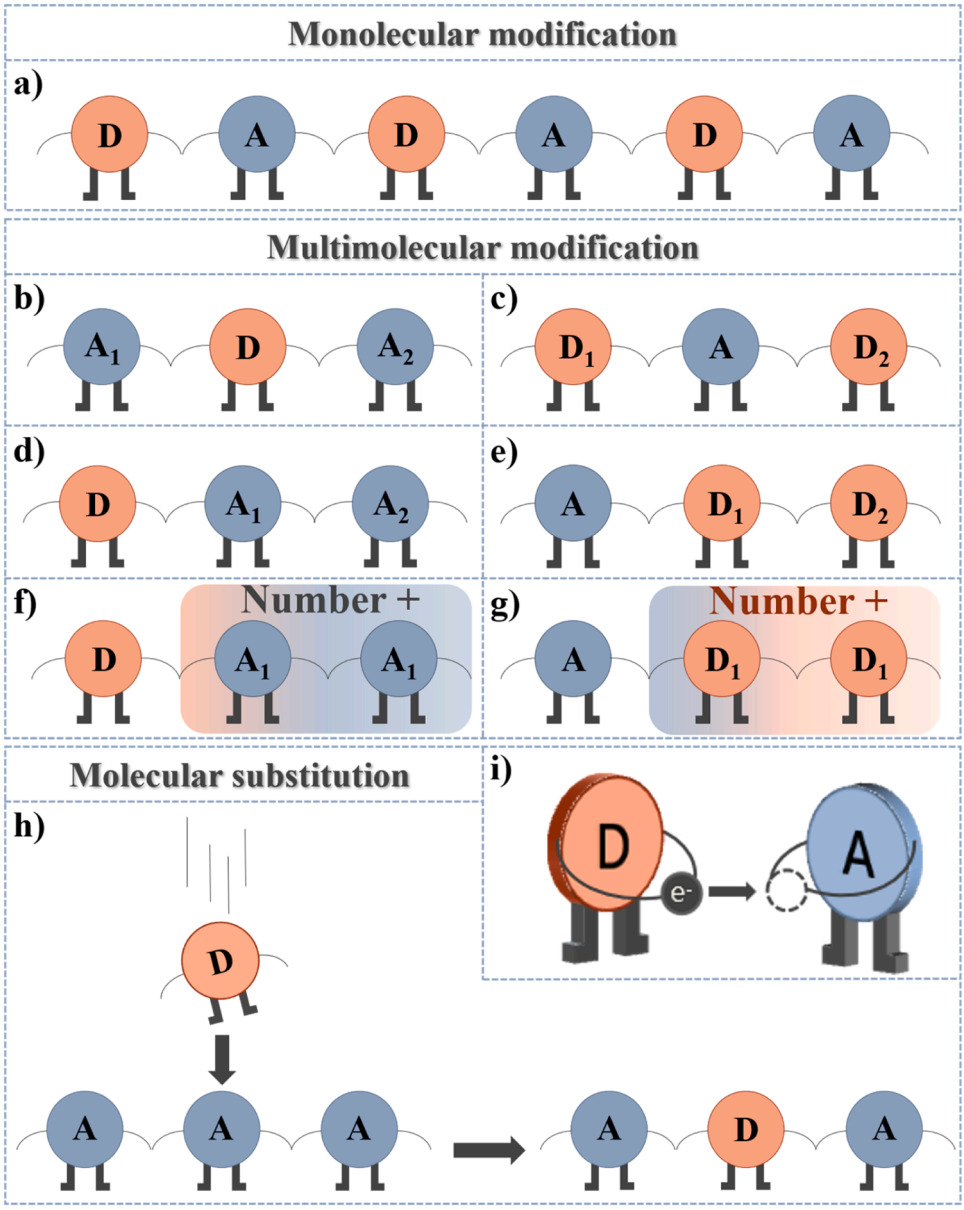

Fig. 3. Illustration of molecular modification types. (a) Monomolecular modification: D-A. Multimolecular modification: (b) A_1-D-A_2; (c) D_1-A-D_2; (d) D-A_1-A_2; (e) A-D_1-D_2; (f) D-A_1-A_1+; (g) A-D_1-D_1+. (h) Molecular substitution. (i) Charge transfer pattern diagram in donor and acceptor. (A_1 and A_2 represent different electron acceptors, D_1 and D_2 represent different electron donors.).

building blocks and uncertain distribution [93,94]. These issues present a significant challenge to determining its electrochemical characteristics and investigating its reaction mechanism. According to the conventional charge transfer direction, the photo-induced electron transfer from D to A (Fig. 3i). And the internal electrochemical mechanism of various D-A OPs photocatalysts has been summarized.

2.1. Monomolecular modification

Monomolecular modification refers to the combination of two organic molecules with different electronegativity to form an organic polymer with an electronic D-A or D-π-A structure [95–97]. A typical characteristic of monomolecular modification is the addition of a single electron donor or acceptor building blocks to the initial OPs. And the synthesis method of the D-A OPs is mostly one-stepping thermal copolymerization reaction, which is easy to operate. Interestingly, the various molecular building block combinations show similar optimization trends in material properties (Table 1). Due to it has such exciting advantages, researchers have been focusing on exploration in recent years [98–100].

Firstly, as different types of molecular building blocks will offer different properties to OPs, validating the optimal combination using the incorporation of different types of molecular building blocks, respectively [101–103]. For example, the carbazole (Cz) as the D unit is linked with different A units, pyrene (Py), triphenyltriazine (TPT), benzothiadiazole (BT), and thiazolylthiazole (TzTz), respectively (Fig. 4a), to construct various D-A conjugated microporous polymers (CMPs) [13]. Similarly, three different COPs are prepared by condensation reaction according different molecules (thiophene, biphenyl, pyrene) as the electron donor unit link with thiazolo[5,4-*d*]thiazole (ThTh) unit, named Ts-ThTh-CMP, Bi-ThTh-CMP and Py-ThTh-CMP [104]. Secondly, based on this theory, the integration of specific molecular building blocks could transform molecules from their inherent planar structure into a two or even three-dimensional structure. This is more conducive to produce reactive oxygen species (ROS) under light exposure. The BF-COFs, which incorporate benzofuran (Fig. 4b), have

Table 1
Summary of recent reports on monomolecular modification.

Donor	Acceptor	Designation	Synthesis method	Bandgap [eV]	BET surface area [$m^2 g^{-1}$]	
4-methoxyphenyl	Polymeric carbon nitride	PCN/4-MI_{75}	Copolymerization reaction	2.45	189.84	[53]
Benzofuran	Hetero radialene	BF-COF1 BF-COF2	Tautomerism strategy	1.87	460	[76]
				1.88	370	
1,4-diformylbenzene	2,4,6-Trimethyl-1,3,5-triazine	g-$C_{18}N_3$-COF	Knoevenagel condensation reaction	2.34	1070	[107]
Polymeric carbon nitride	Benzothiadiazole	PCN-BTD_{008}	Copolymerization reaction	2.64	——	[71]
2,3,10,11,18,19-hexahydroxy-cata-hexabenzo-coronene	Tetrafluorophthalonitrile	HBC-TFPN	Thermal copolycondensation	1.50	681	[74]
5-bromo-2-thiophenecarboxaldehyde	Conjugated g-C_3N_4	TCN-5	Thermal copolymerization reaction	2.22	85.157	[41]
Benzodithiophene	Dibenzo[*b*, *d*]thiophene sulfone	P(BDT-$DBTSO_{79}$)	Thermal copolymerization reaction	2.39	——	[108]
Tetraphenylethene moieties	Anthraquinone moieties	AQTEE-COP	Sonogashira cross-coupling reaction	1.99	396	[97]
1,3,4-thiadiazole ring	Quinone	COF-TD1	One-pot	2.05	29	[109]
1,2,4-thiadiazole ring		COF-TD2		1.76	37	
Triptycene	Polymeric carbon nitride	T-CN-0.010	Thermal copolymerization reaction	2.63	24	[95]
N-phenylthiourea	Polymeric carbon nitride	CNP3	Thermal copolymerization reaction	1.96	8.14	[102]
Polymeric carbon nitride	2,3-diaminopyridine	DAPCN	Thermal copolymerization reaction	2.64	138.92	[101]

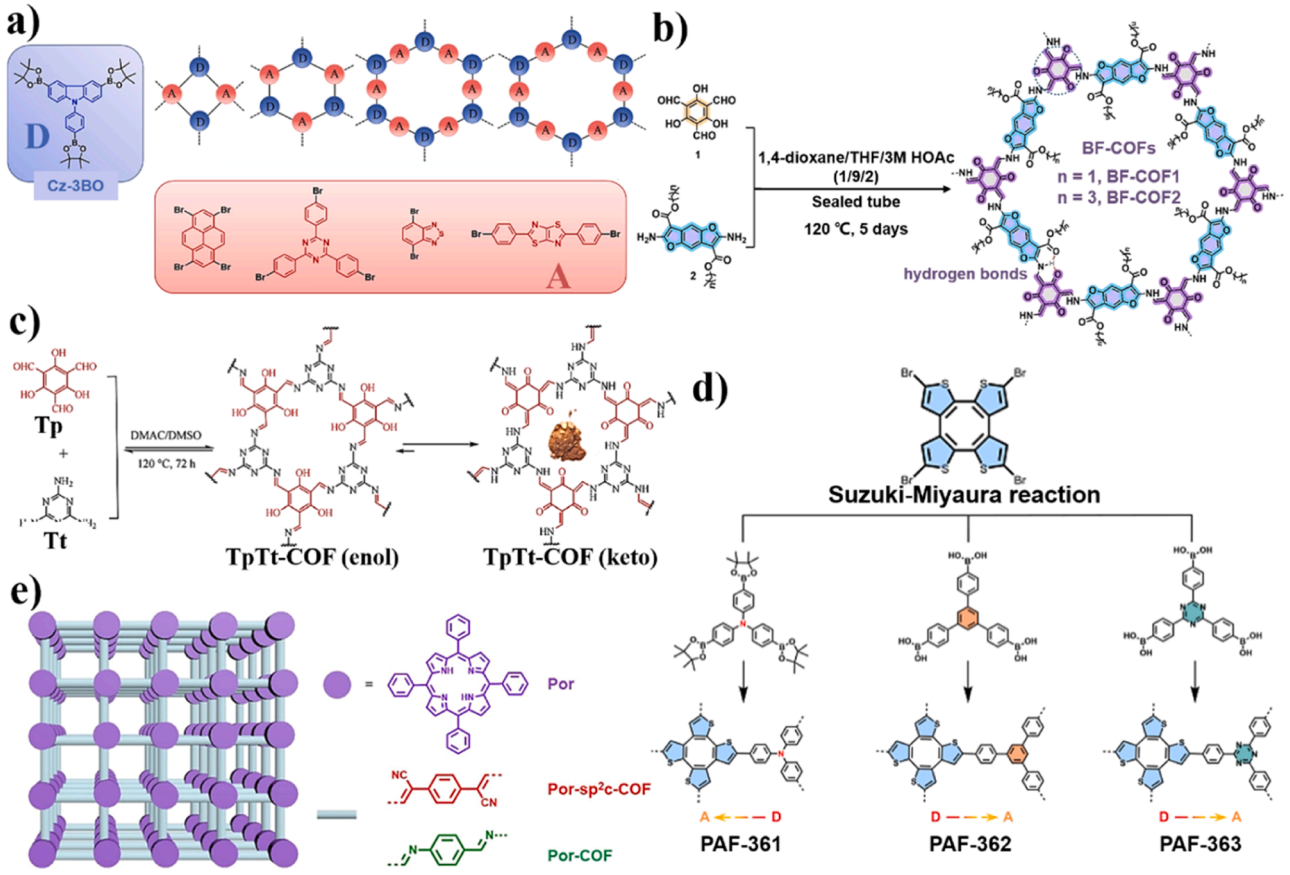

Fig. 4. Synthesis route of monomolecular modification and structure diagram. (a) A carbazole (Cz) unit as the D with diverse A units [13]. (b) Benzofuran-based COFs (BF-COFs) [76]. (c) TpTt-COF [105]. (d) Three kinds of COTh-based D-A OPs. (e) Por-sp^2c-COF and Por-COF [106].

been demonstrated enhanced solvent tolerance by employing a tautomerism strategy [76]. Ultra-linked two-dimensional carbon nanotubes, HBC-TFPN, are synthesized by utilizing hexabenzocoronene as the torsion possessing a fluctuating lattice [74]. Under the above, it realizes the transformation from an ordinary one-dimensional plane to a two-dimensional wave structure. And D-A TpTt-COF (Fig. 4c) is same. The synthesis of this compound is achieved through a reversible Schiff-base condensation reaction, employing 1,3,5-triformylphloroglucinol (Tp) as the donor and 1,3,5-triazine-2,4,6-triamine (Tt) as the acceptor [105]. Finally, it is noteworthy that upon modification and

subsequent combination with diverse molecular building blocks, the role (D or A) of the main molecular unit will undergo alteration in accordance with variations in electronegativity. For instance, three types of photoactive D-A CoTh-based porous aromatic frameworks (CoTh-PAFs) have been synthesized by incorporating cyclooctatetrathiophene (COTh) with three distinct molecular units respectively as the primary building block (Fig. 4d). The role of COTh varies in different combinations due to the disparity in electronegativity between COTh and the incorporated molecular units. And Por-sp^{2}c-COF as a typical porphyrin covalent organic framework is also produced via the Knoevenagel condensation reaction, linking 1,4-phenylenediacetonitrile (PDAN) to 5,10,15,20-tetrakis(4-benzrin) (p-Por-CHO) [84,106] (Fig. 4e). All bonding forms mentioned above fall under the category of monomolecular modification defined earlier.

2.1.1. Energy band adjustment

It has been demonstrated that bandgap structure and its characters in OPs is associated with promoting photochemical water decomposition, photocatalytic oxidation in water, and other applications [110–112]. And in the follow study, researchers have found that monomolecular modification have excellent regulatory capabilities for it [113,114]. Since 2011, Jiang *et al.* [78] have found that modulating fluorescence color emitted by materials could be achieved by introducing different copolymers and altering monomer distribution within OPs. This finding has been consistently supported by subsequent studies [115–118]. Therefore, a growing number of researchers are dedicated to adjust energy band properties of materials through monomolecular modification for enhanced utilization of light energy.

Based on the work of Jiang and his team, Zhang *et al.* [116] have modified conjugated carbon nitride (CN) by incorporating thiophene entities as molecular building blocks to synthesize a novel conjugated polymer, CNA. It has been observed that the addition of thiophene effectively alters the inherent volume and surface structure of CN. The band gap of CNA (1.72 eV) is significantly reduced to CN (2.72 eV), and it could be adjusted accordingly. In the following years, Lan *et al.* [117] have exploited the unique band-gap tunability of COPs to alter the properties of the original triazine polymers in terms of band electron, optical absorption, and redox. This has been achieved by increasing the number of electron-donating benzyl units on the main chain triazine. The obtained CTP-2 (2.66 eV) demonstrates a notably augmented overall water splitting capacity in comparison to CN (2.98 eV), referred to as the combined impact of broadening the light absorption range and enhancing pore oxidation capability. Under identical conditions, CTP-2 demonstrates the hydrogen evolution rate is five times higher than CN, along with the oxygen production rate is three times higher than that of CN. These exciting findings open new avenues for achieving efficient overall water splitting and have sparked great interest in exploring strategies for molecular-level modification of OPs. In the continuous exploration, organic monomer benzothiadiazole (BTD) has been copolymerized with PCN to assemble a photocatalyst with D-π-A structure, COP-2 (2.97 eV) [71]. Remarkably, COP-2 exhibits nearly tenfold higher hydrogen evolution rate and twentyfold higher oxygen evolution rate under visible light irradiation compared to PCN (3.90 eV). Such exceptional photocatalytic performance in overall water splitting could be attributed to the excellent electrochemical properties conferred by the D-π-A structure.

The π-conjugated hybrid structure of PCN is a crucial factor contributing to its pronounced photocatalytic activity [119,120]. Among them, the addition of π-π bonds change the electrochemical properties of the original conjugated polymers (CPs), and enhance the delocalization of π-electrons in the corresponding π-conjugated structure, leading to a notable rise in the quantity of unpaired electrons [120,121]. Due to the unique D-A structure, the separation and transfer of electron-hole pairs are accelerated, and the recombination rate is reduced. Various types of commonly used carbon nitride grafting agents exist, and their reaction processes are analogous; most of them involve straightforward thermal copolymerization procedures (Fig. 5a). Benzene ring is grafted into the carbon nitride skeleton by one-step thermal copolymerization to form D-A type carbon nitride (CNP_x). And, the VB position of the sample gradually increases from CNP0 to CNP4 (the benzene ring concentration gradually increases) (Fig. 5b), while the CB position does not change much and the band gap gradually decreases (2.55 eV~1.82 eV) [102]. Because a benzene ring with π-structure is incorporated into tri-s-triazine, the optical characteristics of carbon nitride are improved, such as expanded spectrum of light absorption and reduced band gap [122,123]. Among all aromatic compounds, the benzene ring exhibits superior electron ionization characteristics due to its higher electron affinity. This integration extends the π-conjugation system and generates a larger conjugated network, resulting in an expanded electron ionization range. Consequently, it facilitates photocatalytic redox reactions by providing favorable conditions (Fig. 5c) [101].

2.1.2. ICT enhancement

The unique D-A structure plays a crucial role in enhancing the optical properties of photocatalysts and improving their photocatalytic efficiency. Additionally, this molecular structure also has an exciting effect on the polymer's built-in field, thereby promoting ICT [88,122]. Currently, electron transport (ET) plays a pivotal role in both biological and chemical processes [48,90]. The high catalytic activity in artificial photocatalytic reaction systems arises from the synergistic effects of light absorption, electron separation, and other factors [124]. Among these factors, the prolonged duration and wide range of charge separation following light energy absorption contribute significantly to the observed high catalytic activity [125]. When the material absorbs light energy, it triggers electron transfer in the photo-excited state. In this process, the electron D-A structure offers significant advantages in terms of enhanced carrier separation and migration capabilities during the reaction, thereby facilitating smooth ICT and effectively inhibiting electron-hole complexation [125–127]. Thus, D-A OPs could improve the original electrochemical properties of the polymers and exhibit excellent photocatalytic performance. Since the initial proposition in 2015 by Fan *et al.* [128], ICT is utilized to elucidate the photocatalytic activity of g-C_3N_4-based photocatalysts with D-A structure (Fig. 6a). The incorporation of molecular building blocks into simple OPs to form D-A structure has emerged as a prominent research focus in recent years, representing a novel approach for molecular modification [107,129]. The charge transfer kinetics of the photocatalyst including PCN [27,77], porphyrin [84], pyrene [104,126], carbazole [130] and their derivatives could be effectively modified by molecular modification. Putting the suitable aromatic organic molecule into original conjugated molecular framework, serving as building blocks, to engender novel OPs. This integration leads to the creation of the D-A structure through leveraging the distinct electrochemical properties displayed by the two constituents within polymers [81]. The molecular building blocks with distinct properties play a pivotal role in altering the electronic structure of the active site, thereby inducing the formation of ICT pathways, and significantly facilitating the separation and translocation of photogenerated charges [83,131].

Furthermore, the formation of a robust build-in electric field requires the presence of a substantial molecular dipole moment [132–134]. The dipole moment of a molecule is directly proportional to the electronegativity at its two ends [135,136]. In other words, higher electronegativity at both ends leads to a greater dipole moment, resulting in a stronger internal electric field and the increased ICT rate. The D-A type OPs exhibit excellent ICT capability could be attributed to the significant electronegativity difference between D and A [137,138]. By capitalizing on this characteristic, the researchers successfully achieved remarkably enhanced photoelectric responsiveness through the identification of molecular modules with greater electronegativity disparities. For example, Deng has proposed a molecular dipole control strategy in his report [88], by exploiting the modularity of molecular units in OPs,

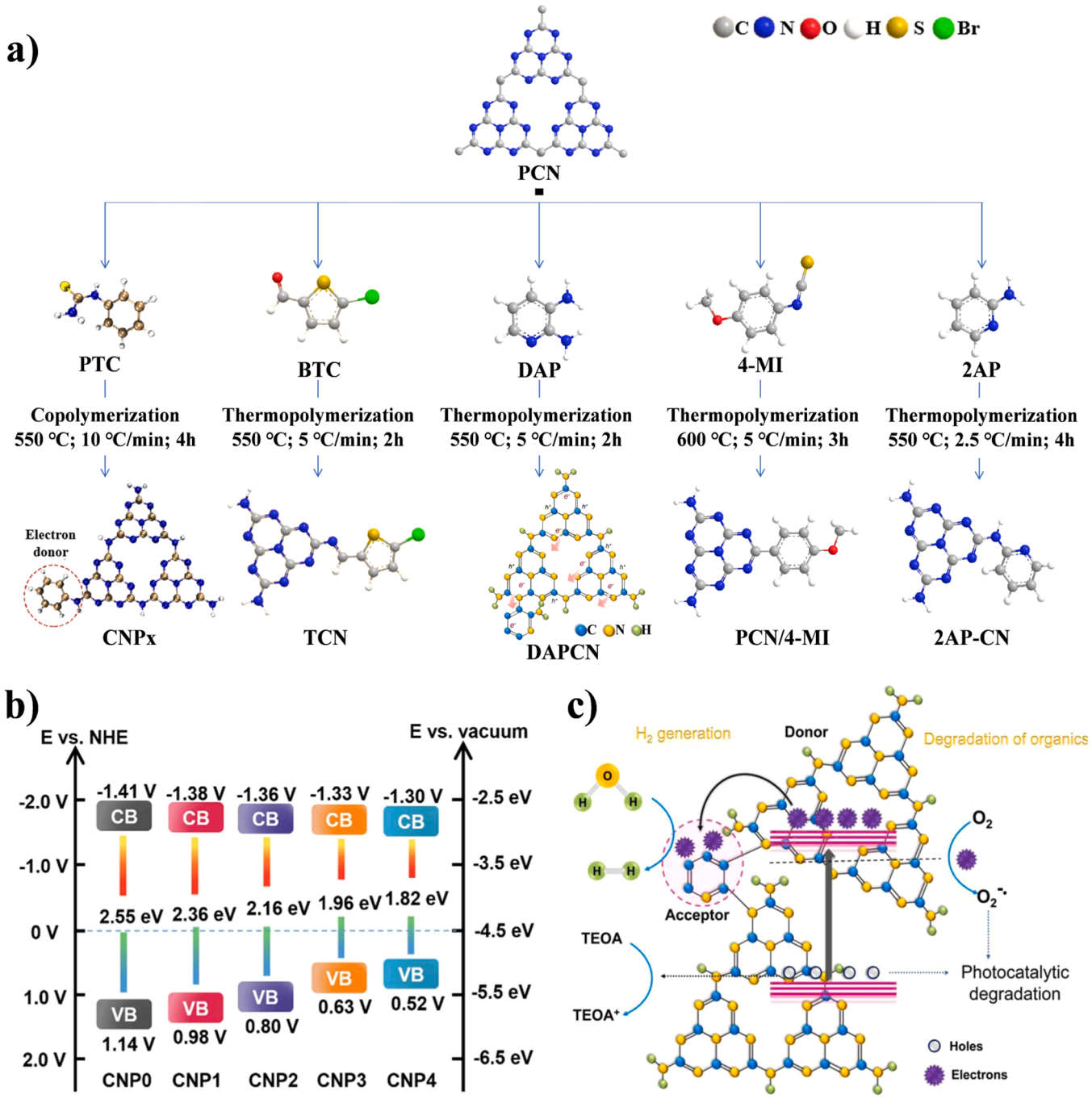

Fig. 5. (a) The typical scheme of single molecule modification of PCN. (b) Energy bandgap structure of CNP_x (x=0–4) [102]. (c) The molecular structure of DAPCN and its process for utilizing light energy to produce hydrogen and break down pollutants [101].

benzene ring, anthraquinone, and 9-fluorenone are covalently tethered to the main chain molecule N-methyl carbazole respectively, thereby enabling precise control over the dipole moment. Among them, the inclusion of 9-fluorenone (CbzCMP-9) induces a significant alteration in the dipole moment, surpassing that of the other two variants (CbzCMP-7,8) by approximately three orders of magnitude (Fig. 6b). So, the optimized CbzCMP-9 has an extremely strong built-in electric field generated by its elevated molecular dipole moment, resulting in a robust driving force for charges. Consequently, it demonstrates exceptional photocatalytic efficacy towards thiocyano chromones and C-3 thiocyanation of indoles (achieving up to 95% and 98% yields, respectively) when compared to alternative photocatalysts. Similarly, the Hirshfeld charge distribution of COF-TD1 and COF-TD2, two covalent organic frameworks obtained through molecular modification (Fig. 6c), reveals a pronounced D-A structural feature, with the thiadiazole center serving as the electron donor unit and the quinone structures acting as the acceptor unit [109]. Subsequent studies revealed that not only modifying the type of D or A unit alters the electronegativity difference, but also enables an increase in electronegativity by substituting the functional group on A unit with a highly electron-absorbing group, such as halogen, hydroxyl, carboxyl, and aldehyde groups [63,130]. For instance, Yu *et al.* [66] have incorporated fluorine, a highly electronegative halogen group, into A unit as a strong electron-withdrawing moiety. By strategically selecting the substitution position and appropriate amount of fluorine, they have successfully synthesized the D-A polymer P1F-T. Notably, P1F-T exhibits a dipole moment (1.788 D) that

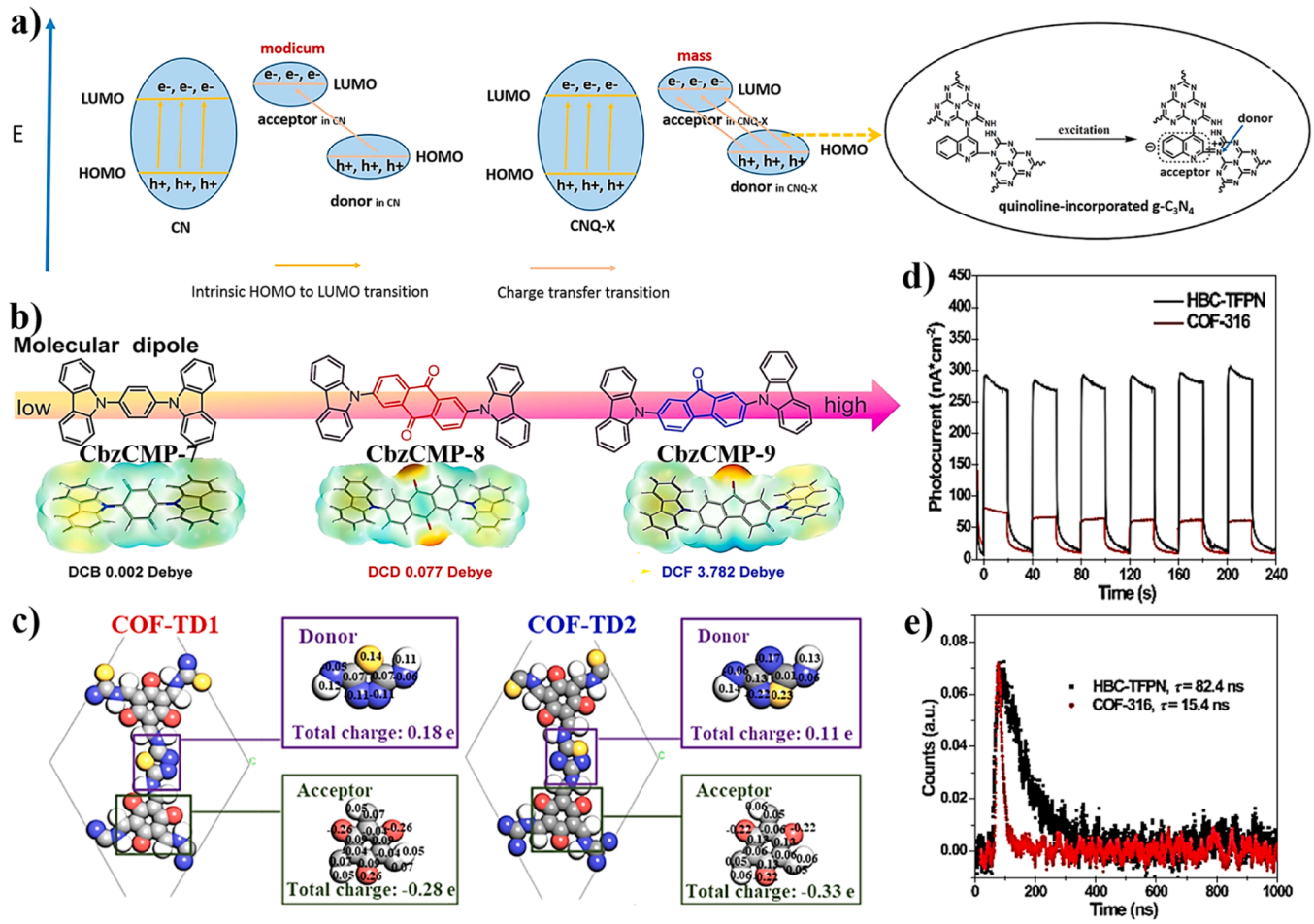

Fig. 6. (a) Schematic diagram of the electron excitation and transition modes in CN and CNQ-X [128]. (b) ESP diagrams and molecular dipoles (unit of dipole moment: Debye) of CbzCMP-n (n = 7–9) [88]. (c) Analysis of the Hirshfeld charge distribution in COF-TD1 and COF-TD2 [109]. Where gray, white, red, blue, and yellow spheres represent C, H, O, N, and S atoms, respectively. (d) Transient photocurrent responses and (e) decay profiles of transient absorption (in acetone suspension, under Ar atmosphere) of HBC-TFPN and COF-316 [74].

is 2.60 and 2.82 times higher than those of polymers P2F-T and P4F-T, respectively.

Apart from the aforementioned molecular dipole, which exerts a significant influence on ICT, the well-ordered molecular arrangement within the 2D COFs layer plays a crucial role in facilitating efficient utilization of photogenerated carriers [139]. Yu *et al.* [74] has reported the synthesis of a wave-like 2D lattice of dioxin-linked COF (HBC-TFPN), utilizing 2,3,10,11,18,19-hexahydroxy-cata-hexabenzo-coronene (HBC) as the electron donor unit and Tetrafluorophthalonitrile (TFPN) as the electron acceptor unit. In this structure, hexabenzocoronene serves as a torsional unit, while the concave-convex complementarity between HBC-TFPN layers effectively mitigates stacking misalignment. This promotes the alignment of HBC and TFPN units into bicontinuous π-pillars, extending the donor-acceptor π-pillar array to enhance carrier transport. The photocurrent response and transient absorption decay curves of HBC-TFPN (Fig. 6d-e), respectively. It could be seen that photocurrent response intensity of HBC-TFPN with 2D wave structure far exceeds that of COFs-316 and has a longer exciton lifetime. The above findings further underscore the unparalleled efficacy of molecular modification in enhancing the charge properties of photocatalysts.

2.1.3. Photocatalyst properties modification

Numerous studies have shown that polymeric materials obtained after monomolecular modification will show variations, and selecting an appropriate combination of molecular modules is crucial for the modification of OPs photocatalysts' properties. As previously mentioned, the appropriate combination of molecular modules could generate a more robust internal electric field, and the physical properties of the OPs photocatalyst could also be tailored to individual preferences for selecting the optimal combination and customizing the polymer's functionality. Particularly when considering customized OPs' physical properties, these alterations could be perceived in a more intuitive manner. Such as color change of the material [113,140], specific surface area change [130,141], increase pore size [100], thinner and smaller nanosheets [23,41], and loosening of texture [74,127]. Specifically, the surface topography of initial CN exhibits a lower degree of sparsity compared to the obtained. But, when the original CN backbone is functionalized with pyridine rings at its edges, the texture of 2AP-CN would become looser [89]. Further, AQTEE-COP (Fig. 7a) is synthesized through the Sonogashira cross-coupling reaction between 2, 6-dibromoanthraquinone (AQ) and 1,1,2,2-tetrakis(4-ethynylphenyl) ethene to incorporate an anthraquinone redox center [97]. Based on the report, NATEE-COP (Fig. 7b) exhibits lower water dispersibility compared to AQTEE-COP. Which is prepared by 2,6-dibromonaphthalene (NA) instead of AQ with 1,1,2,2-tetrakis(4-ethynylphenyl)ethene under the same conditions. The integration of hydrophilic carbonyl groups in AQTEE augments the intensification of interfacial interactions between substrate molecules and active catalytic sites during multiphase catalytic reactions in aqueous environments, thereby facilitating an elevation in efficiency. And the molecularly modified AQTEE-COP exhibits a significantly increased specific surface area (396 m^2 g^{-1}) and excellent porosity. Tris(4-formylphenyl)amine (TFPA) and tris

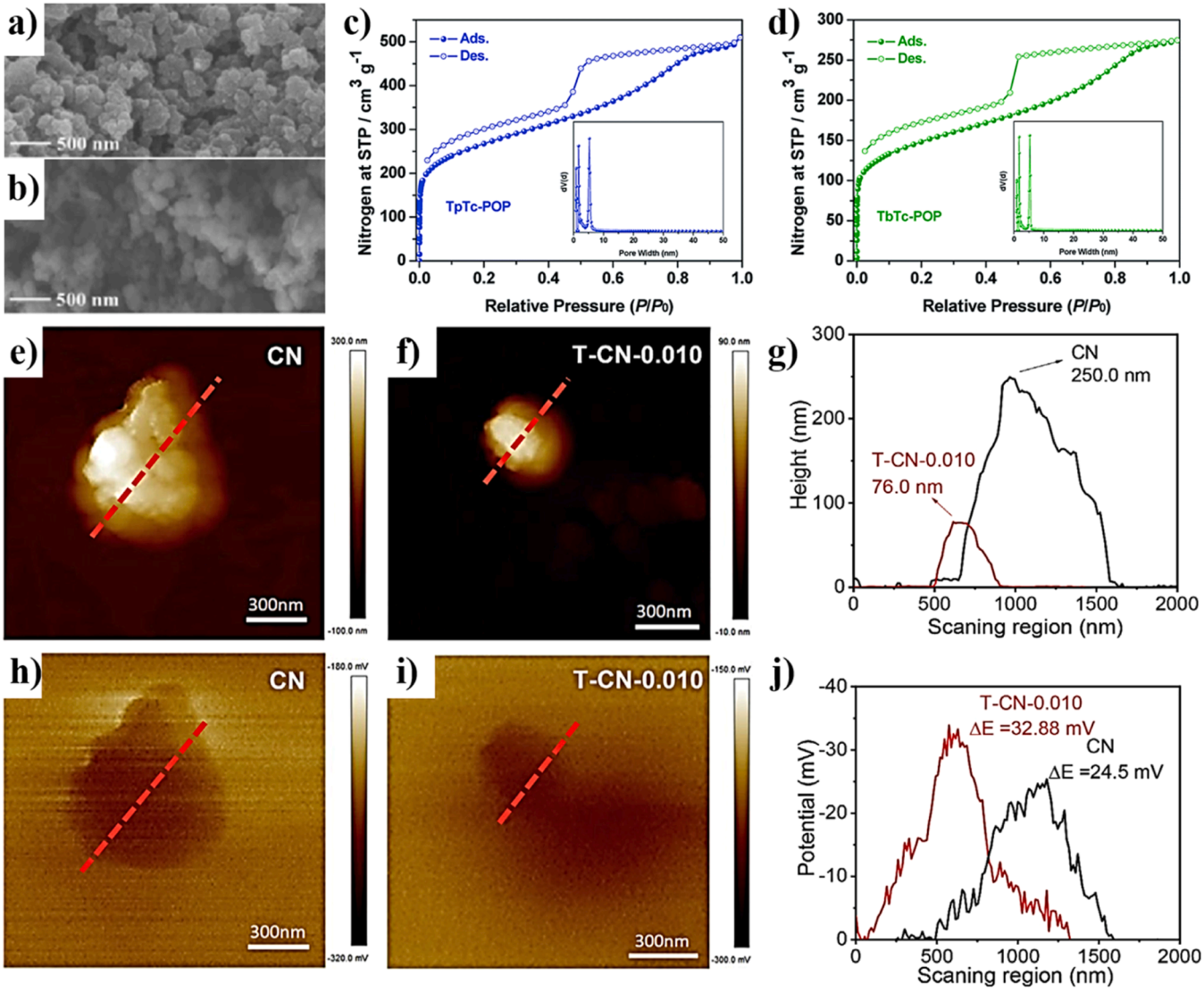

Fig. 7. SEM images of (a) AQTEE-COP and (b) NATEE-COP [97]. The N_2 adsorption, desorption isotherms, and pore size distributions images of (c) TpTc-POP and (d) TbTc-POP [25]. (e, f) The surface morphology and (h, i) surface potential of CN and T-CN-0.010 [95]. (g) The thickness curves in (e) and (f). (j) The image of surface potential liner scanning in (h) and (i).

[1-(10-formyl-4,40-biphenyl)]amine (TFBA) are molecular units derived from the same compound, triphenylamine (TPA). However, they exhibit differences in their electron-rich properties. To investigate the impact of these two units as electron donors on the porous structure of the polymer. Consequently, they undergo polymerization with electron-deficient tricyanomesititene (TCM) molecular units, leading to the synthesis of D-A porous organic polymers (POPs), namely TpTc-POP and TbTc-POP, exhibiting intramolecular electron push and pull electric fields respectively [25]. The porosity difference between the two materials has been investigated using nitrogen adsorption and analytical experiments to determine if it is attributed to variations in the electron donor unit. Notably, TpTc-POP exhibits a higher BET surface area (966 $m^2\ g^{-1}$) compared to TbTc-POP (538 $m^2\ g^{-1}$). Nevertheless, both materials displayed prominent microporous and mesoporous structures (Fig. 7c-d). The surface structure of the aforementioned polymers undergoes the transition from smooth to rough and from compact to loose, resulting in an increased porosity that provides abundant surface reactive sites for the photocatalytic reaction. This augmentation of catalytic active sites facilitates the attachment of the reactants to photocatalyst, enabling multiple simultaneous redox reactions. And it also enhances the utilization of photogenerated carriers under the influence of intramolecular push and pull electric field.

Except modification of the surface properties, the surface potential is also modified due to the D-A structure. For example, Zheng *et al.* [95] have successfully synthesized novel CPs featuring a D-A structure by employing thermal copolymerization, wherein triptycene is incorporated into carbon nitride to prepare T-CN. The atomic force microscope with Antifrictional Metel (AFM) and Kelvin probe (KPFM) are utilized to examine the morphology and surface potentials of CN and T-CN-0.010. Analysis of the AFM images and corresponding height profiles clearly indicates that, because of molecular modification treatment, T-CN-0.010 exhibits a significantly reduced average thickness compared to CN (Fig. 7e-g). Moreover, the surface dot position of T-CN-0.010 has also changed beyond CN (Fig. 7h-j). As for the above mentioned, the surface potential of the modified photocatalytic materials exhibited a pronounced enhancement, indicating an accelerated separation of intermolecular holes and electrons under light conditions, as well as an increased accumulation of photogenerated charge from within the catalyst to its surface. Most studies concur that the presence of a stronger driving force in modified molecules is attributed to the build-in electric field, which serves as a pivotal factor underlying this phenomenon. It is widely acknowledged that the establishment of intramolecular electron

D-A structure represents the most direct and efficacious approach for generating a build-in electric field. The electronegativity difference between the D and A is utilized to establish an electron push-pull field, thereby effectively enhancing the mutual conductivity of the modified OPs. By facilitating the migration of photogenerated charges towards the surface for participation in reactions, this phenomenon leads to an increased photocatalytic activity within the photocatalyst itself, consequently resulting in a notable improvement in the rate of photoreactions.

2.2. Multimolecular modification

The modification of D-A OPs by a single-type molecule building block always presents a bottleneck in terms of electric field intensity and photocatalytic efficiency, imposing inevitable limitations on the function of OPs [142,143]. To overcome these challenges, researchers have proposed leveraging the synergistic effect among multiple molecules to collectively modify the main molecular unit. Based on previous studies, various types of multimolecular modification methods have been comprehensively reviewed [144,145] (Table 2). The concept of multimolecular modification could be categorized into two dimensions: multi-form and multi-number. The "multi-form" refers to the collaboration of two or more distinct molecular modules to collectively modify a shared molecular unit. On the other hand, the "multi-number" denotes increasing the number of D or A module building block based on the original D-A molecular combination unit. The objectives of the multimolecular modification types both are to augment the active site adhesion for photoreaction, while concurrently enhancing the internal electric field within the polymer, thereby elevating photocatalytic efficiency.

According to the function of molecular building blocks in the polymer molecular unit (D or A), the "multi-form" could be roughly divided into four types: A-D_1-D_2, D_1-A-D_2, A_1-D-A_2, and D-A_1-A_2. Among them, compared to several other types, the utilization of the D_1-A-D_2 type OPs as a photocatalyst is less prevalent, which may be attributed to the limitations of current relevant research. However, the D_1-A-D_2 type has gained widespread usage in the field of electrochemistry for enhancing charge transfer between molecules, thus demonstrating its feasibility [146–148]. This aspect also holds potential as a breakthrough focus for comprehensive interdisciplinary research in the future. The A-D_1-D_2, A_1-D-A_2, and D-A_1-A_2 types are widely applied in the field of photocatalysis. For example, Tang *et al.* [75] have used two organic molecules, pyromellitic diimide (PDI) and 3-amino-1,2,4-triazole (TA), to simultaneously modify PCN through multi-step thermal polymerization (Fig. 8a). According the DFT image of TA-CN-PDI, it could be confirmed as A-D_1-D_2 type. The CN and TA as the D unit, respectively; and the PDI as the A unit. This approach has the potential to enhance both the number and quality of photoexcited electrons. Furthermore, to overcome the inherent insolubility of conventional OPs in water, Zhuang *et al.* [91] have constructed a metal-free A_1-D-A_2 type catalyst, named Py-SO_n (Fig. 8b). The main modified molecular unit in this study is Py, with different proportions of dibenzothiophene-S, S-dioxide (FSO) and 2,1,3-benzothiadiazole (BT) building blocks grafted on both sides of the Py. FSO and BT collectively facilitate the absorption of photogenerated charge transmitted from the Py. Besides the above combinations, Liang *et al.* [65] have chosen different two molecular building blocks to modify the electron-rich benzene. Thereinto, benzene is seen as the D unit, dibenzothiophene-S, S-dioxide (SO) as the A_1 and benzothiadiazole (TH) as the A_2. The optimal photocatalytic performance of D-A_1-A_2 type PBSOTH (Fig. 8c) can be achieved by adjusting the ratio between its components, thereby offering a novel approach for efficiently reducing high-valence uranium. It has been clearly pointed out that the benzene exists in the system of D-A_1-A_2 type PBSOTH as D unit. However, it also has been considered as the existence of π-linker in some studies. At present, it is imperative to discern the role of the benzene ring in various OPs systems based on its primary function, particularly in determining

Table 2
Summary of recent reports on multimolecular modification.

$Donor_1$	$Donor_2$	$Acceptor_1$	$Acceptor_2$	Designation	Synthesis method	Bandgap [eV]	BET surface area [$m^2 g^{-1}$]	
Pyrene	——	2,1,3-benzothiadiazole	Dibenzothiophene sulfone	Py-SO_1	Suzuki condensation reaction	2.33	147.36	[91]
pyromellitic diimide	——	Polymeric carbon nitride	3-amino-1, 2, 4-triazole	TA-CN-PDI	Multi-step thermal condensation reaction	1.30	70.07	[75]
1,3,5-triphenylbenzene	Chromenoquinoline ring	Terephthalaldehyde	——	COF 4 P	Povarov reaction	1.25	655.40	[94]
Pyrene	——	4,7-dibromobenzothiadiazole	4,7-dibromobenzothiadiazole	P-PyBT	Trimerization reaction	2.07	13	[129]
Pyrene	Benzene ring	Dibenzothiophene sulfone	——	PyBT-2	Pd(0)-catalyzed Suzuki-Miyaura coupling reaction	2.21	865	[149]
Benzene ring	——	Dibenzothiophene-S, S-dioxide	Benzothiadiazole	PBSOTH-3	Statistical copolymerization	2.21	215.3	[65]

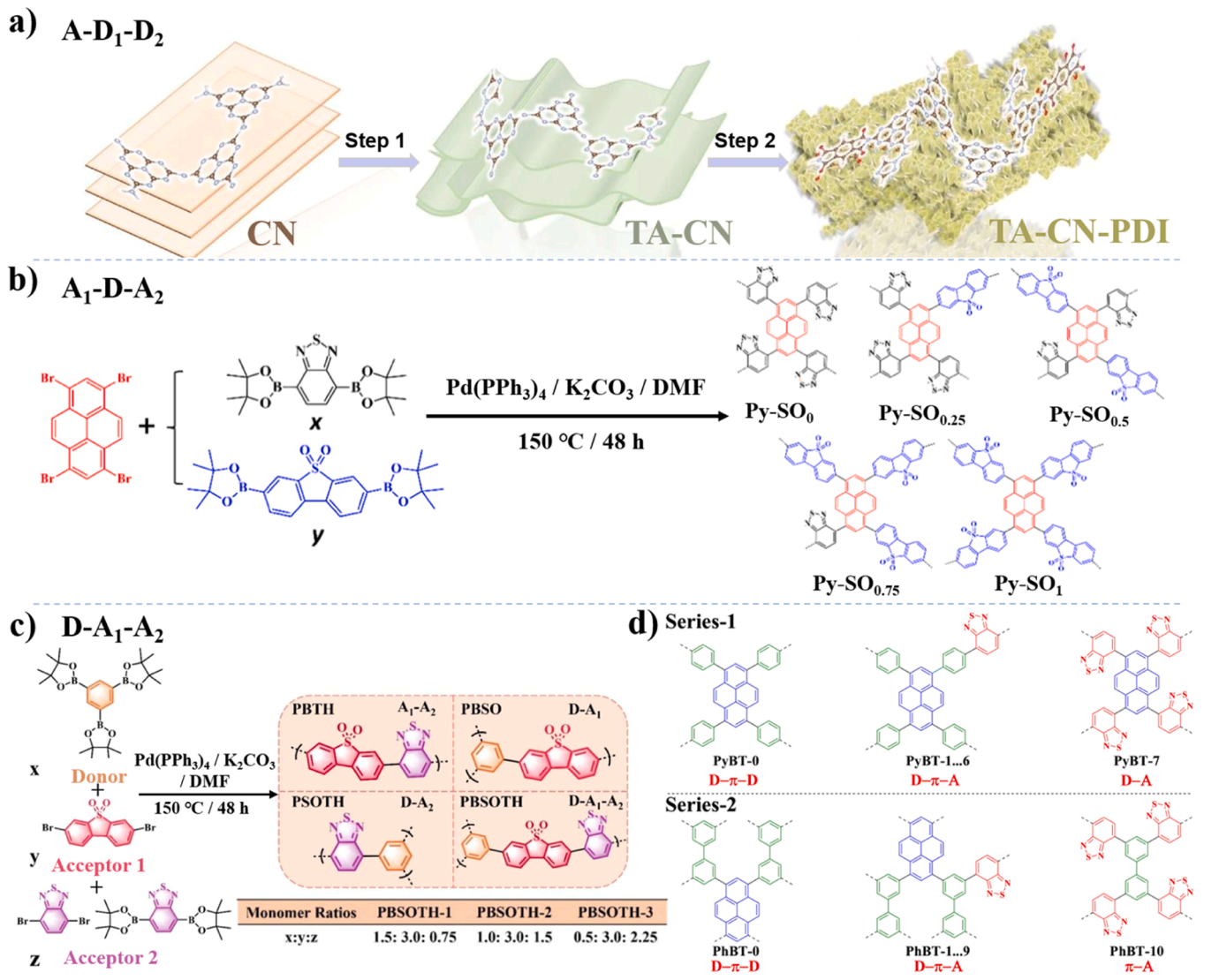

Fig. 8. The molecular images of different types after multimolecular modification. (a) The synthetic process of TA-CN-PDI [75]; (b) Py-SO_n [91]; (c) PBSOTH-n [65]. (d) The molecular structure of PyBT-0–7 and PhBT-0–10 [149].

whether the benzene ring exists catalytic sites that actively participates in the reaction [59,149]. For instance, the benzene (or biphenyl) within the molecular unit of PyBT (or PhBT), as demonstrated by Xu *et al.* [149], serve as the π-linker rather than D or A unit (Fig. 8d). Similarly, the benzene (or thiophene) functions as a π-linker in the molecular unit of the JNU-210 (or JNU-211), while the triazine ring is incorporated as an additional building block, forming a new A_2 unit in JNU-210 (or JNU-211) unlike PyBT [92]. Consequently, despite there are π linkers in JNU-210 (or JNU-211), it still belongs to the A_1-D-A_2 type OPs.

According to the increased number of D or A unit, the "multi-number" could be roughly classified into two types: A-D_1-D_1+ and D-A_1-A_1+ (Fig. 9). In Wang's study [150], the polymer DBTD-CMP1 exists the behavior of a single benzene as electron-donor, and they have compared the impact of photocatalytic effect by increasing the number of benzene ring in D unit. Thus, the A-D_1-D_1+ type DBTD-CMP3 with multiple identical D unit is obtained (Fig. 9a). Under the same way, based on the existing D-A type PDBTSO-T, Liu *et al.* [151] increased the number of thiophene D unit while maintaining the unchanged dibenzothiophene-S, S-dioxide as A unit (Fig. 9b). Consequently, they successfully synthesized the A-D_1-D_1+ type polymer PDBTSO-2 T. In addition to the increasing the molecule number of D unit based on the original D-A OPs structure, other studies will also investigate methods for achieving ultra-high photocatalytic performance by increasing the molecule number of A unit. Recently, Li *et al.* [152] have introduced 1,3,4-oxadiazole units with electron-attracting property into the 1,3,5-triazine-based π-conjugated framework. By increasing the number of 1,3,4-oxadiazole units, the bi-1,3,4-oxadiazole-linked D-A_1-A_1+ type TCP-BOXD (Fig. 9c) has been achieved. And, Xie *et al.* [153] have employed an increased number of dibenzothiophene-S, S-dioxide units as A and a constant number of dibenzo[*g*, *p*]chrysene units as D to construct D-A_1-A_1+ type DBC-BTDO (Fig. 9d). Similarly, the oligomeric dibenzothiophene-S, S-dioxide is also utilized as the A segment in the D-A_1-A_1+ type P (BDT-DBTSO) researched by Li *et al.* [108].

2.2.1. *Energy band adjustment*

As mentioned in previous section, using molecular modification could effectively change the optical properties of the material, including fluorescence intensity and absorption spectral range. The same changes could also occur when the original material is modified with multiple molecules [152,154].

The addition of reactive groups or molecular building blocks to the existing structure to increase the π-conjugation network in OPs as a feasible strategy to improve the photocatalytic activity of OPs [72]. Compared to PDBTSO-T with a single electron donor, the introduction of

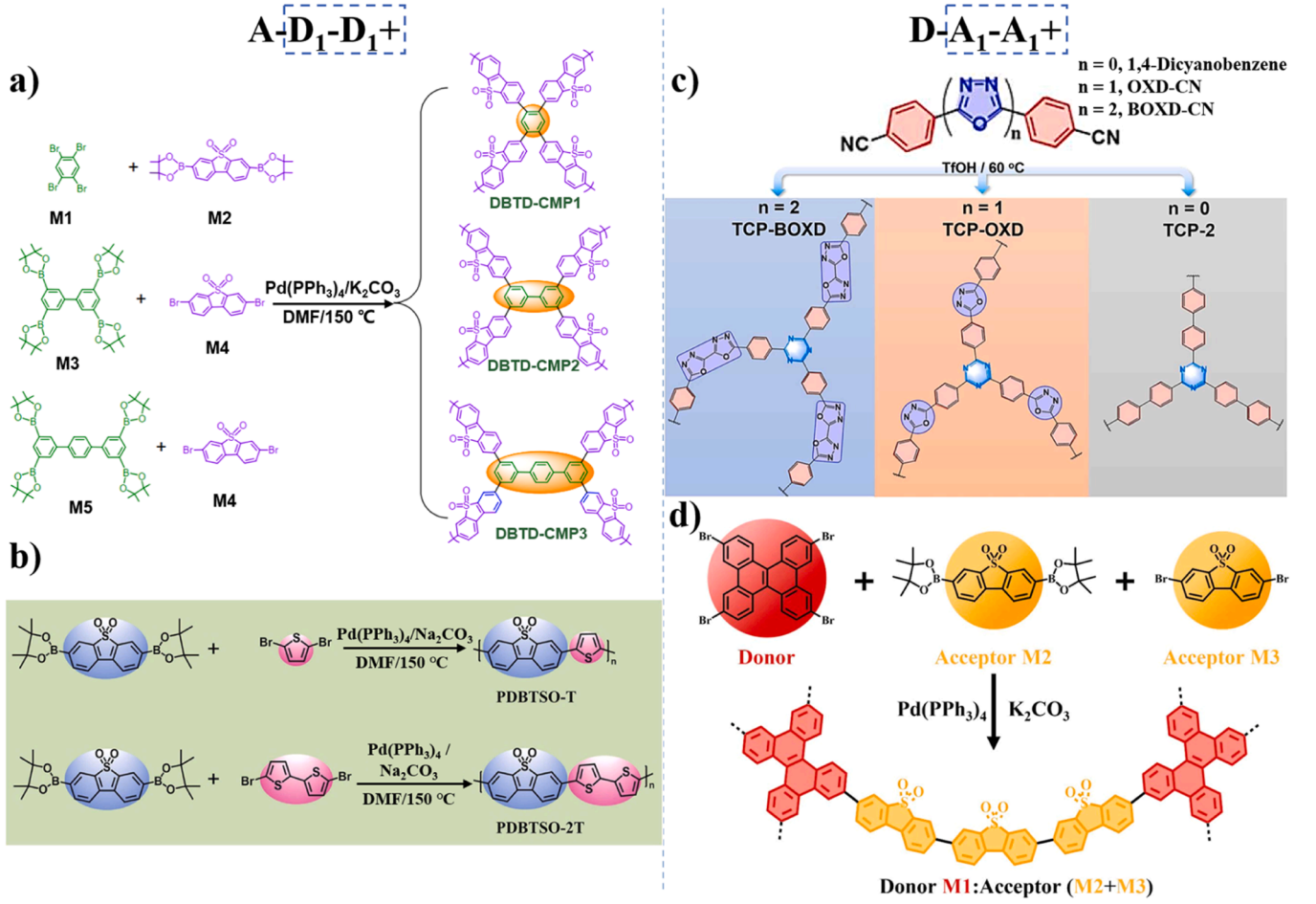

Fig. 9. The synthesis process of A-D_1-D_1+ type: (a) DBTD-CMPn and the representative structures [150]; (b) PDBTSO-T and PDBTSO-2 T [151]. The synthesis process of D-A_1-A_1+ type: (c) TCP-2, TCP-OXD and TCP-BOXD [152]; (d) DBC-BTDO-n [153].

a double electron donor in PDBTSO-2 T results in a narrower band gap (Fig. 10a), thereby enhancing the likelihood of photoreaction hydrogen production [151]. Additionally, a noticeable enhanced electrical signal of in the PDBTSO-2 T molecular skeleton during the photocatalytic hydrogen production process is observed (Fig. 10b). It could shift the maximum absorption peak toward the infrared absorption spectrum region and broaden the absorption peak (Fig. 10c), and the average particle size of polymer Pdots particle becomes smaller (Fig. 10d), which could capture more photons under visible light irradiation and improve solar energy utilization [155]. On the other hand, the addition of strong electron-absorbing molecular building blocks such as thiophene groups [155]; benzene ring [92]; dibenzothiophene groups [150]; benzothiadiazole groups [108]; 1,3,4-oxadiazole groups [152]; and halogen to the π-conjugated backbone of the polymer could lower the polymer LUMO energy level and shorten the band gap [92]. That is why the added electron-absorbing group will have strong attraction to the electrons in the π-principal chain. In addition, increasing the number and type of π-units in the polymer is another effective way to modify the electronic structure and electrochemical properties of organic semiconductors to further improve the intramolecular carrier separation (Fig. 10e).

2.2.2. ICT enhancement

According to the basic electrochemical principles of the D-A structure, it is known that the addition of multiple new molecular building blocks in the original organic polymer, so that they form a conjugated polymer with the D-A structure, which changes the electrochemical properties of the modified polymer itself in several ways. Firstly, altering the uniform charge distribution within the polymer. The charge distribution density of CN modified by PDI and TA showed an obvious non-uniformity (Fig. 11a-b). This also illustrates that PDI as a typical electron-absorbing group breaks the dynamic equilibrium of the charge inside the original CN, and its stronger electron-absorbing ability leads to more electrons migrating to it, which is more favorable to n→π* electron leap (Fig. 11c-d). Not only that, electron spatial configuration in HOMO and LUMO of TACP could reduce carrier recombination [75]. Secondly, enhancing the charge separation within the polymer. The synthesis of TPC-BOXD with bi-1,3,4-oxadiazole linkage, which has a significant increase in carrier lifetime compared to TCP-2, which consists of only triazine groups, and its carrier kinetic model (Fig. 11e) also indicates that it has an enhanced electron-hole separation ability at 350 nm [152]. In addition to this, increasing the number of benzene ring linkages in OPs [149,150,156] or other molecular groups containing multiple π bonds form π-π stacks in polymers as a way to improve the fast carrier separation transfer [104]. Finally, facilitating charge transfer efficiency within polymers. The covalent organic backbone NPT/C-CN was obtained by grafting pyridine conjugate ring at the edge of the CN backbone by a one-step thermal polymerization method while replacing the N atom used as a bridge therein with a C atom. It is not hard to find that the photocurrent density on NPT/C-CN is obviously elevated compared to NPT-CN and CN (Fig. 11f-h), and it shows the lowest charge transfer resistance and the highest charge kinetic, which reinforces the fact that the speed of photogenerated carrier transfer and the separation efficiency of NPT/C-CN are obviously accelerated after the modification [157]. The incorporation of another electron A unit could significantly modulate the charge density distribution within the polymer chain (Fig. 11i) [55,145]. Concurrently, as the number of electron D or A unit

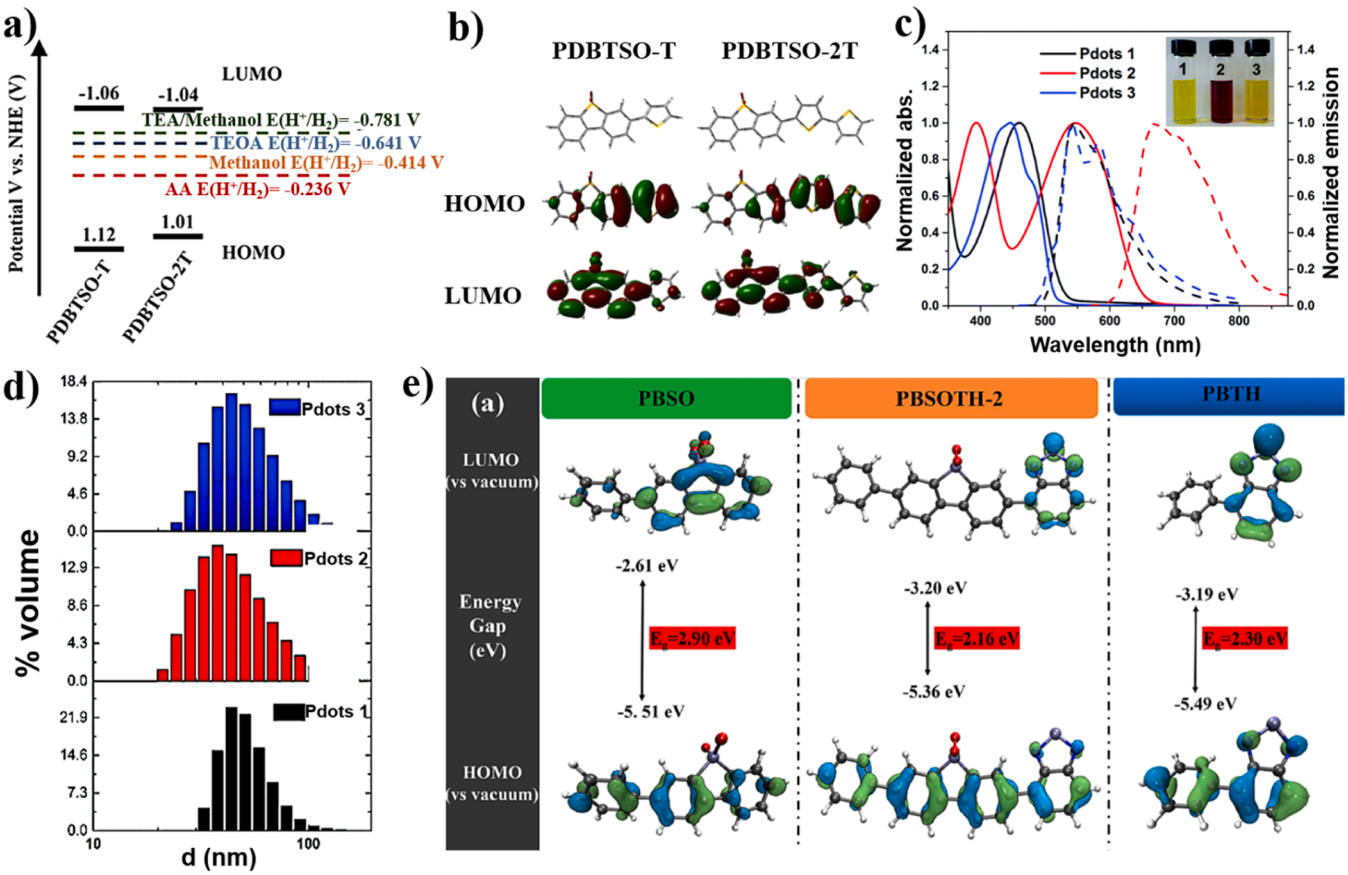

Fig. 10. (a) The energy and (b) molecular structural diagrams of PDBTSO-T and PDBTSO-2 T [151]. (c) The absorption and emission spectra (in an aqueous environment) and (d) the hydrodynamic diameter distribution diagram of Pdots (1, 2 and 3) [155]. (e) The HOMO and LUMO orbital distributions and energy band of PBSO, PBSOTH-2, and PBTH [65].

increases, the degree of charge separation between h^+ and e^- becomes more pronounced (Fig. 11j), leading to an enhanced number of catalytic sites involved in the reaction and improved utilization efficiency [108, 153].

From a comprehensive perspective, it is evident that the simultaneous modification of the OPs by multiple molecular building blocks could readily induce internal multi-component functionalization synergy. This not only optimizes its primary electrochemical properties, such as charge separation ability and migration efficiency, inhibition of carrier complexation, and reduction of internal resistance but also further enhances the other properties of OPs through leveraging the unique characteristics of different substances. For instance, introducing hydrophilic groups or altering the material surface roughness and porosity effectively improves its photocatalytic performance for efficient applications.

2.2.3. *Photocatalyst properties modification*

The surface topographical features of the modified OPs formed after multiple molecular modification also change significantly compared to the original ones. For example, with the increased number of electron A unit, the D-A-A+ type P(BDT-DBTSO$_n$) as photocatalyst has made different colors (Fig. 12a). Moreover, it is also common to utilize multimolecular modifications as an effective means to change the shape of the material. These include B-BO-1,3,5, B-BO-1,2,4, and B-BO-1,2,4,5, respectively, which have been obtained by Wang *et al.* via altering the sites and quantity of benzofurans attached on the benzene ring. The morphological of the samples underwent substantial transformations, evolving from a fibrous B-BO-1,3,5 structure with a diameter of less than 100 nm to a porous sheet-like B-BO-1,2,4 configuration. Subsequent modifications resulted in the formation of B-BO-1,2,4,5, characterized by numerous granular structures fused onto its surface (Fig. 12b) [80]. Furthermore, the D-A_1-A_2 type FS-OHOMe-COF exhibits an excellent BET surface area, 943 m^2 g^{-1} (Fig. 12c), and the pore size of FS-OHOMe-COF (2.6 nm) is evidently smaller compared to that of the other two D-A OPs (Fig. 12d). The interlayer force of the polymer, modified by multi-acceptor molecules, is significantly enhanced (Fig. 12e), thereby achieving heightened stability and enabling a substantial hydrogen peroxide production capacity in the light reaction [144].

2.3. *Molecular substitution*

In addition to monomolecular modification and multimolecular modification, another type of molecular in-situ substitution is employed to investigate the internal structural alteration of the original main material. The molecular substitution of D-A in this paper encompasses molecular ring substitution as well as other forms of molecular substitutions. The general molecular substitution reaction is facile to execute, and the newly obtained photocatalytic materials find extensive applications across diverse domains (Table 3).

The type of modification called molecular substitution are roughly mentioned (Fig. 13), where the C_4N_2 ring in the TAP is utilized to replace the constituent unit of the original CN, named MA, to form TAP-CN with N defect [158] (Fig. 13a); a new photocatalytic organic polymer, TBPA-COF, is formed by introducing acetylene into the olefin-linked TBP-COF in place of the original single chain [52] (Fig. 13b); substitution of the electron donor 1,3,5-triethynylbenzene (TEB) with 1,3-diethynylbenzene (MEB) in the framework of the original D-A CMP yielded a TEB-DBT CMP with partial alkyne defects [159] (Fig. 13c); non-conjugated segments with hydrophilic property are inserted into

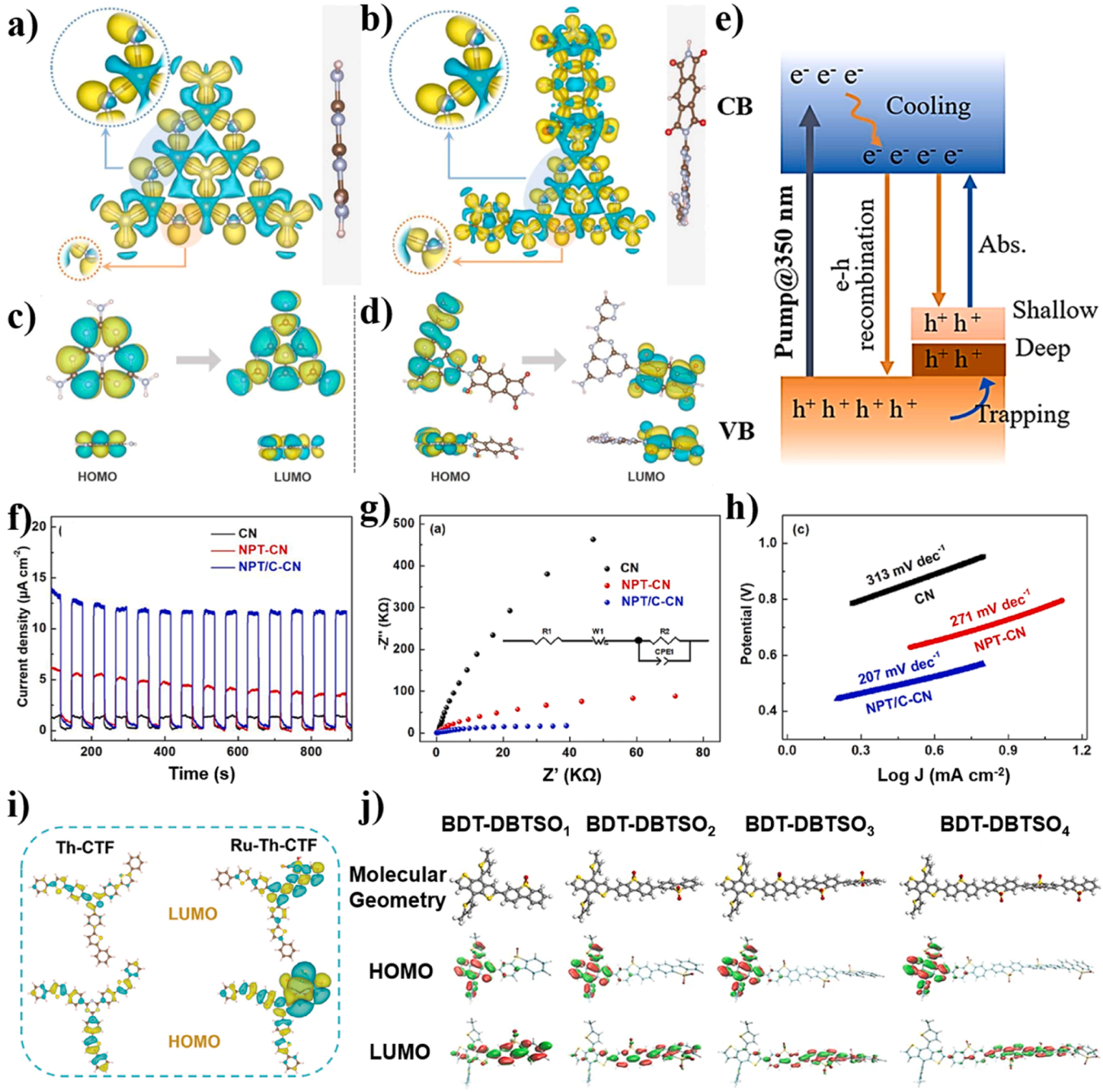

Fig. 11. The 3D schematic depicting charge density and the HOMO/LUMO electronic structure of (a, c) CN and (b, d) TACP [75]. (The yellow and blue regions, respectively, denote electron enrichment and electron depletion zones) (e) The charge carrier dynamics models of TCP-BOXD [152]. (f) Transient photocurrent curves; (g) EIS Nyquist diagrams; (h) Tafel plots of CN, NPT-CN, NPT/C-CN [157]. The molecular structure and charge distribution of (i) Th-CTF and Ru-Th-CTF [145], (j) BDT-DBTSO$_n$ [108].

the primary sequence of the conjugated polymer to change the basic properties of the otherwise conjugated polymer [160] (Fig. 13d).

2.3.1. *Molecular ring substitution*

Generally, PCN with π-conjugated electronic features as a kind of metal-free organic photocatalysts has been broadly used in the photocatalysis field. However, the pristine PCN still suffers from several intrinsic problems, such as the small absorption spectral range, fast charge recombination, low surface void fraction and poor photogenerated carrier transport efficiency [116,158]. The aforementioned factors have considerably hindered the progress of PCN in photocatalysis research. Therefore, breaking the covalent equilibrium of PCN on itself and modulating its π-electronic structure are normally regarded as effective ways to contribute to improving the photocatalytic performance [168,169]. To accomplish these objectives, in addition to the previously mentioned monomolecular/multimolecular modification methods of grafting molecule units into the heptazine ring of PCN via covalent bonding, there is another method named molecular ring substitution [164,169]. When the triazine/heptazine ring in original PCN have been in-situ substituted by other small molecular ring units, the process could be called molecular ring substitution [22,163]. The process is typically accomplished through a one-pot thermal polycondensation procedure. Based on the available reports, this is a methodology for constructing electronic D-A structure within the

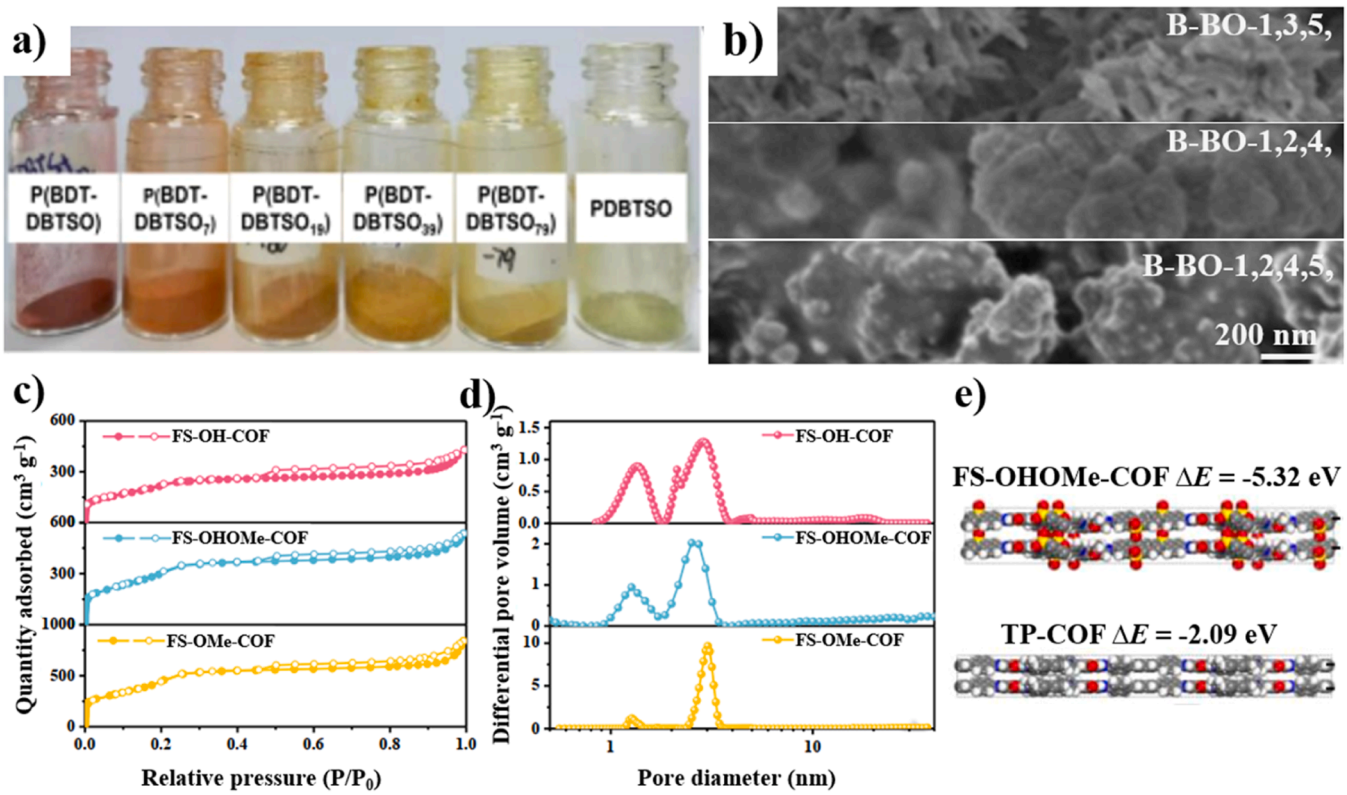

Fig. 12. Schematic diagram of (a) color changes [108] and (b) material morphology [80] after multimolecular modification. (c) The nitrogen adsorption/desorption isotherms and (d) pore size distribution curves of FS-OHOMe-COF. (e) The disparity about layer interaction energy between TP-COF and FS-OHOMe-COF [144].

Table 3
Summary of recent reports on molecular substitution.

Donor	Acceptor	Designation	Substitution type	Synthesis method	Bandgap [eV]	BET surface area [$m^2 g^{-1}$]	Application	
C═O substituted heptazine ring	C═C bond substituted heptazine ring	$OCCN_x$	Functional groups substitution	Nucleophilic substitution/Addition reactions	2.03	18.26	CO_2 reduction	[161]
-OH	g-C_3N_4	CN-OH	Functional groups substitution	Thermal copolymerization	1.76	——	Activating PMS	[162]
Pyrimidine	g-C_3N_4	TKCN	Molecular ring substitution	Copolymerization reaction	1.86	34.2	H_2 production	[163]
Maleic hydrazide	g-C_3N_4	CN-MH	Molecular ring substitution	Thermal polycondensation	2.12	287.37	H_2 production	[164]
Anthrazoline	-NH_2/-CHO	Anthrazoline (1a-1d)	Functional groups substitution	——	——	——	Amination and amidation reaction	[165]
Truxene	ITIC	CP-3	Molecular substitution	Suzuki coupling reaction	1.12	——	H_2O_2 production	[166]
ABPA	CN	CN_{25}	Molecular substitution	Thermal copolymerization	2.68	99	H_2 production	[167]

molecular units of PCN. The differentiation for molecular ring substitution primarily revolves around two key aspects [170]: (1) Small molecular ring in-situ substitution, and (2) manifestation of typical electronic D-A structural characteristics within the molecular ring unit rather than between them. Compared to previous element-substituting doping methods, the molecular ring substituted PCN is typically represented by the in-situ substituted molecular ring as the electron donor/acceptor unit, rather than an individual atom. Furthermore, molecular ring substitution compensates for the fact that the element doping content must be tightly controlled to be optimized, and it greatly exceeds its current capabilities in terms of altering the catalyst crystal structure and lowering the electron transfer barriers [138,169].

The common types of triazine ring-substituted molecules are shown in Fig. 14. Since 2015, Chen *et al.* [170] have obtained CN-DPY with a π-rich aromatic system via thermal copolymerization (550 °C/4 h) of dicyandiamide (DCDA) with 2,6-diaminopyridine (DPY) to substitute the triazine ring in the CN network by doping the pyridine ring with π-deficiencies (Fig. 14a). Following this thought, large number of similar ways to modify pristine CN have subsequently emerged. On the one hand, Ho *et al.* [158] also have substituted the pyrimidine ring for the triazine ring in 2,4,6-triaminopyrimidine (TAP) by thermal copolymerization to form TAP-CN with N-defects; on the other hand, Yan *et al.* [169] have used 2,4,6-trichlorophenol as a precursor and used benzene ring doping to substitute for the triazine ring, obtaining CN-T with an all-carbon aromatic ring structure (Fig. 14b). As the incorporation of TAP could lead to qualitative changes in the internal charge properties of CN. Heymann *et al.* [171] in 2018 have likewise utilized the TAP molecular ring to substitute the triazine ring units in poly(triazine

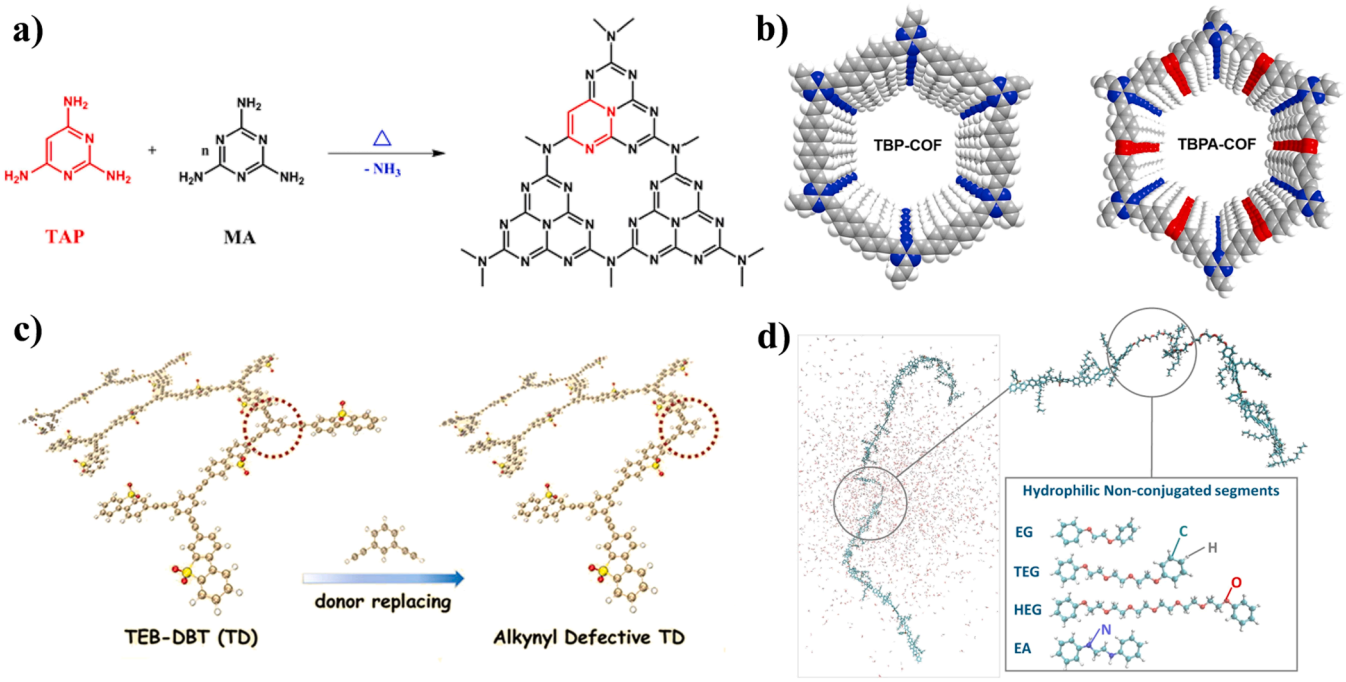

Fig. 13. (a) Incorporation of TAP into the g-C_3N_4 network [140]. (b) Schematic representation of TBP-COF and TBPA-COF [52]. (c) Schematic depiction of the fabrication process for alkynyl defective TEB-DBT CMPs [159]. (d) Schematic depiction of OPs incorporating hydrophilic non-conjugated segments [160].

imide) (PTI) (Fig. 14c). Not only that, Zhang *et al.* [163] have been still in the process of further modification of TAP ring-substituted doped CN, until 2021. This shows that the TAP molecular ring substitution of triazine ring to enhance the catalyst has gained much recognition. In addition to the molecular types mentioned above, other common types are barbituric acid, 2-aminobenzonitrile, pyran, and their derivatives [172–174]. Similarly, the modification method of substituting molecular rings for triazine rings has led to significant improvements in the catalysts in terms of expanding the light absorption range; harmonizing the energy band structure; facilitating the separation of photogenerated carriers; and increasing the electrical conductivity [175,176]. CN-DPY relocates the π-electrons due to the incorporation of the pyridine molecular ring, which leads to an upward shift of the corresponding HOMO by 0.288 eV and a downward shift of the LUMO by 0.068 eV, which in turn decreases the overall bandgap energy of the material from 2.90 eV to 2.54 eV [170]. Moreover, the CN-DPY light absorption range is red-shifted. CN-MH-S with D-A structure (Fig. 14d) is constructed by substituting the triazine ring in CN by maleic hydrazide ring to build a fast channel for charge transfer, and the modification changed the typical nanosheet structure of CN into a three-dimensional lettuce-like nanostructure, which also led to the shortening of the migration distance of carriers [164]. At the same time, the efficient separation of intramolecular photogenerated carriers is induced to improve the charge transfer efficiency in the photoreaction.

Moreover, the incorporation of the molecular ring does not change the intrinsic crystal structure and the core chemical backbone within CN, but results in the change of its morphologic texture and the increase of specific surface area and porosity [177,178]. As shown in the SEM image of TCN (Fig. 14e), the pristine CN modified by 2-thiobarbituric acid (TA) substitution dramatically changes the nanosheet-like morphology compared to the typical smooth surface of pristine CN [168]. With the increase incorporation of TA, the TCN structure underwent a gradual transformation, exhibiting partial curling and dense irregular pores. Furthermore, its visible light absorption edge moves from 450 nm to the infrared range of 700 nm, which could lead to an increase in the number of absorbed photons. Adequate light absorption is the key to enhance the activity of the photocatalyst [179,180].

2.3.2. *Other substitutions*

Currently, relevant experimental studies and theoretical calculations have shown that a certain degree of structural defects will form a typical D-A structure within the polymer, which positively affects its catalytic performance and adsorption capacity [181]. These specifically include: (1) defect content contributes significantly to the material energy level change, intramolecular electron-hole separation transfer, and alteration of photocatalytic active sites [58,182]; (2) introduction of defects enables systematically adjustable absorption edge redshift [183,184]; (3) the improvement of photogenerated carrier transport efficiency effectively promotes ICT and solves the limitation of rapid carrier complexation on photocatalytic performance [58].

As a result, molecular substitution is utilized to replace some of the molecules of the host material with other molecules, resulting in defects in the material itself. As for the specific mechanism, with the continuous deepening of research progress and the continuous progress of research technology in recent years, researchers have made more and more accurate and detailed explanations. Yu *et al.* [185] have proposed a KOH-assisted selective in situ introduction of two N-deficient types with carbon nitride precursors (urea, melamine, or thiourea) via one-step thermal copolymerization to obtain g-C_3N_x. It has been demonstrated that g-C_3N_4 with a certain degree of N-deficiency has a much better energy-band structure (narrow bandgap 2.17 eV) and that the incorporated cyano group (-C≡N) also exists as an active site in the photocatalytic reaction (Fig. 15a-b), significantly enhancing its photocatalytic activity in the visible light. Not only that, the introduction of N defect causes the maximum absorption edge of g-C_3N_4 to migrate purposefully to the infrared range (Fig. 15c-d), thus expanding the number of photons absorbed by the material. In the same thought, Guo *et al.* [58] have prepared crystalline porous carbon nitride (CPCN) by using exciton engineering technique, in which the addition of -C≡N caused the original CN structure to be distorted, breaking the original interfacial energy ordering of CN. The electrons are absorbed and accumulated by -C≡N in large quantities, which leads to the effective dissociation of excitons in CPCN, and its surface charge transfer efficiency rises to 50.8% compared to 36.6% of CN. The implementation of above strategies for molecular substitution in g-C_3N_4 results in the enhancement of

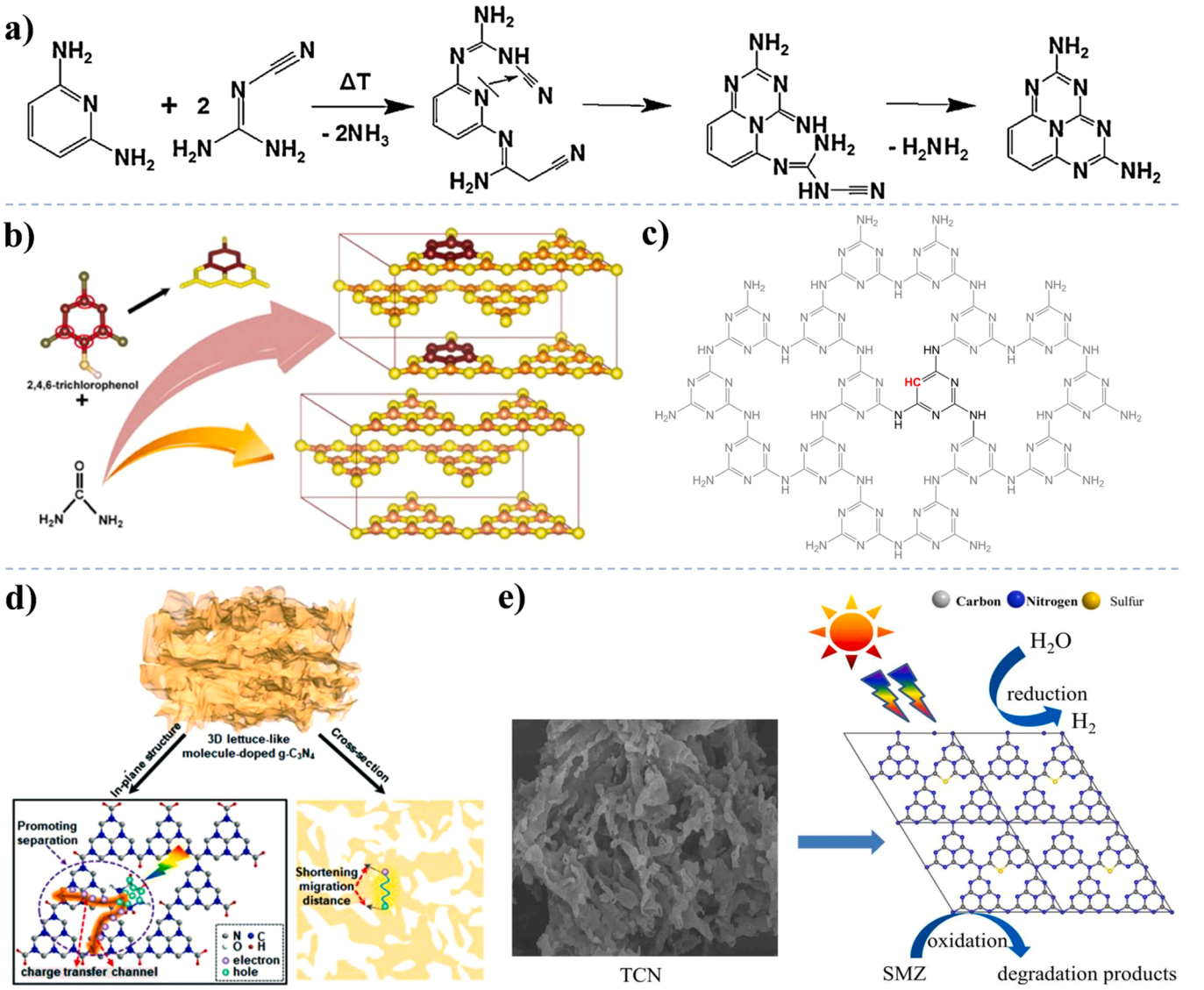

Fig. 14. (a) CN-DPY formation by ring substitution of the pyridine molecule for the triazine ring [170]. (b) Schematic diagram of the ring substitution process of CN-T [169]. (c) Schematic diagram of a pyrimidine unit substituted for the s-triazine unit [158]. (d) Separation and transport mechanism of photo-generated carriers in CN-MH-S [164]. (e) The SEM image of TCN and mechanistic diagram of TCN for photocatalytic hydrogen production and pollutant degradation [168].

the photocatalytic oxidative activation, and further improves the H_2 precipitation efficiency of the material under visible light irradiation conditions. Not only that, in addition to constructing defects on g-C_3N_4, Xiao *et al.* [159] have made the TEB-DBT CMP partially alkyne-deficient by replacing the electron donor 1,3,5-triethynylbenzene (TEB) with 1, 3-diethynylbenzene (MEB) in the original D-A CMP framework. The HOMO and LUMO images of TEB-DBT and Defect-TD-1–4 are obtained based on DFT calculation (Fig. 15g), there is a significant difference between TEB-DBT compared to Defect-TD-1–4, which is also due to the extended π-conjugation system after molecular modification. As the MEB content increases the defect content also increases, the chemical composition of the polymers shows a significant difference, in which the intramolecular charge is transferred from the donor to the acceptor and the charge separation ability is improved.

Through molecular in-situ substitutions a transformation where heterogeneous molecules become an integral part of its structure. This process not only disrupts the internal charge transfer equilibrium of the raw material to form D-A structure but also introduces additional functionalities within the added molecules, thereby enhancing the photocatalytic performance of the material [186]. For example, Wang *et al.* [165] have highlighted the exceptional photocatalytic properties exhibited by organic fluorescent moieties, which have garnered significant attention in the field. Consequently, they employed anthrazolines as the primary framework for the OPs, incorporating tetrahydrofuran and Ni to enhance its performance (Fig. 15e). By harnessing the exceptional optical properties and charge transfer capability of this substituted organic semiconductor material, the authors effectively exploit the synergistic effect of a bi-catalyst to facilitate expeditious cross-coupling reactions and enable C-N bond formation under mild reaction conditions. Under the same theory, Li *et al.* [57] have proposed a new strategy to construct D-A COFs by utilizing different molecules (2, 1,3-benzoselenadiazole-based, 4,4′-([1,2,5]thiadiazolo[3,4-*c*]pyridine-4,7-diyl)-based, 1,4-dimethoxy benzene-based) in situ substitution of the linker (Fig. 15f) resulted in three newly discovered isomeric 2D-COFs (COF-JLU23, COF-JLU24, COF-JLU25) have been synthesized based on pyrene. Similarly, Yu *et al.* [138] have extended the previous research by employing benzene ring, pyridine, and pyrazole as electron-donor units in substitution of the original molecule. This strategic modification effectively regulates the ICT kinetics while altering the number atoms within the molecular framework. The above

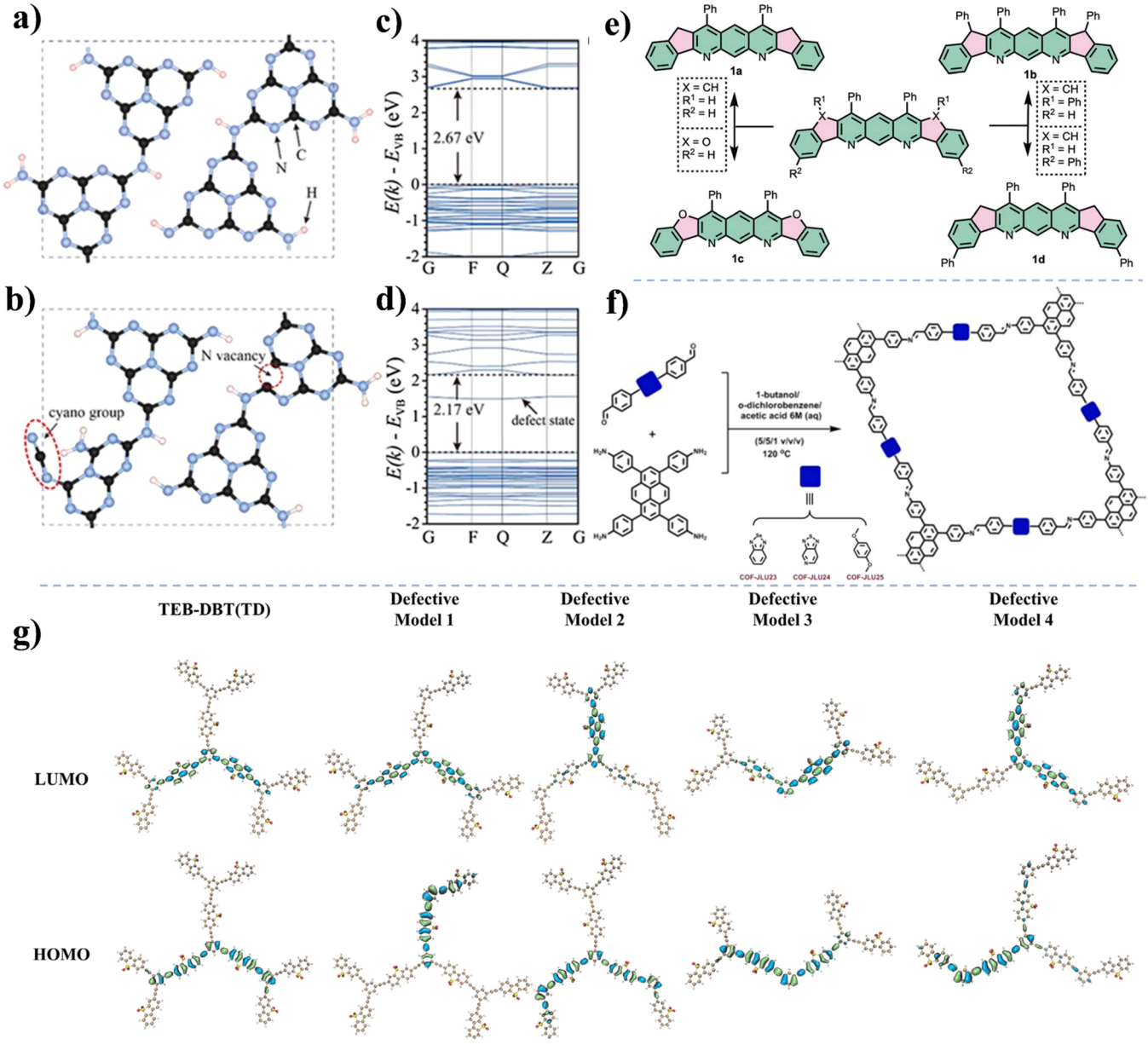

Fig. 15. Structure models and calculated band structures of (a, c) g-C_3N_4 and (b, d) g-C_3N_x with -C≡N [185]. (e) Schematic diagram of ring substitution resulting in anthrazoline derivatives [165]. (f) Diagram of the process of substituting the benzene ring in 1, 4-bis(4-aldehyde phenyl)benzene with 1,3,6,8-tetra(4-aminopheny) pyrene to form COFs [57]. (g) The distributions of LUMO-HOMO orbitals in simplified fragments of TEB-DBT CMPs were analyzed using DFT simulation [159].

substitution modes enhance both the intramolecular oxidative activation reactivity and the hydrophilic dispersion of the organic conjugated molecules due to hydrogen bonding interactions [187].

In addition to the above, most research endeavors to modify substituting molecules without altering the spatial structure of the material itself to enhance the optical properties of OPs. But numerous studies have demonstrated that photocatalysts possessing ordered three-dimensional structure (3D OM) exhibit superior catalytic activity compared to zero-dimensional, one-dimensional, and two-dimensional structures, particularly in regards to photocatalytic pollutant degradation applications [188,189]. To address the limitations of rapid carrier recombination, limited exposure of catalytic active sites, and narrow visible light collection range observed in graphitic phase CN, Zhou *et al.* [167] have used a hot-melt method to thermally induce copolymerization of urea and 3-aminobenzeneboronic acid to obtain CN_{25}, in which the 3-aminobenzeneboronic acid based substitutes for the N-atom position joined with CN to form the D-A structure (Fig. 16a-b). The polymer CN_{25} is characterized by a nanostructure with a lamellar composition that allows for porosity, possesses a significantly increased surface area, exhibits exceptional hydrophilic properties, demonstrates efficient utilization of visible light, and effectively suppresses carrier recombination. Compared with pristine CN, CN_{25} demonstrates enhanced exciton dissociation and more efficient kinetics of carrier migration (Fig. 16c). Finally, the formation of the D-A structure is supported by the analysis of electron density, molecular dipole moment, electrostatic potential, and states density of HOMO/LUMO. Additionally, these findings shed light on the potential mechanism behind enhancing photocatalytic activity [190,191]. Moreover, since the incorporation of alkynes (-C≡C-) into the OPs framework facilitates an extended π-conjugated structure, thereby promoting efficient ICT. For instance, Zhang *et al.* [52] have synthesized D-A COFs, named TBPA-COFs, through a solvent-thermal condensation reaction induced by organic acids. They utilize 2,4,6-trimethyl-1,3,5-triazine (TMT) and bis(4-formylphenyl)acetylene (BFPA) as raw materials to achieve the

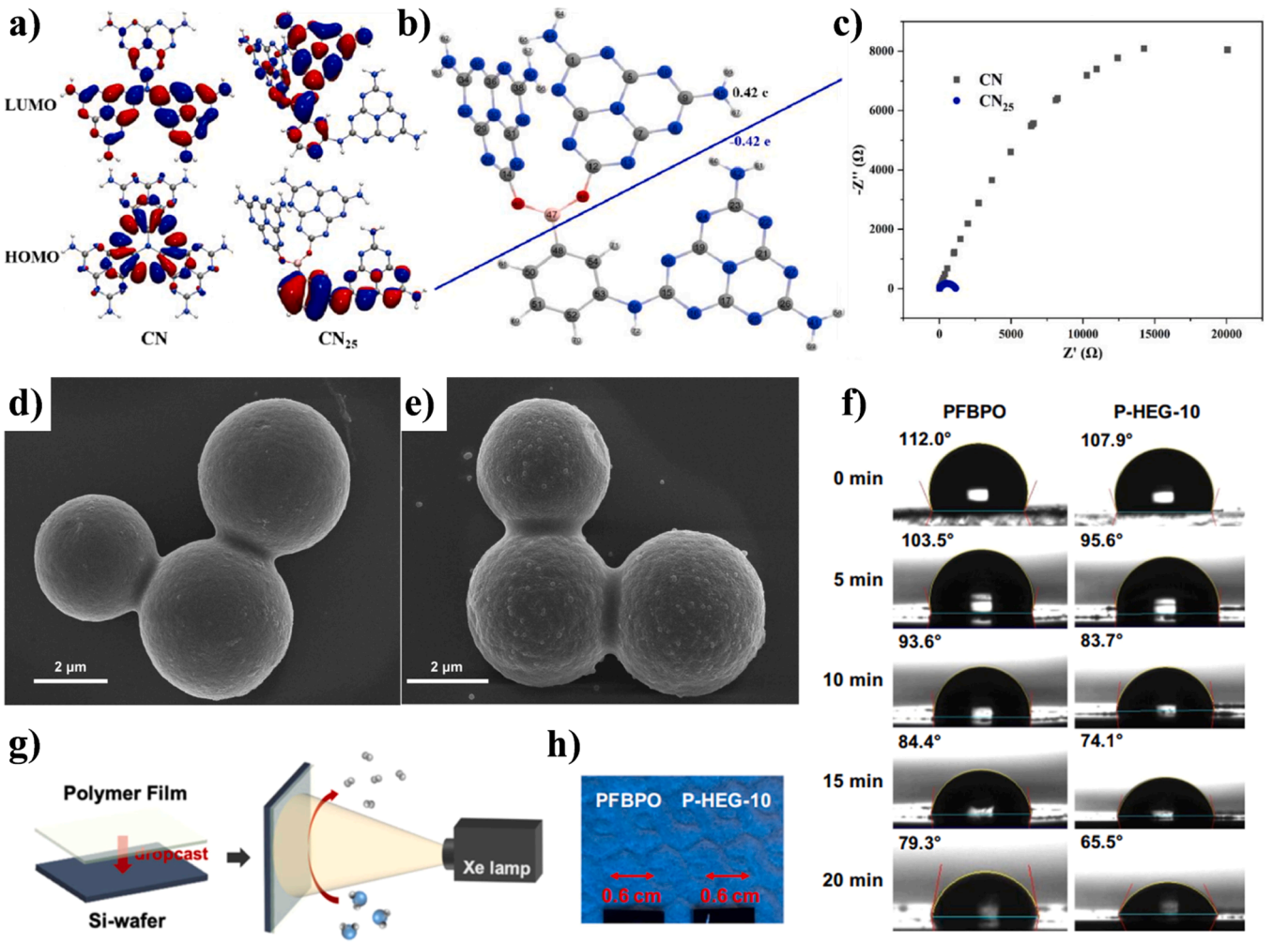

Fig. 16. (a) The HOMO-LUMO energy levels diagram, (b) the APT charge analysis and (c) the EIS image of CN and CN_{25} [167]. The SEM image of (d) TBP-COF and (e) TBPA-COF [52]. (f) Water contact angles of PFBPO and P-HEG-10 films in the light illumination over time. (g) Schematic diagram of photocatalytic HER in PFBPO and P-HEG-10 thin film systems. (h) Images of the 0.6 × 0.6 cm^2 film over PFBPO and P-HEG-10 [160].

synthesis of D-A COFs with the alkyne (-C≡C-) substitution linkage. The -C≡C- substitution not only led to enhancing the selective aerobic oxidation of organic sulfides by TBPA-COF, but also the material surface morphology of TBPA-COF showed rougher and more porous compared to that of the olefinic-linked (-C═C-) TBP-COF, which was more favorable for the adsorption of reactants on the material surface (Fig. 16d-e). In addition, the incorporation of groups with strong electron-absorbing or electron-donating ability by substituting the molecular aryl functionality could also serve the purpose of modifying the modified OPs [192].

Besides the above modification involving the incorporation of OPs through individual molecular substitution, another promising avenue for modification lies in the insertion of molecular segment substitution. For example, Chang *et al.* [160] have effectively created a range of discontinuous conjugated polymers (DCPs) with non-conjugated segments that are hydrophilic, which have been inserted into the original structure of hydrophobic CPs. These enable efficient water penetration, leading to a productive interface between water and polymers. Within the bulk DCPs in both film and solution states (Fig. 16f). The interrupted conjugated DCPs exhibited higher HER compared to hydrophobic photocatalysts under identical conditions. By effectively introducing water into hydrophilic non-conjugated chain fragments of modified DCPs without significantly altering their semiconducting properties, it could overcome the major limitation in this field (Fig. 16g-h).

3. Application of D-A OPs in environment

3.1. Water splitting for H_2 and O_2 production

The photocatalytic water splitting process entails the division of water molecule into hydrogen and oxygen, driven by a positive change in the standard Gibbs free energy change (ΔG_0) with an energy equivalent to 237 kJ mol^{-1} [71]. After molecular modification, the intermolecular D-A structure formed in the pristine photocatalysts enhances the ICT process, leading to an improvement in the separation of photogenerated charges and providing a larger number of catalytic active sites for photo-redox reactions [101,140,154]. Not only that, the modified OPs photocatalyst exhibited excellent recycle capability following an extended period of photocatalytic cycling experiments, while maintaining unaltered photocatalytic performance and a high degree of structural stability [45,126]. In recent years, the application of D-A OPs photocatalytic water splitting is increasing (Table 4). H_2 has long been recognized as a sustainable green energy with high combustion value, non-polluting combustion products, and a wide range of sources [89,187]. The dominance of coal, oil, and natural gas in the traditional energy structure has resulted in a series of severe environmental pollution issues, significantly impeding the sustainable development of society and economy while also posing detrimental effects on public health [149,193]. Thus, the development and utilization of the novel form environmentally-friendly energy source, exemplified by hydrogen,

Table 4
Summary of photocatalysts in HER and OER.

Photocatalyst	Modification type	Sacrificial agent [vol %] /Co-catalyst [wt %]	Visible wavelength (λ) [nm]	Hydrogen production rate [mmol h^{-1} g^{-1}]	Oxygen production rate [μmol h^{-1} g^{-1}]	Apparent quantum Efficiency (AQE) [%]	
PCN-BTD_{008}	Monomolecular modification	——/Pd	420	0.7442	14.8	58.6	[71]
10DAPCN	Monomolecular modification	TEOA (10)/Pt (2)	> 420	26.24	——	3.11	[101]
P-HEG-10	Monomolecular substitution	TEA (33.3)/——	460	16.8	——	17.82	[160]
g-C_3N_4-MF_{100}	Monomolecular modification	TEOA (20)/Pt (3)	> 420	3.613	——	8.6	[140]
BPCN	Multimolecular modification	No/Co (1), Pt (3)	450	0.260	228.67	5.72	[26]
NP-$CN_{0.2}$	Monomolecular modification	TEA (20)/Pt (3)	> 420	2.791	——	6.1	[40]
CTP-2	Monomolecular modification	Co^{2+} (3)	> 300	0.025	12.0	——	[117]
2AP-CN-15	Monomolecular modification	TEOA (20)/Pt (3)	420	6.318	——	20.1	[89]
Tz-COF-3	Monomolecular modification	Ascorbic acid (0.8)/Pt (3)	420	43.2	——	6.9	[93]
P-TAME	Monomolecular modification	Pd (0.46)	420	0.190	1.7	8.9	[126]
Py-ThTh-CMP	Monomolecular modification	Ascorbic acid (0.1)	> 420	1.874	——	3.4	[104]

assumes paramount significance [150]. Currently, researchers have made significant advancements in the exploration of solar energy. Photocatalysts generate robust H_2 and O_2 reactions during photocatalytic water splitting [117,126]. Among these, the utilization of photocatalytic technology enables directly visible-light-driven water splitting to produce pure H_2 and O_2, which solely consumes solar energy without causing secondary pollution.

Molecular modification, as an emerging approach to modify photocatalysts, has been employed in recent years to address the deficiencies of original semiconductor photocatalysts. These deficiencies include unstable movement of photogenerated carriers, high rate of electron-hole recombination, limited light absorption range, low durability, and few reactive sites. Organic molecular groups are introduced through this method to compensate for the internal deficiencies within the material, thereby improving the capability of photocatalytic hydrogen evolution [163]. The hydrogen evolution capacity of PCN as a photocatalyst is inherently stable, and it readily exhibits synergistic effects with introduced small molecular groups, thereby enhancing the efficiency of hydrogen evolution. Consequently, PCN is frequently employed as a substrate for molecular modification to form the D-A structure in combination with diverse small molecular groups. For instance, Li *et al.* [89] have found that grafting the electron-withdrawing pyridine rings in edge of CN framework could drive the photogenerated charge migration. The graft of the electron-absorption structure not only alters the charge dynamics of the material itself, but also augments the number of catalytic active sites for hydrogen production in the novel material D-A 2AP-CN-15. The process of photocatalytic HER by utilizing Pt as the co-catalyst, the number of catalytic active sites capable of efficiently generating HER is significantly enhanced compared to pristine CN (Fig. 17a). And through computation of the Gibbs free energy of hydrogen adsorption (ΔG_{H^*}) at each reaction site, it is observed that the ΔG_{H^*} value at the edge site in the 2AP-CN-15 structure exhibits a notably lower value than that at the central site, which could be attributed to substantial charge transfer from the center to the edge. The Pt are adsorbed onto the edge-active sites, forming Pt (2−5) sites with ΔG_{H^*} values close to 0, thereby enhancing their favorability for efficient generation of photocatalytic HER. 2AP-CN-15 exhibits sustained high hydrogen evolution capacity that are nearly quadrupled compared to that of the original CN (Fig. 17b), and even after undergoing four consecutive hydrogen evolution cycles within 16 h. Besides, the samples have maintained its structural integrity throughout the process. Similarly, Zhou *et al.* [167] have verified that its optimal hydrogen precipitation rate was increased by 5.5 times compared to the pristine CN (Fig. 17c). Through the one-step polymerization scheme of urea, NPT, and β-CD, carbon atoms and conjugated heterocycles are incorporated into CN. C replaces the bridged N, while conjugated heterocycles are grafted onto the periphery of the CN backbone. The resulting synergistic effect between off-domain backbone sensing and edge sensing effectively enhances electron mobility and facilitates directional transfer of photogenerated electrons to the periphery of the CN backbone. In addition to significantly enhancing the photocatalytic performance of the material itself, the incorporation of NPT group, a representative organic ring unit, enables NPT/C-CN to maintain efficient hydrogen production and structural integrity after 6 consecutive cycles of experiments within 24 h. The potential error caused by sample loss in each cycle experiment has been eliminated [157]. Furthermore, Bhoyar *et al.* [101] have successfully synthesized a D-π-A type network via utilizing PCN as the primary material through copolymerization reaction, wherein the nitrogen-rich but π-bonds deficient DAP moiety was incorporated into PCN. The presence of D-π-A structure enhances the electron transfer process from PCN (as donor) to the pyridine ring (as acceptor) to create the ICT channel, promoting efficient electron flow. Meanwhile, it demonstrates a more rapid nonradiative decay of photo-exciton compared to PCN, with an average duration of approximately 0.60 ns. The optimal modification ratio results in a photocatalytic H_2 production rate up to 4.5 times higher than PCN, because of the considerably reduced hydrogen adsorption free energy relative to PCN, D-A DAPCN exhibits a higher H_2 production (Fig. 17d). This reduction in energy level for H_2 production facilitates the reaction. The aforementioned examples further substantiate the evident advantages of employing molecular modification in constructing D-A structural materials, as it effectively enhances the primary charge transfer efficiency and augments the number of photo-reaction sites during the photocatalytic HER process, thereby significantly boosting the rate of hydrogen evolution.

The photocatalytic water splitting is widely acknowledged to yield H_2 and O_2 simultaneously in 2:1. However, empirical evidence suggests that how to utilize photocatalysis to efficiently produce O_2 in large quantities is a difficult problem to overcome compared with H_2 production [174,177]. Recently, remarkable progress has also been made around photocatalytic water splitting for generating O_2 by utilizing innovative D-A structure photocatalysts created through molecular

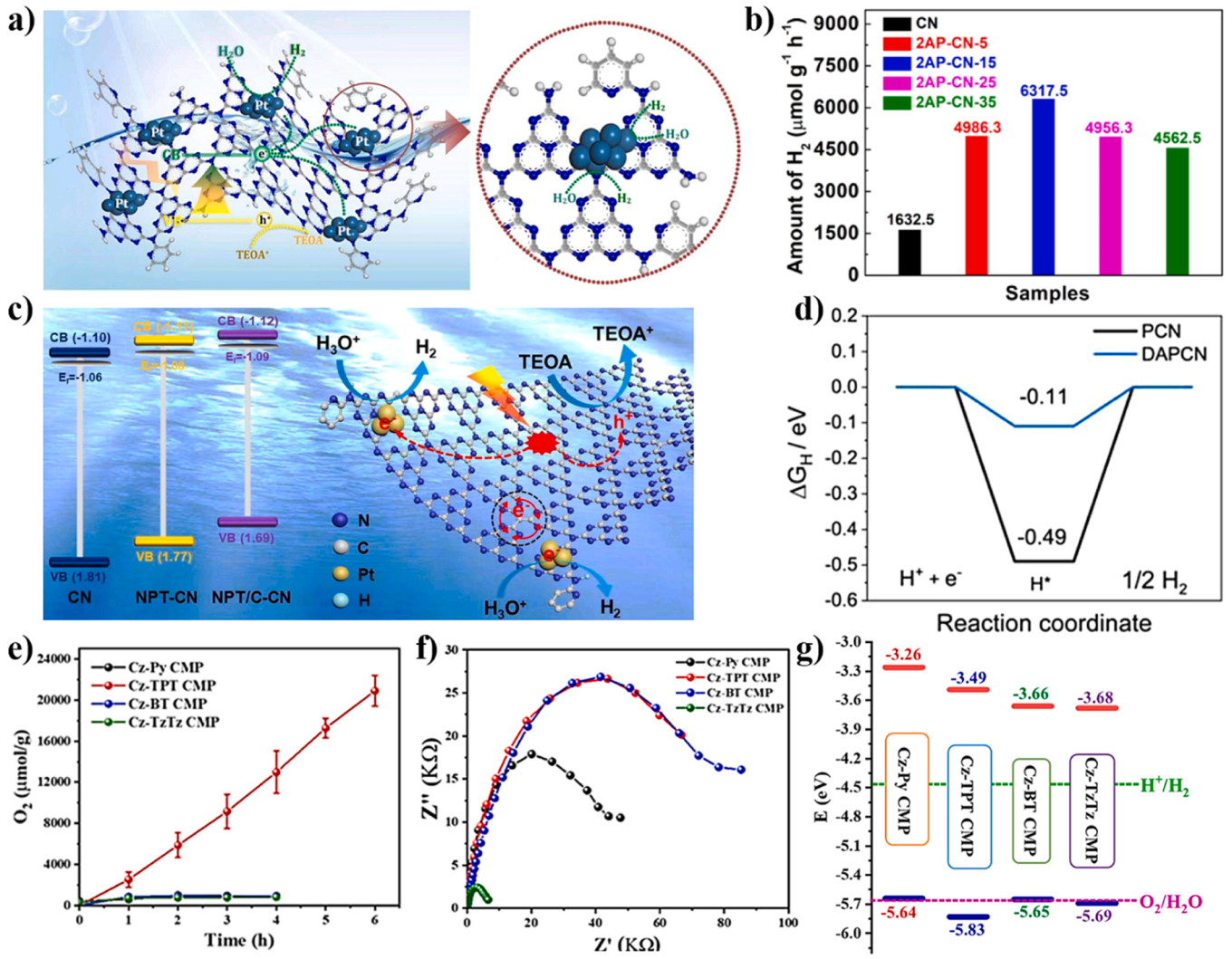

Fig. 17. (a) The photocatalytic H_2 evolution schematic diagram of D-A 2AP-CN-15 sample [89]. (b) The comparison of H_2 evolution rate over the different samples [89]. (c) Possible charge transfer behavior and HER mechanism of NPT/C-CN [157]. (d) Reaction coordinate diagram illustrating the comparative free energy of hydrogen adsorption for PCN and DAPCN [101]. (e) Trend diagram of O_2 production by Cz-n CMP (n = Py, TPT, BT, TZTZ). (f) Nyquist plots, (g) band structure of Cz-n CMP (n = Py, TPT, BT, TZTZ) [13].

modification [95,167]. Yu *et al.* [66] have utilized this tool to target the problem of low O_2 production, and then adjusted the number of F substitutions on the acceptor units in the D-A polymer PxF-T (x = 1,2,4) to increase its electron-absorbing capacity and regulate the overall polarity of the organic molecule. As the electron-absorbing capacity of the polymer acceptor unit increases the HOMO energy level gradually decreases, and the O_2-producing capacity increases. Further, Saber *et al.* [13] have synthesized carbazole (Cz) as the donor unit, while pyrene (Py), triphenyltriazine (TPT), benzothiadiazole (BT), and thiazolylthiazole (TzTz) as the acceptor unit, respectively. Among them, the Cz-TzTz CMP exhibits remarkably low resistivity, leading to its exceptional hydrogen evolution rate of 15.3 mmol g^{-1} h^{-1} when utilizing ascorbic acid as a sacrificial electron donor without the need for additional platinum co-catalyst incorporation. However, when $AgNO_3$ was used as the electron acceptor in solution, the capacity of Cz-TPT CMP to produce O_2 was extremely superior (3387 μmol g^{-1} h^{-1}) compared to all the O_2 precipitation rates reported so far (Fig. 17e-f). This is because Cz-TPT CMP has HOMO potential suitable for O_2 output (Fig. 17g) [13].

3.2. Degradation of environmental pollutants

The escalating levels of environmental contamination present a peril to human existence and the long-term progress of society [194]. With the rapid advancement of modern industry, agriculture, and aquaculture, there is an escalating use of dyes, pesticides, and antibiotics leading to a growing demand for wastewater treatment [195–197]. Wastewater containing these substances has become a significant contributor to urban industrial and domestic sewage in China [198–200]. Consequently, the need for effective treatment methods for this industrial wastewater has gained increasing attention. Compared to traditional physicochemical wastewater treatment technologies and biological wastewater treatment systems, the photocatalytic degradation ability of pollutants in water is highly appealing [201–203]. However, when compared to conventional photocatalysts, molecular modified D-A OPs exhibit superior advantages in terms of enhanced degradation efficiency, better durability, and more comprehensive pollutant degradation. (Table 5).

The distinctive characteristics of dye-contaminated wastewater are evident, especially the presence of commonly used industrial dyes such as methyl orange (MO), methylene blue (MB), and Rhodamine B (Rh B). This encompasses substantial organic content, suboptimal biochemistry, pronounced chromaticity, intricate composition, and inherent toxicity [198,204]. Therefore, wastewater that is discharged directly into the environment without treatment will cause serious pollution to the

Table 5
Summary of photocatalysts in degrading pollutants.

Photocatalyst	Modification type	Major oxidation species	Pollutant type	Targeted pollutant/ TOC Removal rate (%)	Rate constant (k_{obs}) [min^{-1}]	
g-C_3N_4-BTA	Monomolecular modification	$^1O_2$	ATZ	100.0/35.0 (PMS, 5 mM)	0.55	[70]
CN-DPY$_w$	Molecular substitution	$\bullet O_2^-$, •OOH	MO	100.0/—	11.27	[170]
LCN	Molecular substitution	——	Rh B 4-CP Phenol	≥95.0/—	——	[115]
OCN/Py	Monomolecular modification	$\bullet O_2^-$, •OH, $SO_4^{\bullet-}$, $^1O_2$	TC	97.0/97.4 (PMS, 0.5 mM)	0.568	[50]
Triazine-PDI	Multimolecular modification	$\bullet O_2^-$, •OH	Phenol	10.0/79.0	11.46	[90]
COF-TD1	Monomolecular modification	$\bullet O_2^-$	Paracetamol	>98.0/—	——	[109]
CPCN	Molecular substitution	$\bullet O_2^-$, •OH	CIP	85.8/—	0.0219	[58]

environment and may affect people's health in direct or indirect ways through the food chain [195]. Many researchers have devoted themselves to exploring options for photocatalytic degradation of industrial dyes, and so far, several methods have been obtained to efficiently photodegrade industrial dyes represented by MO and Rh B [170,196]. But most pristine photocatalysts suffer from unsuitable VB-edge potentials and poor absorption and oxidization capabilities, which lead to large number of hole buildups and rapid complexation of photogenerated charges during the reaction process [53,178]. D-A OPs obtained by molecular modification, which act as photocatalysts could well solve these problems [58,188]. Xia's team has prepared a conjugated polymer g-$C_{18}N_3$-COF with D-A structure via Knoevenagel condensation reaction for the efficient degradation of Rh B under visible light [73]. Because it possesses a triazine moiety, a molecular structure suitable for photocatalysis, and the protonation of the nitrogen atoms on the triazine ring during the preparation process, the light absorption and the effective charge separation ability of g-$C_{18}N_3$-COF were well enhanced sensitive to visible light, and it showed good photocatalytic degradation of Rh B; the photocatalytic degradation of Rh B at a high concentration of 300 ppm reached the degradation equilibrium in 6 h. The photocatalysts successfully achieved the degradation of Rh B through a high concentration of 300 ppm. And, the photocatalytic degradation of dye pollutants has been investigated through 3 cyclic degradation experiments within 18 h. Despite a slight decrease in catalytic activity, the overall performance remained at a high level, while maintaining the original crystallinity of g-$C_{18}N_3$-COF [73]. Moreover, Mushtaq *et al.* [141] have prepared CMP-P1 with a completely unsaturated π-conjugated backbone capable of degrading MB precisely and efficiently in complex aqueous environments contaminated with mixed dyes; Niu *et al.* [183] have prepared R-melon with significantly improved degradation of Rh B compared to the pristine melon; Ou *et al.* [83] have prepared heptazinocyclic-based melon (DA-HM) with a typical D-A structure that degraded Rh B more than three times as much as the normal HM; Yu *et al.* [74] have prepared D-A HBC-TFPN with a concave interlayer structure that degraded MO more than 1.7 times as much as its precursor COF-316 by 1.7 times. And, the results of the reusability experiments conducted on the modified materials in these studies consistently demonstrate that even after prolonged exposure to light reactions, the materials exhibit a sustained high level of photocatalytic performance.

Likewise, the pollution risks associated with emerging contaminants (ECs), such as tetracycline (TC), nitenpyram (NTP), atrazine (ATZ), 4-clorophenol (4-CP), bisphenol A (BPA), other pharmaceuticals, and endocrine-disrupting chemicals, have progressively garnered attention from researchers [205–207]. In the field of D-A OPs photocatalysis, researchers have explored the incorporation of various organic micromolecular groups as the modification groups, thereby enhancing the visible light-driven ROS generation capability of D-A OPs photocatalysts and ensuring their excellent generating capacity in free radical upon repeated utilization [208–210]. To illustrate this point, Hou *et al.* [109] have prepared D-A COF-TD1 with the incorporation of a 1,3,4-thiadiazole ring as an electron donor and quinone as an electron acceptor. Due to the 1,3,4-thiadiazole ring excites electrons more readily under light conditions and undergoes rapid ICT under the strong electron-absorbing effect of the electron acceptor. The O_2 in solution gains electrons and transforms into $\bullet O_2^-$ radicals, which attack APAP for degradation (Fig. 18a). Consequently, comparative studies between COF-TD1 and COF-TD2, where the latter utilizes a 1,2,4-thiadiazole ring as unit, revealed that under identical conditions, COF-TD1 exhibited a significantly enhanced photodegradation efficiency for paracetamol in water with an increase of approximately 40% (Fig. 18b). And the researchers also have found that COF-TD1 with strong light responsiveness has shown good degradation effect on other common water pollutants such as diclofenac, tetracycline hydrochloride, naproxen, and bisphenol A. For another example, Zhou *et al.* [167] have employed a hot-melt grafting technique to introduce a benzene ring with strong capability in electron absorption into the CN framework, which is subsequently subjected to thermal copolymerization resulting in the synthesis of CN_{25}. The optimized CN_{25} photocatalyst achieved a degradation efficiency of 81.3% for a significantly concentrated TC solution (40 mg L^{-1}) within 100 min, exhibiting an improvement of 6.75 times compared to the unmodified CN. In contrast, Zhang *et al.* [102] have enhanced the π-π interactions in the material by grafting g-C_3N_4 with the benzene ring, leading to a remarkable photodegradation of bisphenol A exceeding 90% within 50 min, which is nearly three times higher than that achieved using the original g-C_3N_4. Likewise, the conventional g-C_3N_4 has been modified with a molecular ring, utilizing 5-bromo-2-thiophenecarboxaldehyde (BTC) grafted to the heptazine ring group to constitute the D-A structure TCN, which generates •OH driven by photogenerated charge for the photodegradation of oxytetracycline hydrochloride (OTC) (Fig. 18c), and the OTC could be photodegraded within 60 min under the visible light [41]. The optimal degradation rate could be as high as 93%. As a further example, Guo *et al.* [173] have fully utilized the substitution of oxygen for g-C_3N_4 to obtain OCN to improve its ability to produce ROS under light condition, and simultaneously produce $\bullet O_2^-$, $^1O_2$, •OH, and H_2O_2, which are the typical types of ROS. As a result, OCN has an extremely strong oxidizing ability, so that it could achieve a photocatalytic degradation rate of 85.76% for OTC within 120 min, as well as also show excellent photodegradation ability for nitroblue tetrazolium (NBT). According to the same idea, Guo *et al.* [58] have again utilized cyano-substitution into CN in order to achieve the enhancement of CN's ability of light-driven molecular oxygen activation in water. CPCN has been successfully obtained to produce $\bullet O_2^-$ and •OH for the oxidative degradation of ciprofloxacin (CIP) under light-driven, and the removal rate of CIP could reach 85.8% in 90 min.

Since pesticides have been abused in earlier years, it has caused serious environmental pollution [211–213]. Recently, photocatalytic technology has also been well developed in degrading pesticide

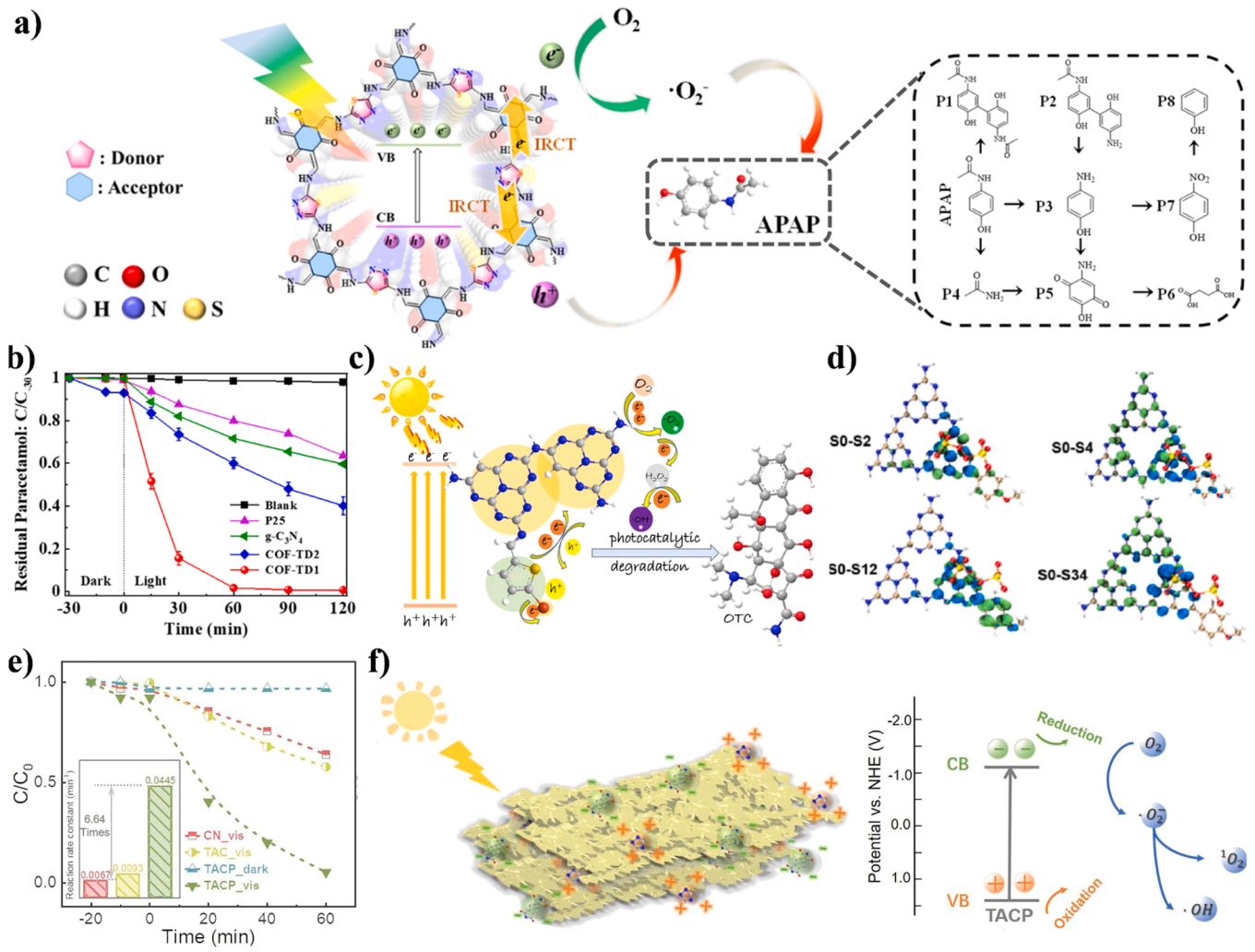

Fig. 18. (a) Schematic diagram of COF-TD1 degradation process of paracetamol under visible light irradiation. (b) Photocatalytic performance for paracetamol degradation by different photocatalysts [109]. (c) The mechanism diagram of the removal of OTC by visible light of the optimized sample (TCN-5) [41]. (d) The distribution of electrons and holes in various excited states of PDS+PCN/4-MI D-A [53]. (green and blue in surface, which represent electron and hole distributions respectively). (e) Comparison of ATZ removal efficiency. (f) Photocatalytic mechanism diagram of ATZ degradation by TACP [75].

residues, which also provides new ideas to reduce the harm of pesticide pollution to the land environment [214,215]. Che's team has copolymerized D-A PCN/4-MI$_x$ with urea and 4-methoxyphenyl isothiocyanate (4-MI) [53]. It has a thinner nanosheet structure and hydrophilicity compared to the original PCN, the specific surface area of it is significantly enhanced compared to pure PCN, with a value of 189.84 $m^2\ g^{-1}$ as opposed to 121.65 $m^2\ g^{-1}$ for pure PCN. On this basis, peroxydisulfate (PDS) is specially added to enhance the oxidizing property in the photoreaction. Electrons are transported to PDS through the phenomenon of electron tunneling under light to activate PDS to produce $\bullet SO_4^-$, which leads to the production of large amounts of ROS such as $\bullet OH$, $\bullet O_2^-$ and $^1O_2$ during the photoreaction process (Fig. 18d). PDS+PCN/4-MI$_{75}$ with D-A structure shows the highest catalytic degradation activity for NTP, reaching 100% degradation within 30 min of the light reaction with 0.115 min^{-1} reaction rate constant (k). This observation suggests that the incorporation of 4-MI as the electron donor unit in PCN not only enhances the efficiency of carrier separation, but also improve the photocatalytic oxidation capability. In addition, Weng *et al.* [70] have utilized the grafting of benzene-tricarboxylic acid (BTA) on the edge of g-C_3N_4 to obtain a photocatalytic material with D-A structure, g-C_3N_4-BTA. And the additional added peroxymonosulfate (PMS) is oxidatively activated by the photogenerated holes accumulated on BTA, resulting in nearly 100% $^1O_2$ generation of the booster in the photoreaction. As a result, g-C_3N_4-BTA+PMS exhibited excellent degradation performance (up to 100% degradation within 60 min) in the photodegradation of ATZ in water [216]. Similarly, Tang *et al.* [75] have also been working on how to efficiently enhance the photodegradation performance of OPs against conventional pesticides. Our team has applied multi-step thermal polycondensation method to prepare the constructed D-π-A type photocatalyst TACP with a thin-walled vesicular structure, which significantly increased the ATZ removal rate up to 95%, and the reaction rate constant (0.0445 min^{-1}) has been improved by a factor of 6.64 compared with that of CN (Fig. 18e). The gradual decrease of photoresistance from CN to TACP and the enhancement of n→π* electronic excitation could be clearly illustrated by electrochemical impedance spectroscopy (EIS), and its photocurrent is more than 5 times that of the pristine CN, which is significantly enhanced to 0.38 μA/cm^2. Under visible light irradiation, the D-π-A structure prompted the electron jump within the TACP (Fig. 18f). Many active electrons accumulate on the CB, making it more favorable to produce active oxides ($\bullet OH$, $\bullet O_2^-$ and $^1O_2$). This is one of the important reasons why TACP possesses an extremely strong ATZ degradation rate.

3.3. CO_2 reduction

The impact of the greenhouse effect on global climate has become

increasingly evident in recent years [5,111]. Specifically, there has been a significant reduction in glacier coverage, accompanied by a rise in sea levels and an escalation in extreme weather events worldwide. The emission of CO_2, a significant greenhouse gas, is primarily attributed to human activities, leading to an annual incremental rise in global temperature. Consequently, the conversion of CO_2 into compound fuels has garnered increasing attention worldwide in recent years [72]. Currently, the existing methods for CO_2 reduction include electrochemical and photochemical reduction. Among them, most of the semiconductor catalysts used in the photochemical reduction process require additional sacrificial agents or organic solvents to achieve efficient CO_2 reduction [28,217]. However, this necessitates secondary treatment after the reaction and may even result in secondary pollution. Therefore, the direct photocatalytic reduction of CO_2 has emerged as a prominent research area in recent years, thus prompting the exploration of photocatalysts. D-A OPs have gained significant attention for its exceptional photoresponse, photoconversion, photogenerated charge migration capabilities, and rich catalysis sites for excellent reducing capacity [100,172].

For instance, the efficient reduction of CO_2 to CO under light condition is achieved by establishing the dual electron transition pathway within $OCCN_x$ [161], which is a type of D-A OPs obtained through molecular modification based on the g-C_3N_4. Under illumination condition, the charge transfer in $OCCN_x$ occurs through both its intrinsic electron transition and the intramolecular charge transfer transition triggered by the D-A structure after molecular modification (Fig. 19a). The combined action of these two electron transition pathways on $OCCN_x$ reaction could be named the charge transfer transition. Driven by ultraviolet light, $OCCN_x$ demonstrates remarkable efficacy in the photocatalytic reduction of CO_2 to CO in aqueous media, obviating the necessity for a catalyst or organic solvent. After 4 h of reaction, $OCCN_{0.25}$ demonstrates the highest CO production (8.11 μmol g^{-1}), which is 4.3 times greater than that achieved by g-C_3N_4 under identical reaction conditions (Fig. 19b). Simultaneously, the precipitation rate of CO remained nearly constant after four consecutive cycles of $OCCN_{0.25}$ reaction. At the conclusion of each reaction, the generated CO is effectively eliminated by N_2 to eliminate any interference, thereby demonstrating that $OCCN_{0.25}$ retains exceptional stability even after prolonged periods of reaction. Moreover, the reduction of CO_2 to CH_4 in aqueous environments is a prominent area of research due to its immense potential as a renewable energy source. The one-step nucleophilic polymerization has been employed to synthesize a D-A structure OPs (TOA-PC) based on cyclotriphosphazene and s-triazine units [63]. The sulfur bridges exist as electronic pathways connecting donor and acceptor. This innovative combination offers a promising solution to address the challenges encountered during the photoreduction process of CO_2 to CH_4 (Fig. 19c). The activity of TOA-PC is significantly reliant on the directional in-built electric field established by the D-A structure and the high-speed electron transfer pathway facilitated by the sulfur bridge connecting the electron donor and acceptor, thereby positively influencing both internal photoinduced charge transfer and surface CO_2 adsorption as well as activation capacity. Even in the absence of photosensitizers and cocatalysts, TOA-PC exhibits remarkably high CH_4 yields, reaching up to 2748 μmol g^{-1} under visible light irradiation (Fig. 19d). Under identical reaction conditions, the recovered TOA-PC have been subjected to 3 h and 5 h tests, respectively, both demonstrating a consistently stable CH_4 output without any observable alteration in material structure (Fig. 19e). The above researches clearly demonstrate that D-A OPs exhibit exceptional performance in promoting photocatalytic reduction of CO_2, and then presenting promising prospects for the advancement of renewable energy technologies.

3.4. Photocatalyst drives other redox reactions

In addition to the previously mentioned applications of D-A OPs in photocatalytic water splitting and pollutants degradation in water, it has become a promising class of methods in chemical synthesis in recent years [79,92]. D-A OPs could assist the formation or cleavage of new covalent bonds in photoreactions with excellent properties such as high efficiency, non-toxicity, stability and recyclability, and low cost, and therefore are gradually being investigated to be used as catalysts in other redox reactions. Designing different D-A OPs, on the one hand, the light reaction induces the aerobic oxidation of amines to generate various

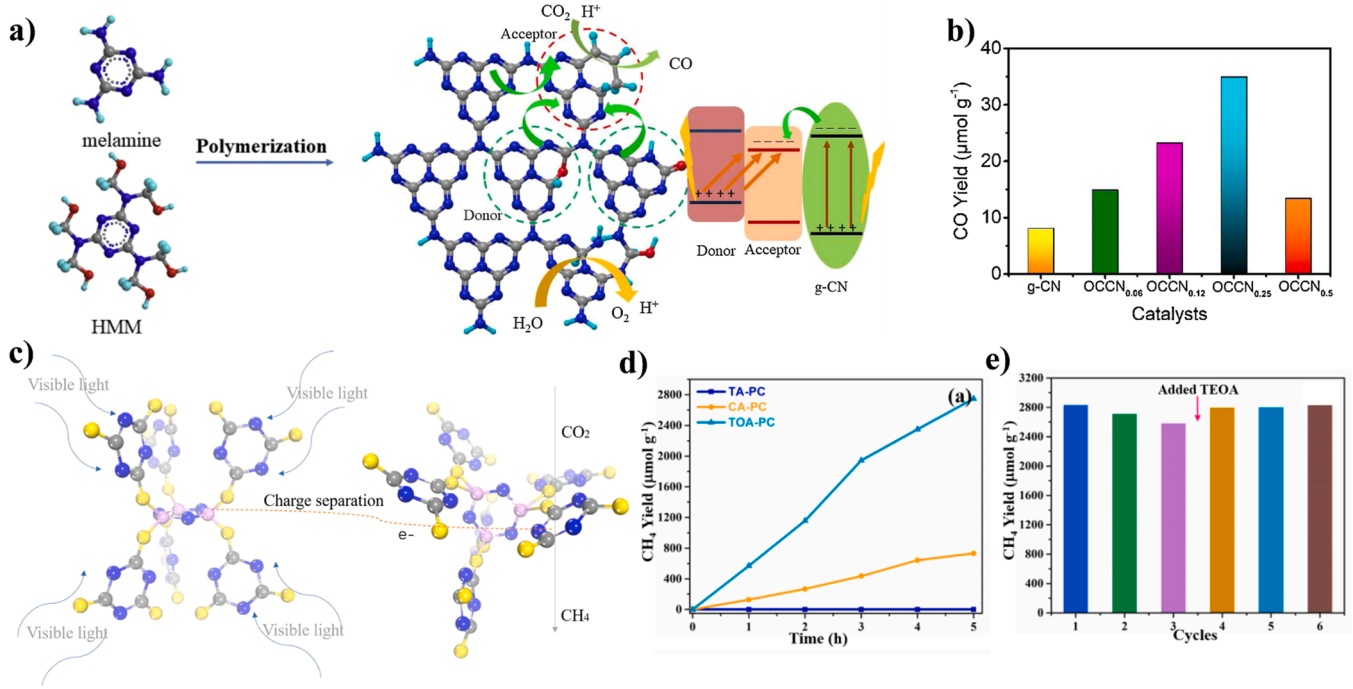

Fig. 19. (a) The preparation process of $OCCN_x$ and the mechanism diagram for photocatalytic reduction of CO_2 to CO. (b) The CO production rate diagram of $OCCN_x$ [161]. (c) The mechanism diagram of TOA-PC photocatalytic reduction of CO_2 to produce CH_4. (d) The CH_4 production rate diagram of TOA-PC. (e) The catalytic stability of TOA-PC [63].

imines [84,106], generating benzimidazole [113,130], hydroxylation of benzene ring [218], C-3 formylation of indoles and its derivatives [57], adding different substituents [165], and reacting with other hazardous substances to harmlessness. On the other hand, it reduces recalcitrant heavy metals in the water through light reactions to reduce its own toxicity to an environmentally safe range [91].

To be more specific, Zhang *et al.* [52] have designed to obtain TBPA-COF, due to the excellent charge transfer property of TBPA-COF contributes to the reaction process of selective photocatalytic aerobic oxidation of sulfide on its surface. Under visible light illumination, charge transfer aggregation occurred on TBPA-COF and reacted with O_2 in water to generate $\bullet O_2^-$ and $^1O_2$ at the same time, which selectively oxidized methyl phenyl sulfide under the joint action of these two radicals. Secondly, TBPA-COF shows excellent promotion of the reaction with 82% conversion of methyl phenyl sulfide at 460 nm light wavelength for 1 h, and the reaction has demonstrated exceptional stability, as it has been successfully repeated three times consecutively without any significant loss in activity (Fig. 20a-b). Based on the same theory, the D-A BF-COFs designed by An *et al.* [76] have also shown the similarly excellent properties of D-A in terms of visible light response range and photogenerated charge separation. BF-COFs promote the reaction of β-ketoate ester and its analogues with NH_4SCN to form C-S bonds under visible light irradiation, generating up to 28 examples of multi-substituted olefins in up to 98% yield (Fig. 20c-d). Moreover, the utilization of L-proline derived olefins enables the further synthesis of chiral amino-substituted thiazoles with a remarkable yield of 99% through identical reaction conditions (Fig. 20e). Thus, these have shown that the OPs modification technology is not only suitable for the application in the field of new energy (hydrogen production, oxygen production, CO_2 reduction, etc.) and the degradation of pollutants in water, but also in the field of chemical and pharmaceutical industry, which is very promising for research.

The application of metal-free organic photocatalytic technology for the treatment of contemporary nuclear power wastewater has been increasingly explored by researchers in recent years [91]. The nuclear wastewater containing a large amount of uranium (U (VI)) exists as a pollutant with radioactive properties for both the environment and living beings. Therefore, how to efficiently reduce the highly dissolved U

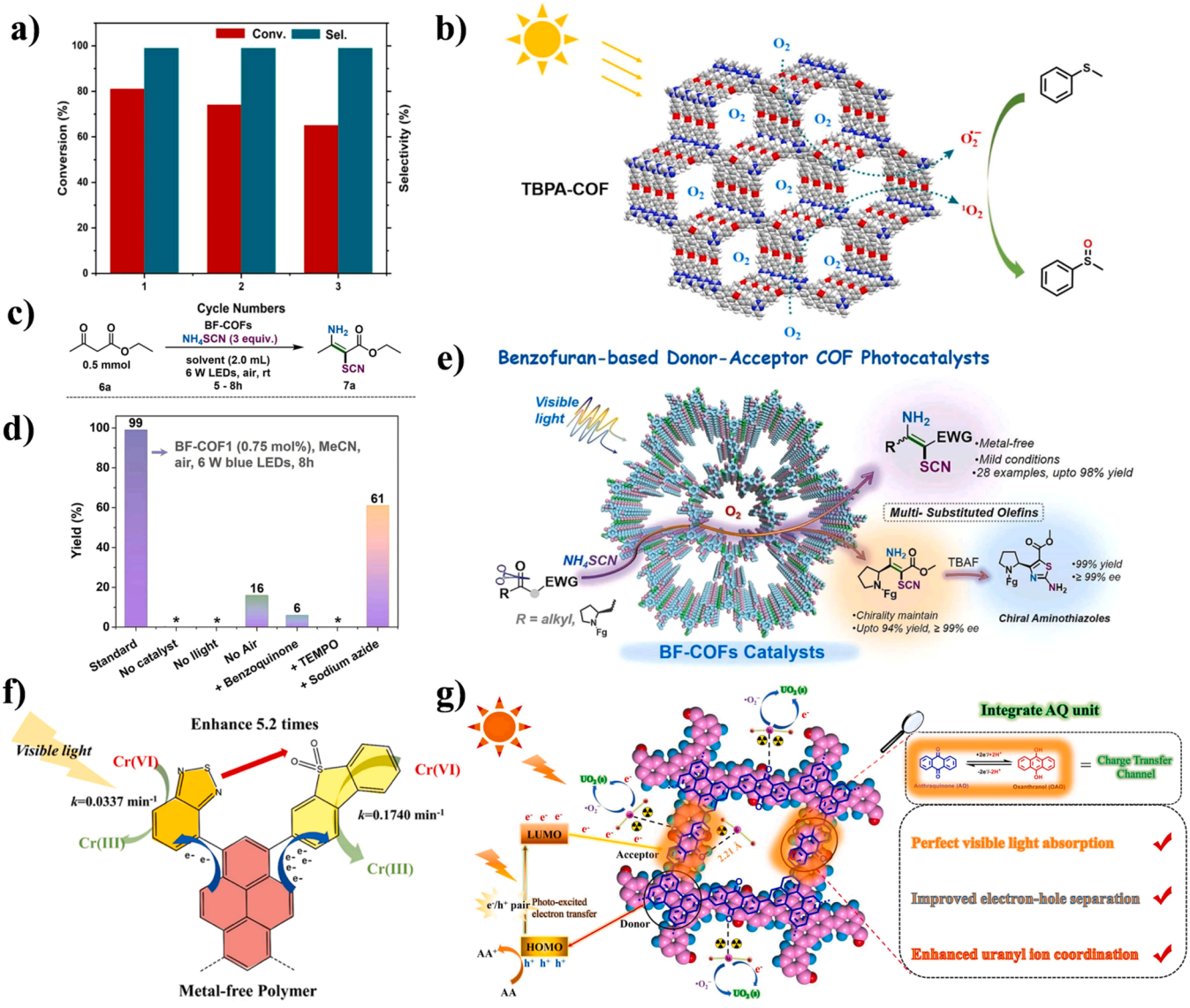

Fig. 20. (a) TBPA-COF photocatalyzed the aerobic oxidation and cycling stability of methyl phenylene sulfide at 460 nm. (b) Mechanism diagram of photocatalytic aerobic oxidation of methyl phenylene sulfide by TBPA-COF under visible light [52]. (c) Preparation of polysubstituted olefin (7a) using BF-COFs as photocatalyst. (d) Effects on photocatalytic synthesis of olefin 7a from specially controlled conditions. (e) Mechanism of photocatalytic reaction of BF-COFs under visible light [76]. (f) Mechanism diagram for the reduction of Cr (VI) to Cr (III) in Py-SO_1 [91]. (g) Reduction mechanism of UO_2^{2+} by ECUT-AQ [127].

(VI) in solution to insoluble U (IV) without generating other hazardous substances is a key issue to be tackled by the researchers. Although some common methods, such as adsorption, ion exchange, evaporation, and co-precipitation, have made some good progress, they have always been limited by technical shortcomings. Recently, due to the flourishing of photocatalytic technology, among which the metal-free D-A OPs have been noticed by more and more researchers because of their diverse designs of molecular building blocks, wide light absorption range, highly sensitive electronic responsiveness, and outstanding material stability [65]. They have concluded that D-A OPs, as photocatalysts, could well compensate for the shortcomings of conventional nuclear wastewater treatment methods. As have been designed by Zhuang *et al.* [91] to obtain Py-SO_1, with two different molecular building blocks (2,1, 3-benzothiadiazole (TB) and dibenzothiophene-S, S-dioxide (FSO)) acting as electron acceptors while modifying the Py-moiety (D). The excellent exciton separation and charge transport properties of Py-SO_1 itself (Fig. 20f) enable the efficient reduction of Cr (VI) to Cr (III) under visible light. Moreover, Yu *et al.* [127] have reported a D-A organic conjugated photocatalyst (ECUT-AQ). Utilizing the remarkable improvement of the D-A structure towards harnessing the inherent electric field within the material, ECUT-AQ facilitates efficient migration and clustering of photoexcited electrons towards anthraquinone groups with electron deficiency under visible light (Fig. 20g). On the one hand, the electrons on the anthraquinone undergo the reaction with O_2 present in water to result in the formation of $\bullet O_2^-$, which participates in the reduction of UO_2^{2+} to UO_2; on the other hand, the anthraquinone moiety also serves as a channel for electron transfer, accelerating the transfer of photogenerated charge from the photocatalyst to UO_2^{2+} for the purpose of reducing UO_2^{2+}. As another example, Wang *et al.* [94] have reported an iso-lattice series of multicomponent COFs. They modify 1,3,5-tris(4-aminophenyl)benzene based on simultaneous modification of the chromoquinoline ring and terephthalaldehyde, and change the functional groups on the benzene ring of terephthalaldehyde as a way to optimize the photovoltaic properties of this COFs. Multi-component COFs were involved in the photocatalytic extraction of uranium from natural seawater (U(VI) to U(IV)), after connecting the benzene ring of terephthalaldehyde by using nitro, bromine, pyridine, p-dihydroxy, o-dihydroxy, and methoxy, respectively. Furthermore, using photocatalytic technology to degrade other harmful heavy metals (such as Cr, Mn, Cd, Hg, Co, Cu) in water have gradually attracted the attention of researchers in recent years. The metal-free D-A OPs do not have the risk of secondary metal contamination after the reaction, and its powerful built-in electric field and light response capability also provide a guarantee for the harmless treatment of heavy metals in water.

4. Conclusions and outlook

The existing reviews on D-A OPs photocatalysts primarily focuses on a single category of OPs, such as conjugated polymers or covalent organic frameworks [49,139,219]. And, one of the primary materials discussed in these published reviews is g-C_3N_4 [176,220], cyanoarenes-based organic photocatalysts [85], and other specific materials [221]. Moreover, while most of the discussion centers on elucidating the mechanism and advantages of D-A structure in facilitating charge transfer during photoreactions, a specific methodology for constructing such the D-A structure has not been explicitly proposed [36, 125,172]. Furthermore, the portion of the discussions pertaining to material applications is confined to one side of photocatalytic hydrogen generation, CO_2 reduction, conversion of organic substances, or degradation of pollutants [107,129,222]. Distinguishing itself from the prevalent issues of limited content and superficial discussions have found in previous review papers of similar nature, our review provides a comprehensive analysis and discussion on D-A OPs. It delves into the synthesis method and mechanism, as well as proposes specific measures for addressing environmental and energy challenges using D-A OPs photocatalyst. Besides, it presents potential research directions that have the potential to overcome current bottlenecks.

Firstly, our work stands out by categorizing molecular modification methods into three distinct approaches (monomolecular modification, multimolecular modification, and molecular substitution) and providing comprehensive definitions and detailed discussions on their respective main modification mechanisms. Among them, although single-molecule modification has exhibited remarkable development in the field of modifying OPs, it is important to acknowledge that the modified OPs achieved through single-type micromolecule units are inherently constrained when compared to multi-type. Consequently, exploring the research domain encompassing the modification of multi-type molecular units holds immense scientific value and warrants significant attention. Secondly, this paper highlights the significance of the molecular modular architecture existed in OPs as a key factor contributing to their exceptional suitability for molecular modifications. Furthermore, an innovative concept of functional customization through molecular modification is introduced. It indicates that the D-A structure photocatalyst not only reduces the band gap and broadens the optical properties of the material, but also enhance molecular dipole moment and facilitates intramolecular charge separation and transfer. In this manner, it could compensate for the deficiencies inherent in the original OPs, thereby enhancing the efficiency of material photocatalysis. Finally, we present a comprehensive discourse on the application of modified D-A OPs in the domains of environment and energy, with a particular emphasis on multifaceted approaches to photodegradation pollutants rather than limiting our discussion to a singular aspect. The photocatalytic technology finds extensive applications in renewable energy utilization, environmental pollutant degradation, and redox reaction promotion. Consequently, molecular modification approaches hold immense potential in advancing photocatalysis as they pave a novel pathway towards efficient solar energy utilization within energy and environment-related domains.

The limitations of the current researches on D-A OPs and recommendations for future development are summarized as follows：

(1) The potential of a single substance is inherently limited, necessitating the exploitation of synergistic effects between substances to maximize its photocatalytic performance. In this regard, the selection of molecular building blocks assumes paramount importance. The integration of molecular building blocks with π-bonds into the OPs framework enables the formation of a D-π-A structured OPs. This incorporation not only significantly reduces the charge migration distance within the framework due to the presence of π-π bonds but also facilitates interlayer and intralayer charge transfer to the catalyst surface as delocalized electrons, thereby effectively enhancing charge separation and migration capabilities.

(2) When designing molecular building block compositions, it is advisable to consider combining multiple building blocks with distinct exceptional properties to create a novel polymer that could fully exploit multimolecular synergy. Moreover, considering the generally higher cost of metal-free OPs compared to metal catalysts, identifying cost-effective alternatives while maintaining comparable photocatalytic efficiency becomes a key focus in the subsequent industrialization and commercialization of D-A OPs.

(3) The addition of molecular bridges between electron donors and acceptors increased attention. Molecular bridges serve as the high-speed access for photogenerated charge transfer, facilitating rapid charge transfer in electron donor-acceptor structures and enhancing photocatalytic efficiency.

(4) The D-A OPs synthesized through molecular modification, exhibit remarkable advantages in the selective generation of ROS under light conditions, rapid activation of PMS/PDS, efficient production of H_2/O_2, degradation of pollutants, and promotion of other redox reactions. Compared to conventional metal composite

photocatalysts, the metal-free OPs eliminate the risk of secondary pollution caused by the catalyst itself. Moreover, the D-A structure facilitates the establishment of an internal electric field within the photocatalyst. However, using D-A OPs to product H_2/O_2 at present, most processes still require additional metal-assisted catalysts such as Pt, TiO_2, ZnO, Fe_2O_3 etc., necessitating subsequent treatment for metal degradation in wastewater. Therefore, it is imperative to design OPs with exceptional catalytic performance for H_2/O_2 production without co-catalysts. Additionally, another challenge that needs to be addressed in future studies is how to efficiently activate PMS/PDS while selectively generating a substantial amount of target ROS.

(5) Piezoelectric photocatalysis has gained attention as a potential area of study in the past few years, wherein the material deformation under force generates an internal electric field that enhances pollutant adsorption during degradation and promotes intermolecular charge transfer. By exploring the impact of molecular modification on the piezoelectric properties of OPs through interdisciplinary approaches, it has the potential to create opportunities for enhanced and adaptable utilization of photocatalytic materials.

(6) Most of the theoretical molecular modification results are satisfactory and highly promising, but going down to the molecular level there are still many uncontrollable uncertainties that make it difficult to industrially scale up many excellent ideas.

CRediT authorship contribution statement

Yu Shi: Writing – original draft, Validation, Conceptualization, Investigation. **Yaocheng Deng:** Resources, Methodology, Funding acquisition, Conceptualization, Writing – review & editing. **Rongdi Tang:** Writing – review & editing, Funding acquisition. **Ling Li:** Writing – review & editing. **Sheng Xiong:** Visualization. **Zhanpeng Zhou:** Writing – review & editing, Visualization. **Wenbo Li:** Writing – review & editing. **Ying Huang:** Resources, Funding acquisition. **Jiawei Liu:** Visualization.

Declaration of Competing Interest

No conflict of interest exits in the submission of this manuscript, and the manuscript has approved by all authors for publication. The authors would like to declare that the manuscript is original and has not been published previously, and is not under consideration for publication elsewhere, in whole or in part.

Data Availability

Data will be made available on request.

Acknowledgement

The study was financially supported by the National Natural Science Foundation of China (Grant No.52270156, 51909089), Excellent Youth Project of Hunan Provincial Education Department, China (Grant No. 23B0226), Training Program for Excellent Young Innovators of Changsha (Grant No. kq2209015), China Postdoctoral Science Foundation (Grant No. 2023M731056).

Appendix A. Supporting information

Supplementary data associated with this article can be found in the online version at doi:10.1016/j.apcatb.2024.124043.

References

[1] W.B. Tiffany, H.W. Moos, A.L. Schawlow, Selective laser photocatalysis of bromine reactions: laser light excites gaseous bromine molecules to single bound quantum states near the dissociation continuum, Science 157 (1967) 40–43.
[2] C. Bie, H. Yu, B. Cheng, W. Ho, J. Fan, J. Yu, Design, fabrication, and mechanism of nitrogen-doped graphene-based photocatalyst, Adv. Mater. 33 (2021) e2003521.
[3] J. Zhang, J. Tian, J. Fan, J. Yu, W. Ho, Graphdiyne: a brilliant hole accumulator for stable and efficient planar perovskite solar cells, Small 16 (2020) 1907290.
[4] P. Xia, S. Cao, B. Zhu, M. Liu, M. Shi, J. Yu, Y. Zhang, Designing a 0D/2D S-scheme heterojunction over polymeric carbon nitride for visible-light photocatalytic inactivation of bacteria, Angew. Chem. Int. Ed. 59 (2020) 5218–5225.
[5] F. Xu, K. Meng, B. Zhu, H. Liu, J. Xu, J. Yu, Graphdiyne: a new photocatalytic CO_2 reduction cocatalyst, Adv. Funct. Mater. 29 (2019) 1904256.
[6] A. Schmidt, M. Albrecht, Photocatalytically active materials with pyridinium-enolate partial structures, Edition. Z. Naturforsch., 63b (2008) 465-472.
[7] L. Tang, Y. Deng, G. Zeng, W. Hu, J. Wang, Y. Zhou, J. Wang, J. Tang, W. Fang, CdS/Cu_2S co-sensitized TiO_2 branched nanorod arrays of enhanced photoelectrochemical properties by forming nanoscale heterostructure, J. Alloy. Compd. 662 (2016) 516–527.
[8] Y. Deng, L. Tang, G. Zeng, H. Dong, M. Yan, J. Wang, W. Hu, J. Wang, Y. Zhou, J. Tang, Enhanced visible light photocatalytic performance of polyaniline modified mesoporous single crystal TiO_2 microsphere, Appl. Surf. Sci. 387 (2016) 882–893.
[9] Y. Deng, L. Tang, G. Zeng, C. Feng, H. Dong, J. Wang, H. Feng, Y. Liu, Y. Zhou, Y. Pang, Plasmonic resonance excited dual Z-scheme $BiVO_4$/Ag/Cu_2O nanocomposite: synthesis and mechanism for enhanced photocatalytic performance in recalcitrant antibiotic degradation, Environ. Sci. Nano 4 (2017) 1494–1511.
[10] Y. Deng, L. Tang, G. Zeng, J. Wang, Y. Zhou, J. Wang, J. Tang, Y. Liu, B. Peng, F. Chen, Facile fabrication of a direct Z-scheme Ag_2CrO_4/g-C_3N_4 photocatalyst with enhanced visible light photocatalytic activity, J. Mol. Catal. A-Chem. 421 (2016) 209–221.
[11] Y. Deng, L. Tang, G. Zeng, Z. Zhu, M. Yan, Y. Zhou, J. Wang, Y. Liu, J. Wang, Insight into highly efficient simultaneous photocatalytic removal of Cr(VI) and 2,4-diclorophenol under visible light irradiation by phosphorus doped porous ultrathin g-C_3N_4 nanosheets from aqueous media: performance and reaction mechanism, Appl. Catal. B-Environ. 203 (2017) 343–354.
[12] G. Algara-Siller, N. Severin, S.Y. Chong, T. Björkman, R.G. Palgrave, A. Laybourn, M. Antonietti, Y.Z. Khimyak, A.V. Krasheninnikov, J.P. Rabe, U. Kaiser, A. I. Cooper, A. Thomas, M.J. Bojdys, Triazine-Based Graphitic Carbon Nitride: a Two-Dimensional Semiconductor, Angew. Chem. Int. Ed. 53 (2014) 7450–7455.
[13] A.F. Saber, A.M. Elewa, H.-H. Chou, A.F.M. El-Mahdy, Donor-acceptor carbazole-based conjugated microporous polymers as photocatalysts for visible-light-driven H_2 and O_2 evolution from water splitting, Appl. Catal. B-Environ. 316 (2022) 121624.
[14] X. Gong, S. Yu, M. Guan, X. Zhu, C. Xue, Pyrene-functionalized polymeric carbon nitride with promoted aqueous-organic biphasic photocatalytic CO_2 reduction, J. Mate. Chem. A 7 (2019) 7373–7379.
[15] S. Xiong, Y. Deng, D. Gong, R. Tang, J. Zheng, L. Li, Z. Zhou, L. Su, C. Liao, L. Yang, Magnetically modified in-situ N-doped Enteromorpha prolifera derived biochar for peroxydisulfate activation: Electron transfer induced singlet oxygen non-radical pathway, Chemosphere 284 (2021) 131404.
[16] Y. Deng, L. Tang, G. Zeng, J. Wang, Y. Zhou, J. Wang, J. Tang, L. Wang, C. Feng, Facile fabrication of mediator-free Z-scheme photocatalyst of phosphorous-doped ultrathin graphitic carbon nitride nanosheets and bismuth vanadate composites with enhanced tetracycline degradation under visible light, J. Colloid Interf. Sci. 509 (2018) 219–234.
[17] Y. Deng, L. Tang, C. Feng, G. Zeng, J. Wang, Y. Zhou, Y. Liu, B. Peng, H. Feng, Construction of plasmonic Ag modified phosphorous-doped ultrathin g-C_3N_4 nanosheets/$BiVO_4$ photocatalyst with enhanced visible-near-infrared response ability for ciprofloxacin degradation, J. Hazard. Mater. 344 (2018) 758–769.
[18] Y. Deng, L. Tang, C. Feng, G. Zeng, J. Wang, Y. Lu, Y. Liu, J. Yu, S. Chen, Y. Zhou, Construction of plasmonic Ag and nitrogen-doped graphene quantum dots codecorated ultrathin graphitic carbon nitride nanosheet composites with enhanced photocatalytic activity: Full-spectrum response ability and mechanism insight, Acs Appl. Mater. Inter. 9 (2017) 42816–42828.
[19] R. Tang, D. Gong, Y. Deng, S. Xiong, J. Deng, L. Li, Z. Zhou, J. Zheng, L. Su, L. Yang, π-π stacked step-scheme PDI/g-C_3N_4/TiO_2@Ti_3C_2 photocatalyst with enhanced visible photocatalytic degradation towards atrazine via peroxymonosulfate activation, Chem. Eng. J. 427 (2022) 131809.
[20] H. Liu, D. Chen, Z. Wang, H. Jing, R. Zhang, Microwave-assisted molten-salt rapid synthesis of isotype triazine-/heptazine based g-C_3N_4 heterojunctions with highly enhanced photocatalytic hydrogen evolution performance, Appl. Catal. B-Environ. 203 (2017) 300–313.
[21] Y. Li, F. Gong, Q. Zhou, X. Feng, J. Fan, Q. Xiang, Crystalline isotype heptazine-/triazine-based carbon nitride heterojunctions for an improved hydrogen evolution, Appl. Catal. B-Environ. 268 (2020) 118381.
[22] Y. Deng, L. Li, H. Zeng, R. Tang, Z. Zhou, Y. Sun, C. Feng, D. Gong, J. Wang, Y. Huang, Unveiling the origin of high-efficiency charge transport effect of C_3N_5/C_3N_4 homojunction for activating peroxymonosulfate to degrade atrazine under visible light, Chem. Eng. J. 457 (2023) 141261.
[23] R. Tang, D. Gong, Y. Zhou, Y. Deng, C. Feng, S. Xiong, Y. Huang, G. Peng, L. Li, Unique g-C_3N_4/PDI-g-C_3N_4 homojunction with synergistic piezo-photocatalytic

effect for aquatic contaminant control and H_2O_2 generation under visible light, Appl. Catal. B-Environ. 303 (2022) 120929.
[24] J. Yang, Y. Liang, K. Li, G. Yang, K. Wang, R. Xu, X. Xie, One-step synthesis of novel K^+ and cyano groups decorated triazine-/heptazine-based g-C_3N_4 tubular homojunctions for boosting photocatalytic H_2 evolution, Appl. Catal. B-Environ. 262 (2020) 118252.
[25] B. Wu, X. Jiang, Y. Liu, Q.-Y. Li, X. Zhao, X.-J. Wang, Vinylene-bridged donor-acceptor type porous organic polymers for enhanced photocatalysis of amine oxidative coupling reactions under visible light, RSC Adv. 11 (2021) 33653–33660.
[26] Z. Xie, W. Wang, X. Ke, X. Cai, X. Chen, S. Wang, W. Lin, X. Wang, A heptazine-based polymer photocatalyst with donor-acceptor configuration to promote exciton dissociation and charge separation, Appl. Catal. B-Environ. 325 (2023) 122312.
[27] Y. Zhang, Q. Cao, A. Meng, X. Wu, Y. Xiao, C. Su, Q. Zhang, Molecular Heptazine-Triazine Junction over Carbon Nitride Frameworks for Artificial Photosynthesis of Hydrogen Peroxide, Adv. Mater. 35 (2023) 2306831.
[28] Z. Fu, X. Wang, A.M. Gardner, X. Wang, S.Y. Chong, G. Neri, A.J. Cowan, L. Liu, X. Li, A. Vogel, R. Clowes, M. Bilton, L. Chen, R.S. Sprick, A.I. Cooper, A stable covalent organic framework for photocatalytic carbon dioxide reduction, Chem. Sci. 11 (2020) 543–550.
[29] A.P. Coté, A.I. Benin, N.W. Ockwig, M. O'Keeffe, A.J. Matzger, O.M. Yaghi, Porous, Crystalline, Covalent Organic Frameworks, Science 310 (2005) 1166–1170.
[30] Y. Deng, L. Tang, C. Feng, G. Zeng, Z. Chen, J. Wang, H. Feng, B. Peng, Y. Liu, Y. Zhou, Insight into the dual-channel charge-charrier transfer path for nonmetal plasmonic tungsten oxide based composites with boosted photocatalytic activity under full-spectrum light, Appl. Catal. B-Environ. 235 (2018) 225–237.
[31] Y. Liu, Q. Chen, Y. Tong, Y. Ma, 9,9-dimethyl dihydroacridine-based organic photocatalyst for atom transfer radical polymerization from modifying "unstable" electron donor, Macromolecules 53 (2020) 7053–7062.
[32] C.-L. Chang, A.M. Elewa, J.H. Wang, H.-H. Chou, A.F.M. El-Mahdy, Donor–acceptor conjugated microporous polymers based on Thiazolo[5,4-d] thiazole building block for high-performance visible-light-induced H_2 production, Microporous Mesoporous. Mater. 345 (2022) 112258.
[33] B.P. Biswal, H.A. Vignolo-González, T. Banerjee, L. Grunenberg, G. Savasci, K. Gottschling, J. Nuss, C. Ochsenfeld, B.V. Lotsch, Sustained solar H_2 evolution from a thiazolo[5,4-d]thiazole-bridged covalent organic framework and nickel-thiolate cluster in water, J. Am. Chem. Soc. 141 (2019) 11082–11092.
[34] L. Guo, S. Jin, Stable covalent organic frameworks for photochemical applications, Chemphotochem 3 (2019) 973–983.
[35] W. Zhang, Z. Deng, J. Deng, C.-T. Au, Y. Liao, H. Yang, Q. Liu, Regulating the exciton binding energy of covalent triazine frameworks for enhancing photocatalysis, J. Mater. Chem. A 10 (2022) 22419–22427.
[36] C. Yang, B. Cheng, J. Xu, J. Yu, S. Cao, Donor-acceptor-based conjugated polymers for photocatalytic energy conversion, Energychem (2023) 100116.
[37] F.F. Giuseppe, Mattioli, and aldo amore bonapasta, reaction intermediates in the photoreduction of oxygen molecules at the (101) TiO_2 (Anatase) Surface, J. Am. Chem. Soc. 128 (2006) 13772–13780.
[38] P.V. Kamat, Meeting the clean energy demand: nanostructure architectures for solar energy conversion, , J. Phys. Chem. C 111 (2007) 2834–2860.
[39] E.M. Kosower, H. Dodiuk, K. Tanizawa, M. Ottolenghi, N. Orbach, Intramolecular donor-acceptor systems. Radiative and nonradiative processes for the excited states of 2-N-arylamino-6-naphthalenesulfonat, J. Am. Chem. Soc. 97 (1975) 2167–2178.
[40] R. Jiang, G. Lu, J. Liu, D. Wu, Z. Yan, Y. Wang, Incorporation of π-conjugated molecules as electron donors in g-C_3N_4 enhances photocatalytic H_2-production, Renew. Energy 164 (2021) 531–540.
[41] C. Zhang, Z. Ouyang, Y. Yang, X. Long, L. Qin, W. Wang, Y. Zhou, D. Qin, F. Qin, C. Lai, Molecular engineering of donor-acceptor structured g-C_3N_4 for superior photocatalytic oxytetracycline degradation, Chem. Eng. J. 448 (2022) 137370.
[42] Q. Zhang, J. Chen, H. Che, P. Wang, B. Liu, Y. Ao, Recent advances in g-C_3N_4-based donor–acceptor photocatalysts for photocatalytic hydrogen evolution: an exquisite molecular structure engineering, ACS Mater. Lett. 4 (2022) 2166–2186.
[43] K.S. Kei Ohkubo, Kohei Morikawa, Shunichi Fukuzumi, Selective oxygenation of ring-substituted toluenes with electron-donating and -withdrawing substituents by molecular oxygen via photoinduced electron transfer, J. Am. Chem. Soc. 125 (2003) 12850–12859.
[44] M. Karnahl, C. Kuhnt, F. Ma, A. Yartsev, M. Schmitt, B. Dietzek, S. Rau, J. Popp, Tuning of photocatalytic hydrogen production and photoinduced intramolecular electron transfer rates by regioselective bridging ligand substitution, Chemphyschem 12 (2011) 2101–2109.
[45] X. Zhou, B. Xu, J. Zhang, Q. Zhao, C. Li, H. Dong, X. Wang, J. Yang, Regulated effect of organic small molecular doped in carbon nitride skeleton for boosting photocatalytic hydrogen evolution, Int. J. Hydrog. Energ. 46 (2021) 38299–38309.
[46] H.A. Al Attar, A.P. Monkman, Electric field induce blue shift and intensity enhancement in 2D exciplex organic light emitting diodes; controlling electron-hole separation, Adv. Mater. 28 (2016) 8014–8020.
[47] A. Liu, S. Zhao, S.B. Rim, J. Wu, M. Könemann, P. Erk, P. Peumans, Control of electric field strength and orientation at the donor–acceptor interface in organic solar cells, Adv. Mater. 20 (2008) 1065–1070.
[48] W.-J. Sun, H.-Q. Ji, L.-X. Li, H.-Y. Zhang, Z.-K. Wang, J.-H. He, J.-M. Lu, Built-in electric field triggered interfacial accumulation effect for efficient nitrate removal at ultra-low concentration and electroreduction to ammonia, Angew. Chem. Int. Ed. 60 (2021) 22933–22939.
[49] J. Zhao, J. Ren, G. Zhang, Z. Zhao, S. Liu, W. Zhang, L. Chen, Donor-acceptor type covalent organic frameworks, Chem. -Eur. J. 27 (2021) 10781–10797.
[50] H. Fang, J. Gao, J. Wang, J. Xu, L. Wang, Oxygen-doped and pyridine-grafted g-C_3N_4 for visible-light driven peroxymonosulfate activation: Insights of enhanced tetracycline degradation mechanism, Sep. Purif. Technol. 314 (2023) 123565.
[51] W. Xing, F. Ma, Z. Li, A. Wang, M. Liu, J. Han, G. Wu, W. Tu, Edge effect-modulated exciton dissociation and charge transfer in porous ultrathin tubular graphitic carbon nitride for boosting photoredox activity, J. Mate. Chem. A 10 (2022) 18333–18342.
[52] F. Zhang, X. Ma, X. Dong, X. Miao, X. Lang, Inserting acetylene into an olefin-linked covalent organic framework for boosting the selective photocatalytic aerobic oxidation of sulfides, Chem. Eng. J. 451 (2023) 138802.
[53] H. Che, P. Wang, J. Chen, X. Gao, B. Liu, Y. Ao, Rational design of donor-acceptor conjugated polymers with high performance on peroxydisulfate activation for pollutants degradation, Appl. Catal. B-Environ. 316 (2022) 121611.
[54] O.M. Yaghi, H. Li, C. Davis, D. Richardson, T.L. Groy, Synthetic strategies, structure patterns, and emerging properties in the chemistry of modular porous solids, Acc. Chem. Res. 31 (1998) 474–484.
[55] S. Tang, Y.-S. Xu, X.-L. Hu, W.-D. Zhang, Bifunctionalization of carbon nitride by incorporation of thiophene ring and polar nickel complex to promote photocatalytic activity for hydrogen evolution, J. Colloid Interf. Sci. 648 (2023) 898–906.
[56] L. Li, X. Tang, S. Huang, C. Lu, D. Lützenkirchen-Hecht, K. Yuan, X. Zhuang, Y. Chen, Longitudinally Grafting of Graphene with Iron Phthalocyanine-based Porous Organic Polymer to Boost Oxygen Electroreduction, Angew. Chem. Int. Ed. 62 (2023) e202301642.
[57] Z. Li, S. Han, C. Li, P. Shao, H. Xia, H. Li, X. Chen, X. Feng, X. Liu, Screening metal-free photocatalysts from isomorphic covalent organic frameworks for the C-3 functionalization of indoles, J. Mate. Chem. A 8 (2020) 8706–8715.
[58] H. Guo, C.-G. Niu, C. Liang, H.-Y. Niu, Y.-Y. Yang, H.-Y. Liu, N. Tang, H.-X. Fang, Highly crystalline porous carbon nitride with electron accumulation capacity: Promoting exciton dissociation and charge carrier generation for photocatalytic molecular oxygen activation, Chem. Eng. J. 409 (2021) 128030.
[59] S. Li, L. Li, Y. Li, L. Dai, C. Liu, Y. Liu, J. Li, J. Lv, P. Li, B. Wang, Fully conjugated donor-acceptor covalent organic frameworks for photocatalytic oxidative amine coupling and thioamide cyclization, ACS Catal. 10 (2020) 8717–8726.
[60] J. Xiao, X. Liu, L. Pan, C. Shi, X. Zhang, J.-J. Zou, Heterogeneous photocatalytic organic transformation reactions using conjugated polymers-based materials, ACS Catal. 10 (2020) 12256–12283.
[61] B. Yin, Z. Chen, S. Pang, X. Yuan, Z. Liu, C. Duan, F. Huang, Y. Cao, The renaissance of oligothiophene-based donor-acceptor polymers in organic solar cells, Adv. Energy Mater. 12 (2022) 210450.
[62] F. Wang, R. Liao, F. Wang, Pathway Control of π-Conjugated Supramolecular Polymers by Incorporating Donor-Acceptor Functionality, Angew. Chem. Int. Ed. 62 (2023) e202305827.
[63] G. Tang, J. Li, Y. Lu, T. Song, S. Yin, G. Mao, B. Long, A. Ali, G.-J. Deng, Donor-acceptor organic polymer with sulfur bridge for superior photocatalytic CO_2 reduction to CH_4 under visible light illumination, Chem. Eng. J. 451 (2023) 138744.
[64] Z. Luo, X. Chen, Y. Hu, X. Chen, W. Lin, X. Wu, X. Wang, Side-chain molecular engineering of triazole-based donor-acceptor polymeric photocatalysts with strong electron push-pull interactions, Angew. Chem. Int. Ed. 62 (2023) e202304875.
[65] R. Liang, J. Luo, S. Lin, Z. Li, Z. Dong, Y. Wu, Y. Wang, X. Cao, C. Meng, F. Yu, Y. Liu, Z. Zhang, Boosting the photoreduction uranium activity for donor-acceptor-acceptor type conjugated microporous polymers by statistical copolymerization, Sep. Purif. Technol. 312 (2023) 123291.
[66] X. Yu, Y. Xu, Y. Tian, Z. Li, Z. Wang, Y. Weng, J. Wu, Y. Wu, B. Tian, Engineering D-A polymer polarity in heterostructure photocatalyst for improved interfacial charge transfer efficiency, Appl. Surf. Sci. 637 (2023) 157918.
[67] C.N.R. Rao, S.N. Bhat, P.C. Dwedi, Spectroscopy of electron donor-acceptor systems, Appl. Spectrosc. Rev. 5 (1972) 1–170.
[68] A. Ayyappanpillai, Donor-acceptor type low band gap polymers: polysquaraines and related systems, Chem. Soc. Rev. 32 (2003) 181–191.
[69] B. Albinsson, M.P. Eng, K. Pettersson, M.U. Winters, Electron and energy transfer in donor-acceptor systems with conjugated molecular bridges, Phys. Chem. Chem. Phys. 9 (2007) 5847–5864.
[70] Z. Weng, Y. Lin, B. Han, X. Zhang, Q. Guo, Y. Luo, X. Ou, Y. Zhou, J. Jiang, Donor-acceptor engineered g-C_3N_4 enabling peroxymonosulfate photocatalytic conversion to $^1O_2$ with nearly 100% selectivity, J. Hazard. Mater. 448 (2023) 130869.
[71] A. Hayat, M. Sohail, U. Anwar, T.A. Taha, K.S. El-Nasser, A.M. Alenad, A.G. Al-Sehemi, N. Ahmad Alghamdi, O.A. Al-Hartomy, M.A. Amin, A. Alhadhrami, A. Palamanit, S.K.B. Mane, W.I. Nawawi, Z. Ajmal, Enhanced photocatalytic overall water splitting from an assembly of donor-π-acceptor conjugated polymeric carbon nitride, J. Colloid Interf. Sci. 624 (2022) 411–422.
[72] S. Cao, H. Liu, Z. Jia, M. Guo, W. Gao, Z. Ding, W. Yang, L. Chen, W. Wang, Controllable adsorption groups on amine-functionalized carbon nitride for enhanced photocatalytic CO_2 reduction, Chem. Eng. J. 455 (2023) 140746.
[73] T. Xia, Z. Wu, Y. Liang, W. Wang, Y. Li, Z. Sui, L. Shan, C. Li, R. Fan, Q. Chen, sp^2 carbon-conjugated covalent organic frameworks for efficient photocatalytic degradation and visualized pH detection, Mater. Today Chem. 25 (2022) 100962.
[74] H.-Y. Yu, J.-S. Wang, F.-Y. Xie, Q. Yang, Y. Chen, L. Zhao, Y. Li, W.-J. Ruan, A stack-guiding unit constructed 2D COF with improved charge carrier transport and versatile photocatalytic functions, Chem. Eng. J. 445 (2022) 136713.

[75] R. Tang, H. Zeng, D. Gong, Y. Deng, S. Xiong, L. Li, Z. Zhou, J. Wang, C. Feng, L. Tang, Thin-walled vesicular Triazole-CN-PDI with electronic n→π* excitation and directional movement for enhanced atrazine photodegradation, Chem. Eng. J. 451 (2023) 138445.
[76] W.-K. An, S.-J. Zheng, X. Xu, L.-J. Liu, J.-S. Ren, L. Fan, Z.-K. Yang, Y. Ren, C. Xu, Integrating benzofuran and heteroradialene into donor-acceptor covalent organic frameworks for photocatalytic construction of multi-substituted olefins, Appl. Catal. B-Environ. 316 (2022) 121630.
[77] L. Li, H. Zeng, R. Tang, Z. Zhou, S. Xiong, W. Li, Y. Huang, Y. Deng, Carbon nitride with grafted molecular as electron acceptor and active site to achieve efficient photo-activated peroxymonosulfate for organic pollutants removal, Appl. Catal. B-Environ. 345 (2024) 123693.
[78] J.-X. Jiang, A. Trewin, D.J. Adams, A.I. Cooper, Band gap engineering in fluorescent conjugated microporous polymers, Chem. Sci. 2 (2011) 1777–1781.
[79] G.H. Bertrand, V.K. Michaelis, T.C. Ong, R.G. Griffin, M. Dinca, Thiophene-based covalent organic frameworks, Pnas 110 (2013) 4923–4928.
[80] Z. Wang, S. Ghasimi, K. Landfester, K.A. Zhang, Molecular structural design of conjugated microporous poly(Benzooxadiazole) networks for enhanced photocatalytic activity with visible light, Adv. Mater. 27 (2015) 6265–6270.
[81] L. Ascherl, T. Sick, J.T. Margraf, S.H. Lapidus, M. Calik, C. Hettstedt, K. Karaghiosoff, M. Döblinger, T. Clark, K.W. Chapman, F. Auras, T. Bein, Molecular docking sites designed for the generation of highly crystalline covalent organic frameworks, Nat. Chem. 8 (2016) 310–316.
[82] F. Auras, L. Ascherl, A.H. Hakimioun, J.T. Margraf, F.C. Hanusch, S. Reuter, D. Bessinger, M. Doblinger, C. Hettstedt, K. Karaghiosoff, S. Herbert, P. Knochel, T. Clark, T. Bein, Synchronized offset stacking: A concept for growing large-domain and highly crystalline 2D covalent organic frameworks, J. Am. Chem. Soc. 138 (2016) 16703–16710.
[83] H. Ou, X. Chen, L. Lin, Y. Fang, X. Wang, Biomimetic donor-acceptor motifs in conjugated polymers for promoting exciton splitting and charge separation, Angew. Chem. Int. Ed. 57 (2018) 8729–8733.
[84] R. Chen, J.L. Shi, Y. Ma, G. Lin, X. Lang, C. Wang, Designed synthesis of a 2D porphyrin-based sp^2 carbon-conjugated covalent organic framework for heterogeneous photocatalysis, Angew. Chem. Int. Ed. 58 (2019) 6430–6434.
[85] H.M. Ko, C.W. Lee, M.S. Kwon, Degradation Behavior of Donor-acceptor Cyanoarenes-based Organic Photocatalysts, ChemCatChem 15 (2023) e202300661.
[86] H. Fattahimoghaddam, B.-K. Lee, A concise review of recent advances in carbon nitride-based intramolecular donor–acceptor architectures for photocatalytic hydrogen production: Heteromolecular coupling of organic compounds, J. Alloy. Compd. 968 (2023) 172000.
[87] Y. Hou, F. Liu, C. Nie, Z. Li, M. Tong, Boosting exciton dissociation and charge transfer in triazole-based covalent organic frameworks by increasing the donor unit from one to two for the efficient photocatalytic elimination of emerging contaminants, Environ. Sci. Technol. 57 (2023) 11675–11686.
[88] Z. Deng, H. Zhao, X. Cao, S. Xiong, G. Li, J. Deng, H. Yang, W. Zhang, Q. Liu, Enhancing built-in electric field via molecular dipole control in conjugated microporous polymers for boosting charge separation, ACS Appl. Mater. Inter. 14 (2022) 35745–35754.
[89] C. Li, H. Wu, D. Zhu, T. Zhou, M. Yan, G. Chen, J. Sun, G. Dai, F. Ge, H. Dong, High-efficient charge separation driven directionally by pyridine rings grafted on carbon nitride edge for boosting photocatalytic hydrogen evolution, Appl. Catal. B-Environ. 297 (2021) 120433.
[90] H. Zhang, X. Chen, Z. Zhang, K. Yu, W. Zhu, Y. Zhu, Highly-crystalline Triazine-PDI Polymer with an Enhanced Built-in Electric Field for Full-Spectrum Photocatalytic Phenol Mineralization, Appl. Catal. B-Environ. 287 (2021) 119957.
[91] Q. Zhuang, H. Chen, C. Zhang, S. Cheng, W. Dong, A. Xie, Rapid chromium reduction by metal-free organic polymer photocatalysis via molecular engineering, J. Hazard. Mater. 434 (2022) 128938.
[92] K. Wu, X.-Y. Liu, M. Xie, P.-W. Cheng, J. Zheng, W. Lu, D. Li, Rational design of D-π-A-π-D porous organic polymer with polarized π for photocatalytic aerobic oxidation, Appl. Catal. B-Environ. 334 (2023) 122847.
[93] F. Liu, Y. He, X. Liu, Z. Wang, H.-L. Liu, X. Zhu, C.-C. Hou, Y. Weng, Q. Zhang, Y. Chen, Regulating Excitonic Effects in Covalent Organic Frameworks to Promote Free Charge Carrier Generation, Acs Catal. 12 (2022) 9494–9502.
[94] H. Yang, M. Hao, Y. Xie, X. Liu, Y. Liu, Z. Chen, X. Wang, G.I.N. Waterhouse, S. Ma, Tuning local charge distribution in multicomponent covalent organic frameworks for dramatically enhanced photocatalytic uranium extraction, Angew. Chem. Int. Ed. 62 (2023) e202303129.
[95] Y. Zheng, L. Zhang, Y. Li, Y. Wang, J. Chen, B. Lin, Y. Zheng, L. Cheng, S. Wang, Y. Chen, Triptycene incorporated carbon nitride based donor-acceptor conjugated polymers with superior visible-light photocatalytic activities, J. Colloid Interf. Sci. 622 (2022) 675–689.
[96] J. Yang, S. Ghosh, J. Roeser, A. Acharjya, C. Penschke, Y. Tsutsui, J. Rabeah, T. Wang, S.Y. Djoko Tameu, M.Y. Ye, J. Gruneberg, S. Li, C. Li, R. Schomacker, R. Van De Krol, S. Seki, P. Saalfrank, A. Thomas, Constitutional isomerism of the linkages in donor-acceptor covalent organic frameworks and its impact on photocatalysis, Nat. Commun. 13 (2022) 6317.
[97] X. Xu, R. Sa, W. Huang, Y. Sui, W. Chen, G. Zhou, X. Li, Y. Li, H. Zhong, Conjugated organic polymers with anthraquinone redox centers for efficient photocatalytic hydrogen peroxide production from water and oxygen under visible light irradiation without any additives, Am. Chem. Soc. 12 (2022) 12954–12963.
[98] C. Yang, B. Wang, L. Zhang, L. Yin, X. Wang, Synthesis of layered carbonitrides from biotic molecules for photoredox transformations, Angew. Chem. Int. Ed. 129 (2017) 1–6.
[99] Y. Shiraishi, T. Takii, T. Hagi, S. Mori, Y. Kofuji, Y. Kitagawa, S. Tanaka, S. Ichikawa, T. Hirai, Resorcinol-formaldehyde resins as metal-free semiconductor photocatalysts for solar-to-hydrogen peroxide energy conversion, Nat. Mater. 18 (2019) 985–993.
[100] Z. Teng, W. Cai, S. Liu, C. Wang, Q. Zhang, S. Chenliang, T. Ohno, Bandgap engineering of polymetric carbon nitride copolymerized by 2,5,8-triamino-tri-s-triazine (melem) and barbituric acid for efficient nonsacrificial photocatalytic H_2O_2 production, Appl. Catal. B-Environ. 271 (2020) 118917.
[101] T. Bhoyar, D.J. Kim, B.M. Abraham, S. Tonda, N.R. Manwar, D. Vidyasagar, S. S. Umare, Tailoring photoactivity of polymeric carbon nitride via donor-π-acceptor network, Appl. Catal. B-Environ. 310 (2022) 121347.
[102] Q. Zhang, J. Chen, X. Gao, H. Che, P. Wang, B. Liu, Y. Ao, Enhanced photocatalytic degradation of bisphenol A by a novel donor-acceptor g-C_3N_4: π-π interactions boosting the adsorption and electron transfer behaviors, Sep. Purif. Technol. 300 (2022) 121947.
[103] J.B. ÜNSOW, T.S. Kelby, W.T.S. Huck, Polymer brushes: Routes toward mechanosensitive surfaces, Acc. Chem. Res. 43 (2009) 466–474.
[104] M. Mohamed Samy, I.M.A. Mekhemer, M.G. Mohamed, M. Hammad Elsayed, K.-H. Lin, Y.-K. Chen, T.-L. Wu, H.-H. Chou, S.-W. Kuo, Conjugated microporous polymers incorporating thiazolo[5,4-d]thiazole moieties for sunlight-driven hydrogen production from water, Chem. Eng. J. 446 (2022) 137158.
[105] J. Feng, J. Cheng, J. Pang, M. Tang, Z. Liu, C. Rong, R. Tan, Donor–acceptor covalent organic framework promotes visible light-induced oxidative coupling of amines to imines in air, Catal. Sci. Technol. 12 (2022) 6865–6874.
[106] J.L. Shi, R. Chen, H. Hao, C. Wang, X. Lang, 2D sp^2 carbon-conjugated porphyrin covalent organic framework for cooperative photocatalysis with TEMPO, Angew. Chem. Int. Ed. 59 (2020) 9088–9093.
[107] T.-X. Wang, H.-P. Liang, D.A. Anito, X. Ding, B.-H. Han, Emerging applications of porous organic polymers in visible-light photocatalysis, J. Mater. Chem. A 8 (2020) 7003–7034.
[108] Q. Li, J. Li, W.R. Wang, L.N. Liu, Z.W. Xu, G. Xie, J. Li, J. Yao, W.S. Li, Tuning acceptor length in photocatalytic donor-acceptor conjugated polymers for efficient solar-to-hydrogen energy conversion, Chin. J. Chem. 40 (2022) 2457–2467.
[109] Y. Hou, F. Liu, B. Zhang, M. Tong, Thiadiazole-Based Covalent Organic Frameworks with a Donor-Acceptor Structure: Modulating Intermolecular Charge Transfer for Efficient Photocatalytic Degradation of Typical Emerging Contaminants, Environ. Sci. Technol. 56 (2022) 16303–16314.
[110] Y. Wang, F. Silveri, M.K. Bayazit, Q. Ruan, Y. Li, J. Xie, C.R.A. Catlow, J. Tang, Bandgap engineering of organic semiconductors for highly efficient photocatalytic water splitting, Adv. Energy Mater. 8 (2018) 1801084.
[111] Y. Yan, J. Chen, N. Li, J. Tian, K. Li, J. Jiang, J. Liu, Q. Tian, P. Chen, Systematic bandgap engineering of graphene quantum dots and applications for photocatalytic water splitting and CO_2 reduction, ACS Nano 12 (2018) 3523–3532.
[112] M.G. Schwab, M. Hamburger, X. Feng, J. Shu, H.W. Spiess, X. Wang, M. Antonietti, K. Mullen, Photocatalytic hydrogen evolution through fully conjugated poly(azomethine) networks, Chem. Commun. 46 (2010) 8932–8934.
[113] S. Han, Z. Li, S. Ma, Y. Zhi, H. Xia, X. Chen, X. Liu, Bandgap engineering in benzotrithiophene-based conjugated microporous polymers: a strategy for screening metal-free heterogeneous photocatalysts, J. Mater. Chem. A 9 (2021) 3333–3340.
[114] Z.J. Wang, S. Ghasimi, K. Landfester, K.A.I. Zhang, Bandgap engineering of conjugated nanoporous poly-benzobis-thiadiazoles via copolymerization for enhanced photocatalytic 1,2,3,4-tetrahydroquinoline synthesis under visible light, Adv. Synth. Catal. 358 (2016) 2576–2582.
[115] Y. Cui, Z. Ding, X. Fu, X. Wang, Construction of conjugated carbon nitride nanoarchitectures in solution at low temperatures for photoredox catalysis, Angew. Chem. Int. Ed. 51 (2012) 11814–11818.
[116] J. Zhang, M. Zhang, S. Lin, X. Fu, X. Wang, Molecular doping of carbon nitride photocatalysts with tunable bandgap and enhanced activity, J. Catal. 310 (2014) 24–30.
[117] Z.-A. Lan, Y. Fang, Y. Zhang, X. Wang, Photocatalytic oxygen evolution from functional triazine-based polymers with tunable band structures, Angew. Chem. Int. Ed. 130 (2018) 479–483.
[118] J. Chen, L. Han, S. Wang, Y. Zhang, J. Zhang, S. Feng, J. Du, Tris(4-ethynylphenyl)amine-Based Conjugated Microporous Polymers and Its Photocatalytic Water Splitting Hydrogen Evolution, Chin. J. Org. Chem. 42 (2022) 2967–2974.
[119] Y. Deng, Z. Zhou, H. Zeng, R. Tang, L. Li, J. Wang, C. Feng, D. Gong, L. Tang, Y. Huang, Phosphorus and kalium co-doped g-C_3N_4 with multiple-locus synergies to degrade atrazine: Insights into the depth analysis of the generation and role of singlet oxygen, Appl. Catal. B-Environ. 320 (2023) 121942.
[120] R. Tang, D. Gong, Y. Deng, S. Xiong, J. Zheng, L. Li, Z. Zhou, L. Su, J. Zhao, π-π stacking derived from graphene-like biochar/g-C_3N_4 with tunable band structure for photocatalytic antibiotics degradation via peroxymonosulfate activation, J. Hazard. Mater. 423 (2022) 126944.
[121] R. Tang, H. Zeng, C. Feng, S. Xiong, L. Li, Z. Zhou, D. Gong, L. Tang, Y. Deng, Twisty C-TiO_2/PCN S-scheme heterojunction with enhanced n→π * electronic excitation for promoted piezo-photocatalytic effect, Small 19 (2023) 2207636.
[122] Z. Zhou, H. Zeng, L. Li, R. Tang, S. Xiong, D. Gong, Y. Huang, Y. Deng, Internal electric fields drive dual S-scheme heterojunctions: insights into the role of the triple interlaced lattice, J. Colloid Interf. Sci. 650 (2023) 1138–1151.

[123] R. Tang, H. Zeng, Y. Deng, S. Xiong, L. Li, Z. Zhou, J. Wang, L. Tang, Dual modulation on peroxymonosulfate activation site and photocarrier separation in carbon nitride for efficient photocatalytic organics degradation: efficacy and mechanism evaluation, Appl. Catal. B-Environ. 336 (2023) 122918.
[124] Z.A. Lan, G. Zhang, X. Chen, Y. Zhang, K.A.I. Zhang, X. Wang, Reducing the exciton binding energy of donor-acceptor-based conjugated polymers to promote charge-induced reactions, Angew. Chem. Int. Ed. 58 (2019) 10236–10240.
[125] C. Müller, S. Bold, M. Chavarot-Kerlidou, B. Dietzek-Ivanšić, Photoinduced electron transfer in triazole-bridged donor-acceptor dyads-a critical perspective, Coord. Chem. Rev. 472 (2022) 214764.
[126] Z. Luo, X. Chen, Y. Hu, X. Chen, W. Lin, X. Wu, X. Wang, Side-Chain Molecular Engineering of Triazole-Based Donor-Acceptor Polymeric Photocatalysts with Strong Electron Push-Pull Interactions, Angew. Chem. Int. Ed. 62 (2023) e202304875.
[127] F. Yu, Z. Zhu, C. Li, W. Li, R. Liang, S. Yu, Z. Xu, F. Song, Q. Ren, Z. Zhang, A redox-active perylene-anthraquinone donor-acceptor conjugated microporous polymer with an unusual electron delocalization channel for photocatalytic reduction of uranium (VI) in strongly acidic solution, Appl. Catal. B-Environ. 314 (2022) 121467.
[128] X. Fan, L. Zhang, R. Cheng, M. Wang, M. Li, Y. Zhou, J. Shi, Construction of g-C_3N_4-based intramolecular donor-acceptor conjugated copolymers for photocatalytic hydrogen evolution, ACs Catal. 5 (2015) 5008–5015.
[129] C. Zhao, Z. Chen, R. Shi, X. Yang, T. Zhang, Recent Advances in Conjugated Polymers for Visible-Light-Driven Water Splitting, Adv. Mater. 32 (2020) e1907296.
[130] P. Sun, P. Wang, D. Yan, Q. Liu, W. Zhang, J. Deng, Q. Liu, Boosting charge separation in conjugated microporous polymers via fluorination for enhancing photocatalysis, Catal. Sci. Technol. 12 (2022) 5942–5951.
[131] R.S. Sprick, B. Bonillo, R. Clowes, P. Guiglion, N.J. Brownbill, B.J. Slater, F. Blanc, M.A. Zwijnenburg, D.J. Adams, A.I. Cooper, Visible-light-driven hydrogen evolution using planarized conjugated polymer photocatalysts, Angew. Chem. Int. Ed. 128 (2016) 1824–1828.
[132] R. Yin, Y. Li, K. Zhong, H. Yao, Y. Zhang, K. Lai, Multifunctional property exploration: $Bi_4O_5I_2$ with high visible light photocatalytic performance and a large nonlinear optical effect, RSC Adv. 9 (2019) 4539–4544.
[133] Y. Liu, W. Yao, D. Liu, R. Zong, M. Zhang, X. Ma, Y. Zhu, Enhancement of visible light mineralization ability and photocatalytic activity of $BiPO_4$/BiOI, Appl. Catal. B-Environ. 163 (2015) 547–553.
[134] C. Xia, W. Xiong, J. Du, T. Wang, Y. Peng, J. Li, Universality of electronic characteristics and photocatalyst applications in the two-dimensional Janus transition metal dichalcogenides, Phys. Rev. B 98 (2018) 165424.
[135] Z. Lou, P. Wang, B. Huang, Y. Dai, X. Qin, X. Zhang, Z. Wang, Y. Liu, Enhancing charge separation in photocatalysts with internal polar electric fields, Chemphotochem 1 (2017) 136–147.
[136] Z. Li, Y. Dai, X. Ma, Y. Zhu, B. Huang, Tuning photocatalytic performance of the near-infrared-driven photocatalyst $Cu_2(OH)PO_4$ based on effective mass and dipole moment, Phys. Chem. Chem. Phys. 16 (2014) 3267–3273.
[137] H. Liu, C. Li, H. Li, Y. Ren, J. Chen, J. Tang, Q. Yang, Structural engineering of two-dimensional covalent organic frameworks for visible-light-driven organic transformations, Acs Appl. Mater. Inter. 12 (2020) 20354–20365.
[138] J. Yu, S. Chang, X. Xu, X. He, C. Zhang, Photocatalytic hydrogen evolution based on nitrogen-containing donor-acceptor (D-A) organic conjugated small molecules, ACS Sustain. Chem. Eng. 8 (2020) 14253–14261.
[139] Y. Jing, X. Zhu, S. Maier, T. Heine, 2D conjugated polymers: exploiting topological properties for the rational design of metal-free photocatalysts, Trends Chem. 4 (2022) 792–806.
[140] H. Che, C. Liu, G. Che, G. Liao, H. Dong, C. Li, N. Song, C. Li, Facile construction of porous intramolecular g-C_3N_4-based donor-acceptor conjugated copolymers as highly efficient photocatalysts for superior H_2 evolution, Nano Energy 67 (2020) 104273.
[141] S. Mushtaq, S. Bi, F. Zhang, M.M. Naseer, Fully unsaturated all-carbon bifluorenylidene-based polymeric frameworks: synthesis and efficient photocatalysis, N. J. Chem. 46 (2022) 17374–17385.
[142] W. Chen, Z. Yang, Z. Xie, Y. Li, X. Yu, F. Lu, L. Chen, Benzothiadiazole functionalized D-A type covalent organic frameworks for effective photocatalytic reduction of aqueous chromium(VI), J. Mater. Chem. A 7 (2019) 998–1004.
[143] S.-N. Zhang, Q.-Y. Li, Y.-X. Lin, S.-Y. Xia, D. Xu, J.-S. Chen, X.-H. Li, Solar-driven C–H functionalization over metal-free polymer with tunable donor–acceptor interface, ACS Catal. 13 (2023) 12917–12923.
[144] C. Shu, X. Yang, L. Liu, X. Hu, R. Sun, X. Yang, A.I. Cooper, B. Tan, X. Wang, Mixed-linker strategy for the construction of sulfone-containing D-A-A covalent organic frameworks for efficient photocatalytic hydrogen peroxide production, Angew. Chem. Int. Ed. (2024) e202403926.
[145] L. Wang, L. Wang, Y. Xu, G. Sun, W. Nie, L. Liu, D. Kong, Y. Pan, Y. Zhang, H. Wang, Y. Huang, Z. Liu, H. Ren, T. Wei, Y. Himeda, Z. Fan, Schottky Junction and D-A_1-A_2 System Dual Regulation of Covalent Triazine Frameworks for Highly Efficient CO_2 Photoreduction, Adv. Mater. 36 (2023) 2309376.
[146] Tianshi Qin, Wojciech Zajaczkowski, Wojciech Pisula, Martin Baumgarten, Ming Chen, Mei Gao, Gerry Wilson, Christopher D. Easton, Klaus Müllen, S. E. Watkins, Tailored donor-acceptor polymers with an A-D1-A-D2 structure: controlling intermolecular interactions to enable enhanced polymer photovoltaic devices, J. Am. Chem. Soc. 136 (2014) 6049–6055.
[147] M. Jeong, S. Chen, S.M. Lee, Z. Wang, Y. Yang, Z.G. Zhang, C. Zhang, M. Xiao, Y. Li, C. Yang, Feasible D1-A-D2-A random copolymers for simultaneous high-performance fullerene and nonfullerene solar cells, Adv. Energy Mater. 8 (2017) 1702166.
[148] I. Shin, Hj Ahn, J.H. Yun, J.W. Jo, S. Park, Sy Joe, J. Bang, H.J. Son, High-performance and uniform 1 cm^2 polymer solar cells with D1-A-D2-A-type random terpolymers, Adv. Energy Mater. 8 (2017) 1701405.
[149] Y. Xu, N. Mao, C. Zhang, X. Wang, J. Zeng, Y. Chen, F. Wang, J.-X. Jiang, Rational design of donor-π-acceptor conjugated microporous polymers for photocatalytic hydrogen production, Appl. Catal. B-Environ. 228 (2018) 1–9.
[150] Z. Wang, X. Yang, T. Yang, Y. Zhao, F. Wang, Y. Chen, J.H. Zeng, C. Yan, F. Huang, J.-X. Jiang, Dibenzothiophene dioxide based conjugated microporous polymers for visible-light-driven hydrogen production, Acs Catal. 8 (2018) 8590–8596.
[151] Y. Liu, J. Wu, F. Wang, Dibenzothiophene-S,S-dioxide-containing conjugated polymer with hydrogen evolution rate up to 147 mmol g^{-1} h^{-1}, Appl. Catal. B-Environ. 307 (2022) 121144.
[152] Z. Li, H. Fang, Z. Chen, W. Zou, C. Zhao, X. Yang, Regulating donor-acceptor interactions in triazine-based conjugated polymers for boosted photocatalytic hydrogen production, Appl. Catal. B-Environ. 312 (2022) 121374.
[153] P. Xie, C. Han, S. Xiang, S. Jin, M. Ge, C. Zhang, J.-X. Jiang, Toward high-performance dibenzo[g,p]chrysene-based conjugated polymer photocatalysts for photocatalytic hydrogen production through donor-acceptor-acceptor structure design, Chem. Eng. J. 459 (2023) 141553.
[154] K. Kailasam, M.B. Mesch, L. Möhlmann, M. Baar, S. Blechert, M. Schwarze, M. Schröder, R. Schomäcker, J. Senker, A. Thomas, Donor-acceptor-type heptazine-based polymer networks for photocatalytic hydrogen evolution, Energy Technol. -Ger. 4 (2016) 744–750.
[155] P.B. Pati, G. Damas, L. Tian, D.L.A. Fernandes, L. Zhang, I.B. Pehlivan, T. Edvinsson, C.M. Araujo, H. Tian, An experimental and theoretical study of an efficient polymer nano-photocatalyst for hydrogen evolution, Energ, Environ. Sci. 10 (2017) 1372–1376.
[156] H. Yan, Y. Deng, M. Shen, Y.-X. Ye, F. Zhu, X. Yang, G. Ouyang, Regulation the reactive oxygen species on conjugated polymers for highly efficient photocatalysis, Appl. Catal. B-Environ. 314 (2022) 121488.
[157] T. Zhou, P. Zhang, D. Zhu, S. Cheng, H. Dong, Y. Wang, G. Che, Y. Niu, M. Yan, C. Li, Synergistic effect triggered by skeleton delocalization and edge induction of carbon nitride expedites photocatalytic hydrogen evolution, Chem. Eng. J. 442 (2022) 136190.
[158] W. Ho, Z. Zhang, W. Lin, S. Huang, X. Zhang, X. Wang, Y. Huang, Copolymerization with 2,4,6-triaminopyrimidine for the rolling-up the layer structure, tunable electronic properties, and photocatalysis of g-C_3N_4, Acs Appl. Mater. Inter. 7 (2015) 5497–5505.
[159] J. Xiao, X. Liu, X. Gao, J. Hu, L. Pan, C. Shi, X. Zhang, J.-J. Zou, Controllable construction of alkynyl defective dibenzo[b,d]thiophenesulfone-based conjugated microporous polymers for enhanced photocatalytic performance, J. Catal. 414 (2022) 155–162.
[160] C.-L. Chang, W.-C. Lin, L.-Y. Ting, C.-H. Shih, S.-Y. Chen, T.-F. Huang, H. Tateno, J. Jayakumar, W.-Y. Jao, C.-W. Tai, C.-Y. Chu, C.-W. Chen, C.-H. Yu, Y.-J. Lu, C.-C. Hu, A.M. Elewa, T. Mochizuki, H.-H. Chou, Main-chain engineering of polymer photocatalysts with hydrophilic non-conjugated segments for visible-light-driven hydrogen evolution, Nat. Commun. 13 (2022) 5460.
[161] X. Song, X. Li, X. Zhang, Y. Wu, C. Ma, P. Huo, Y. Yan, Fabricating C and O co-doped carbon nitride with intramolecular donor-acceptor systems for efficient photoreduction of CO_2 to CO, Appl. Catal. B-Environ. 268 (2020) 118736.
[162] K. Xu, K. Cui, M. Cui, X. Liu, X. Chen, X. Tang, X. Wang, Electronic structure modulation of g-C_3N_4 by Hydroxyl-grafting for enhanced photocatalytic peroxymonosulfate Activation: Combined experimental and theoretical analysis, Sep. Purif. Technol. 294 (2022) 121246.
[163] G. Zhang, Y. Xu, H. Mi, P. Zhang, H. Li, Y. Lu, Donor Bandgap Engineering without Sacrificing the Reduction Ability of Photogenerated Electrons in Crystalline Carbon Nitride, Chemsuschem 14 (2021) 4516–4524.
[164] Y. Zhang, Z. Huang, J. Shi, X. Guan, C. Cheng, S. Zong, Y. Huangfu, L. Ma, L. Guo, Maleic hydrazide-based molecule doping in three-dimensional lettuce-like graphite carbon nitride towards highly efficient photocatalytic hydrogen evolution, Appl. Catal. B-Environ. 272 (2020) 119009.
[165] D. Wang, H. Huang, X. Zhou, Development of anthrazoline photocatalysts for promoting amination and amidation reactions, ChemComm 58 (2022) 3529–3532.
[166] S. Wang, G. Kumar, H. Tian, Organic Polymer Dots Based on Star-Shaped Truxene-Core Polymers for Photocatalytic H2O2 Production, Sol. RrL 6 (2022) 2200755.
[167] T. Zhou, T. Li, J. Hou, Y. Wang, B. Hu, D. Sun, Y. Wu, W. Jiang, G. Che, C. Liu, Tailoring boron doped intramolecular donor–acceptor integrated carbon nitride skeleton with propelling photocatalytic activity and mechanism insight, Chem. Eng. J. 445 (2022) 136643.
[168] C. Zhou, P. Xu, C. Lai, C. Zhang, G. Zeng, D. Huang, M. Cheng, L. Hu, W. Xiong, X. Wen, L. Qin, J. Yuan, W. Wang, Rational design of graphic carbon nitride copolymers by molecular doping for visible-light-driven degradation of aqueous sulfamethazine and hydrogen evolution, Chem. Eng. J. 359 (2019) 186–196.
[169] W. Yan, Y. Yu, H. Zou, X. Wang, P. Li, W. Gao, J. Wang, S. Wu, K. Ding, Promoted photocatalytic hydrogen evolution by molecular ring-substituting doping and regulation of charge carrier migration in graphitic carbon nitride, Sol. RrL 2 (2018) 1800058.
[170] Z. Chen, P. Sun, B. Fan, Q. Liu, Z. Zhang, X. Fang, Textural and electronic structure engineering of carbon nitride via doping with π-deficient aromatic pyridine ring for improving photocatalytic activity, Appl. Catal. B-Environ. 170 (2015) 10–16.

[171] L. Heymann, S.C. Bittinger, C. Klinke, Molecular doping of electrochemically prepared triazine-based carbon nitride by 2,4,6-triaminopyrimidine for improved photocatalytic properties, Acs Omega 3 (2018) 17042–17048.
[172] Q. Lu, K. Eid, W. Li, A.M. Abdullah, G. Xu, R.S. Varma, Engineering graphitic carbon nitride (g-C_3N_4) for catalytic reduction of CO_2 to fuels and chemicals: strategy and mechanism, Green. Chem. 23 (2021) 5394–5428.
[173] H. Guo, C.-G. Niu, C.-Y. Feng, C. Liang, L. Zhang, X.-J. Wen, Y. Yang, H.-Y. Liu, L. Li, L.-S. Lin, Steering exciton dissociation and charge migration in green synthetic oxygen-substituted ultrathin porous graphitic carbon nitride for boosted photocatalytic reactive oxygen species generation, Chem. Eng. J. 385 (2020) 123919.
[174] J. Zhang, G. Zhang, X. Chen, S. Lin, L. Mohlmann, G. Dolega, G. Lipner, M. Antonietti, S. Blechert, X. Wang, Co-monomer control of carbon nitride semiconductors to optimize hydrogen evolution with visible light, Angew. Chem. Int. Ed. 124 (2012) 3237–3241.
[175] X. Zhu, C. Tian, G.M. Veith, C.W. Abney, J. Dehaudt, S. Dai, An in situ doping strategy for the preparation of conjugated triazine frameworks displaying efficient CO_2 capture performance, J. Am. Chem. Soc. 138 (2016) 11497–11500.
[176] Z. Zhou, Y. Zhang, Y. Shen, S. Liu, Y. Zhang, Molecular engineering of polymeric carbon nitride: advancing applications from photocatalysis to biosensing and more, Chem. Soc. Rev. 47 (2018) 2298–2321.
[177] H. Zhang, J. Lin, Z. Li, T. Li, X. Jia, X.-L. Wu, S. Hu, H. Lin, J. Chen, J. Zhu, Organic dye doped graphitic carbon nitride with a tailored electronic structure for enhanced photocatalytic hydrogen production, Cata. Sci. Technol. 9 (2019) 502–508.
[178] M. Jing, H. Zhao, L. Jian, C. Pan, Y. Dong, Y. Zhu, Coral-like B-doped g-C_3N_4 with enhanced molecular dipole to boost photocatalysis-self-Fenton removal of persistent organic pollutants, J. Hazard. Mater. 449 (2023) 131017.
[179] Y. Tang, H. Zheng, X. Zhou, Z. Tang, W. Ma, H. Yan, Molecular doping increases the semitransparent photovoltaic performance of dilute bulk heterojunction film with discontinuous polymer donor networks, Small Methods 6 (2022) e2101570.
[180] D. Ravelli, M. Fagnoni, A. Albini, Photoorganocatalysis. What for? Chem. Soc. Rev. 42 (2013) 97–113.
[181] Z. Wang, X. Lin, Y. Tang, D. Miao, J. Huang, Y. Lu, S. Liu, R. Fu, D. Wu, Facile and universal defect engineering toward highly stable carbon-based polymer brushes with high grafting density, Small 19 (2023) 2207821.
[182] Y. Qian, Y. Han, X. Zhang, G. Yang, G. Zhang, H.-L. Jiang, Computation-based regulation of excitonic effects in donor-acceptor covalent organic frameworks for enhanced photocatalysis, Nat. Commun. 14 (2023) 3083.
[183] P. Niu, L.C. Yin, Y.Q. Yang, G. Liu, H.M. Cheng, Increasing the visible light absorption of graphitic carbon nitride (melon) photocatalysts by homogeneous self-modification with nitrogen vacancies, Adv. Mater. 26 (2014) 8046–8052.
[184] P. Niu, M. Qiao, Y. Li, L. Huang, T. Zhai, Distinctive defects engineering in graphitic carbon nitride for greatly extended visible light photocatalytic hydrogen evolution, Nano Energy 44 (2018) 73–81.
[185] H. Yu, R. Shi, Y. Zhao, T. Bian, Y. Zhao, C. Zhou, G.I.N. Waterhouse, L.Z. Wu, C. H. Tung, T. Zhang, Alkali-assisted synthesis of nitrogen deficient graphitic carbon nitride with tunable band structures for efficient visible-light-driven hydrogen evolution, Adv. Mater. 29 (2017) 1605148.
[186] Y. Shen, M. Wan, In situ doping polymerization of pyrrole with sulfonic acid as a dopant, Synth. Met. 96 (1998) 127–132.
[187] D.J. Woods, R.S. Sprick, C.L. Smith, A.J. Cowan, A.I. Cooper, A solution-processable polymer photocatalyst for hydrogen evolution from water, Adv. Energy Mater. 7 (2017) 1700479.
[188] J.-C. Jin, K.-Y. Wang, M. Afzal, A. Alarifi, S.W. Gosavi, R. Chauhan, L. Botha, W.-G. Chang, New Cu(II)-based three dimensional supramolecular coordination polymer as photocatalyst for the degradation of methylene blue, J. Mol. Struct. 1266 (2022) 133533.
[189] Q. Guo, L. Jing, Y. Lan, M. He, Y. Xu, H. Xu, H. Li, Construction 3D rod-like $Bi_{3.64}Mo_{0.36}O_{6.55}$/$CuBi_2O_4$ photocatalyst for enhanced photocatalytic activity via a photo-Fenton-like Cu^{2+}/Cu^{+} redox cycle, Sep. Purif. Technol. 254 (2021) 117546.
[190] Y. Zhang, S. Zhang, G. Liu, Q. Sun, S. Xue, W. Yang, Rational molecular and doping strategies to obtain organic polymers with ultralong RTP, Chem. Sci. 14 (2023) 5177–5181.
[191] H. Zhang, X. Zhang, Y. Li, G. Huang, W. Du, J. Shi, B. Wang, S. Li, T. Jiang, J. Zhang, Q. Cheng, J. Chen, B. Han, X. Liu, Y. Zhang, H. Zhou, Interfacial Molecular Doping at Donor and Acceptor Interface in Bilayer Organic Solar Cells, Sol. RrL 6 (2022) 2101096.
[192] J. Dostanic, D. Loncarevic, M. Zlatar, F. Vlahovic, D.M. Jovanovic, Quantitative structure-activity relationship analysis of substituted arylazo pyridone dyes in photocatalytic system: Experimental and theoretical study, J. Hazard. Mater. 316 (2016) 26–33.
[193] S. Qiao, M. Di, J.-X. Jiang, B.-H. Han, Conjugated porous polymers for photocatalysis: the road from catalytic mechanism, molecular structure to advanced applications, Energychem 4 (2022) 100094.
[194] J. Wilkinson, P.S. Hooda, J. Barker, S. Barton, J. Swinden, Occurrence, fate and transformation of emerging contaminants in water: an overarching review of the field, Environ. Pollut. 231 (2017) 954–970.
[195] M. Ismail, K. Akhtar, M.I. Khan, T. Kamal, M.A. Khan, M.A. A, J. Seo, S.B. Khan, Pollution, toxicity and carcinogenicity of organic dyes and their catalytic bio-remediation, Curr. Pharm. Des. 25 (2019) 3653–3671.
[196] N.Y. Donkadokula, A.K. Kola, I. Naz, D. Saroj, A review on advanced physico-chemical and biological textile dye wastewater treatment techniques, Rev. Environ. Sci. Bio. 19 (2020) 543–560.
[197] A.A. Oladipo, M. Gazi, A.S. Oladipo, A.O. Ifebajo, E.O. Ahaka, Photocatalytic degradation of toxic pesticides: Mechanistic insights, Photocatal. Adv. Oxid., Pro. Wast. Treat. (2020) 95–138.
[198] P.O. Oladoye, T.O. Ajiboye, E.O. Omotola, O.J. Oyewola, Methylene blue dye: Toxicity and potential elimination technology from wastewater, Results Eng. 16 (2022) 100678.
[199] S. Wang, Z. Zhu, J. He, X. Yue, J. Pan, Z. Wang, Steroidal and phenolic endocrine disrupting chemicals (EDCs) in surface water of Bahe River, China: Distribution, bioaccumulation, risk assessment and estrogenic effect on Hemiculter leucisculus, Environ. Pollut. 243 (2018) 103–114.
[200] W. Duan, F. Meng, H. Cui, Y. Lin, G. Wang, J. Wu, Ecotoxicity of phenol and cresols to aquatic organisms: A review, Ecotoxicol. Environ. Saf. 157 (2018) 441–456.
[201] M.F.R. Samsudin, N. Bacho, S. Sufian, Y.H. Ng, Photocatalytic degradation of phenol wastewater over Z-scheme g-C_3N_4/CNT/$BiVO_4$ heterostructure photocatalyst under solar light irradiation, J. Mol. Liq. 277 (2019) 977–988.
[202] R. Wang, X. Zhao, N. Jia, L. Cheng, L. Liu, C. Gao, Superwetting oil/water separation membrane constructed from in situ assembled metal-phenolic networks and metal-organic frameworks, ACS Appl. Mater. Inter. 12 (2020) 10000–10008.
[203] C. Liu, M. Zhang, H. Gao, L. Kong, S. Fan, L. Wang, H. Shao, M. Long, X. Guo, Cyclic coupling of photocatalysis and adsorption for completely safe removal of N-nitrosamines in water, Water Res 209 (2022) 117904.
[204] K. Maheshwari, M. Agrawal, A.B. Gupta, Dye Pollution in Water and Wastewater, Nov. Mater. Dye. Waste Treat. (2021) 1–25.
[205] Y. Yang, X. Zhang, J. Jiang, J. Han, W. Li, X. Li, K.M.Y. Leung, S.A. Snyder, P.J. J. Alvarez, Which Micropollutants in Water Environments Deserve More Attention Globally? Environ. Sci. Technol. 56 (2022) 13–29.
[206] Y. Deng, C. Feng, L. Tang, Y. Zhou, Z. Chen, H. Feng, J. Wang, J. Yu, Y. Liu, Ultrathin low dimensional heterostructure composites with superior photocatalytic activity: insight into the multichannel charge transfer mechanism, Chem. Eng. J. 393 (2020) 124718.
[207] Y. Wang, Y. Deng, D. Gong, L. Yang, L. Li, Z. Zhou, S. Xiong, R. Tang, J. Zheng, Visible light excited graphitic carbon nitride for efficient degradation of thiamethoxam: Removal efficiency, factors effect and reaction mechanism study, J. Environ. Chem. Eng. 9 (2021) 105739.
[208] Y. Wang, W. Hao, H. Liu, R. Chen, Q. Pan, Z. Li, Y. Zhao, Facile construction of fully sp^2-carbon conjugated two-dimensional covalent organic frameworks containing benzobisthiazole units, Nat. Commun. 13 (2022) 100.
[209] R. Luo, H. Lv, Q. Liao, N. Wang, J. Yang, Y. Li, K. Xi, X. Wu, H. Ju, J. Lei, Intrareticular charge transfer regulated electrochemiluminescence of donor-acceptor covalent organic frameworks, Nat. Commun. 12 (2021) 6808.
[210] L. Li, X. Yuan, Z. Zhou, R. Tang, Y. Deng, Y. Huang, S. Xiong, L. Su, J. Zhao, D. Gong, Research progress of photocatalytic activated persulfate removal of environmental organic pollutants by metal and nonmetal based photocatalysts, J. Clean. Prod. 372 (2022) 133420.
[211] E. Pellzzett, Photocatalytic degradation of atrazine and other S-triazine herbicides, Environ. Sci. Technol. 24 (1990) 1559–1565.
[212] Rodr, Iacute, L. Guez-Castellanos, J.C. Sanchez-Hernandez, Earthworm biomarkers of pesticide contamination: Current status and perspectives, J. Pestic. Sci. 32 (2007) 360–371.
[213] F.-J. Zhao, Y. Ma, Y.-G. Zhu, Z. Tang, S.P. McGrath, Soil contamination in china: Current status and mitigation strategies, Environ. Sci. Technol. 49 (2014) 750–759.
[214] M. Yeganeh, E. Charkhloo, H.R. Sobhi, A. Esrafili, M. Gholami, Photocatalytic processes associated with degradation of pesticides in aqueous solutions: Systematic review and meta-analysis, Chem. Eng. J. 428 (2022) 130081.
[215] F.S. Bruckmann, C. Schnorr, L.R. Oviedo, S. Knani, L.F.O. Silva, W.L. Silva, G. L. Dotto, C.R. Bohn Rhoden, Adsorption and Photocatalytic Degradation of Pesticides into Nanocomposites: A Review, Molecules 27 (2022) 6261.
[216] J. Zhang, X. Zhao, Y. Wang, Y. Gong, D. Cao, M. Qiao, Peroxymonosulfate-enhanced visible light photocatalytic degradation of bisphenol a by perylene imide-modified g-C_3N_4, Appl. Catal. B-Environ. 237 (2018) 976–985.
[217] C. Gan, M. Sheng, Z. Hu, Y. Li, Y. Peng, Z. Xiang, B. Sun, H. Jiang, Novel and efficient strategy for chlorophenols and CO_2 transformation over carbon nitride nanotubes: Effect of the hydroxyl grafting and surface electron polarization, J. Catal. 413 (2022) 636–647.
[218] E. Jin, S. Fu, H. Hanayama, M.A. Addicoat, W. Wei, Q. Chen, R. Graf, K. Landfester, M. Bonn, K.A.I. Zhang, H.I. Wang, K. Mullen, A. Narita, A Nanographene-Based Two-Dimensional Covalent Organic Framework as a Stable and Efficient Photocatalyst, Angew. Chem. Int. Ed. 61 (2022) e202114059.
[219] Q. Yang, M. Luo, K. Liu, H. Cao, H. Yan, Covalent organic frameworks for photocatalytic applications, Appl. Catal. B-Environ. 276 (2020) 119174.
[220] N.S.N. Hasnan, M.A. Mohamed, Z.A. Mohd Hir, Surface Physicochemistry Modification and Structural Nanoarchitectures of g-C_3N_4 for Wastewater Remediation and Solar Fuel Generation, Adv. Mater. Technol. 7 (2021) 2100993.
[221] T.-Y. Shang, L.-H. Lu, Z. Cao, Y. Liu, W.-M. He, B. Yu, Recent advances of 1,2,3,5-tetrakis(carbazol-9-yl)-4,6-dicyanobenzene (4CzIPN) in photocatalytic transformations, Chem. Commun. 55 (2019) 5408–5419.
[222] T. Banerjee, F. Podjaski, J. Kröger, B.P. Biswal, B.V. Lotsch, Polymer photocatalysts for solar-to-chemical energy conversion, Nat. Rev. Mater. 6 (2020) 168–190.